Journal of Medicinal Chemistry

pubs.acs.org/jmc

Perspective

Conjugated Photosensitizers for Imaging and PDT in Cancer Research

João C. S. Simões, Sophia Sarpaki, Panagiotis Papadimitroulas, Bruno Therrien,* and George Loudos*

Cite This: *J. Med. Chem.* 2020, 63, 14119−14150

Read Online

ACCESS | Metrics & More | Article Recommendations

ABSTRACT: Early cancer detection and perfect understanding of the disease are imperative toward efficient treatments. It is straightforward that, for choosing a specific cancer treatment methodology, diagnostic agents undertake a critical role. Imaging is an extremely intriguing tool since it assumes a follow up to treatments to survey the accomplishment of the treatment and to recognize any conceivable repeating injuries. It also permits analysis of the disease, as well as to pursue treatment and monitor the possible changes that happen on the tumor. Likewise, it allows screening the adequacy of treatment and visualizing the state of the tumor. Additionally, when the treatment is finished, observing the patient is imperative to evaluate the treatment methodology and adjust the treatment if necessary. The goal of this review is to present an overview of conjugated photosensitizers for imaging and therapy.

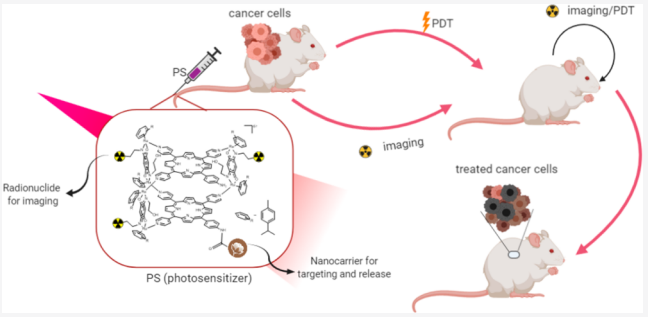

1. INTRODUCTION

Photodynamic therapy (PDT) is an attractive cancer theranostic platform, mainly due to its precise controllability, minimal invasiveness, and high spatiotemporal accuracy.[1] It works by combining photosensitizers (PS) with negligible cytotoxicity and excitation light in compatible doses to produce cytotoxic reactive oxygen species (ROS), which eradicate cancer cells.[2] PDT presents, therefore, several unique and distinct characteristics, which make it a very advantageous therapy not only as a stand-alone treatment but also in combination with other established modalities.

Although conventional imaging remains critical to the management of patients with cancer, molecular imaging can provide additional information. Imaging, in such manner, is an extremely intriguing tool since it is not only assuming an essential role after treatment to access its success and recognize any conceivable repeating injuries, but also because it allows an examination of the disease and to investigate whether the behavior of the tumor has changed. Additionally, when the treatment is finished, observing the patient is vital in order to evaluate the outcome and, if necessary, to revise the protocol.[3] Imaging, in combination with PDT, may therefore be used not only for research but also as a tool for studying basic PDT mechanisms, developing models of diseases, understanding PDT tissue interactions,[4,5] and even as a therapy response.[6] Moreover, it can provide a basis to establish the prospect of success of new therapeutic approaches.[7−11]

PDT imaging can be divided into different modalities: optical, ultrasound, magnetic resonance, and nuclear imaging, according to the mechanism of action.[12] This can either be through radioactive compounds that produce a flag on a screen (PET or SPECT), by utilization of nonradioactive materials that may enhance the contrast of tumors (computer tomography (CT) and magnetic resonance imaging (MRI)) or through acoustic (ultrasound and photoacoustic) and fluorescence signals upon activation (Figure 1).

While both, optical and nonoptical imaging, have been used to monitor PDT, the outcomes are often assessed too late, usually when the disease has progressed more than expected. This creates a new challenge for developing online or early monitoring strategies to envision as soon as possible a new approach to treat a disease.[13] Imaging techniques combined with PDT offer new opportunities for the treatment of different cancers. This concept introduces the so-called theranostic agent, a single compound that inherently possesses both imaging and treatment properties, allowing for the visualization of the problem while being able to treat the condition.[3,14] These modalities have correlative properties that make them appropriate for various kinds of *in vivo* imaging applications. They are overall conceivable to be conjugated

Received: January 10, 2020
Published: September 29, 2020

https://dx.doi.org/10.1021/acs.jmedchem.0c00047
J. Med. Chem. 2020, 63, 14119−14150

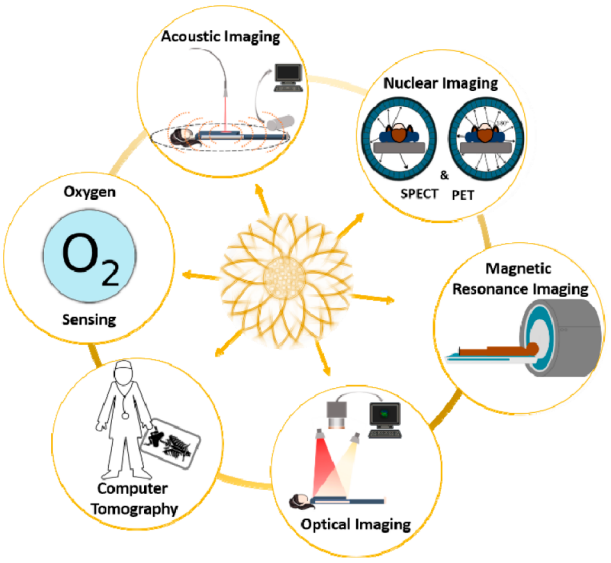

Figure 1. Imaging applications in photodynamic therapy.

with PDT agents so as to accomplish a definitive objective of having a single agent that does "all".[3,15]

Theranostic agents are commonly divided into two groups according to their design: (1) an agent with both properties, imaging and therapeutic, and (2) double-functionalized nanoparticles (theranostic particles) that are modified with an assortment of imaging and therapeutic moieties.[3] Exploiting the same biodistribution such theranostic agents can pave the way to personalized medicine (Figure 2).[16−19] Due to the development of instruments for imaging and PDT treatment, several imaging and therapeutic modalities have been combined, using different assembly strategies, to develop novel theranostic agents.[20]

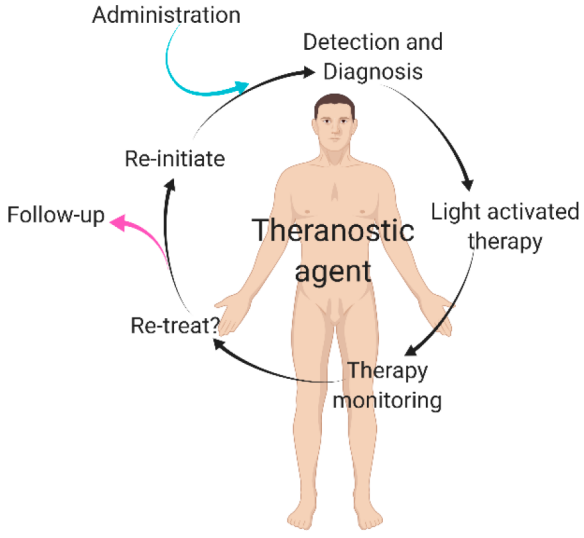

Figure 2. Cartoon depicting personalized medicine with theranostic agents.

2. BASIC PRINCIPLES OF PHOTODYNAMIC THERAPY (PDT) AND PHOTOSENSITIZERS

2.1. Photodynamic Therapy (PDT). The true potential of PDT was only realized after the extensive work of Dougherty and co-workers who, between 1975 and 1980, reported a complete cure of malignant tumors by combining an HpD (hematoporphyrin derivative) and red light.[21] Initially, it was applied in a breast cancer model and later in patients with skin, prostate, breast, or colon tumors. These promising results were later confirmed in clinical trials with improved versions of HpDs in patients with skin or bladder cancer. At the same time, Weishaupt and his colleagues postulated that singlet oxygen ($^1O_2$) generated in PDT was the cytotoxic agent responsible for the destruction of tumor cells.[22,23] Finally, in 1993, a landmark for PDT was achieved with the regulatory approval in Canada of porfimer sodium, a semipurified version of HpD, for the treatment of bladder cancer.

Light, oxygen, and PS precise cooperation are key for the efficacy of PDT to trigger the production of ROS, responsible for the inactivation and destruction of tumor cells. Furthermore, PDT provides spatiotemporal control through the photosensitizer and the light source.[13] The PS can reach the tumor compartment utilizing various targeted methodologies,[24] such as immunoconjugates or nanotechnologies.[25] A localized light activation ensures an optimal treatment, thus sparing surrounding tissues. While a specific location of light illumination provides spatial control, a time delay between PS administration and light irradiation provides a temporal control of the therapy.

Nevertheless, the combination of light, oxygen, and PS represents a great challenge in the optimization of therapeutic protocols. To obtain the desired therapeutic effect, a great number of factors should be considered, namely, the type of PS, the dose administered, the intracellular location, the drug to light interval (DLI), the total light dose applied, its wavelength and fluence rate, tumor characteristics, and local availability of oxygen. Since the PS is only activated in the presence of light, PDT presents several advantages over other conventional cancer treatments such as low systemic toxicity and the capability to destroy tumor cells selectively. Furthermore, it can also be applied in combination with other therapeutic modalities and is often cheaper than other cancer treatments.[26,27] On the other hand, PDT presents some disadvantages including the fact that most of the PS used in PDT are hydrophobic molecules, they show a poor cell specificity, and light penetration through tissues is minimal, thus limiting PDT treatments to superficial tumors such as skin cancer, nasopharyngeal cancer, and oral cancer.[28−32]

2.2. Photosensitizers in PDT. When developing new photosensitizers, there are a series of advantages and limitations that we can find. The limitations include photosensitivity after treatment, the fact that the treatment efficacy depends on optimal light activation to the tumor, and the presence of oxygen remains crucial to PDT. Another big disadvantage is that no current photosensitizer can treat metastatic cancers.[33] The advantages, on the other side, make for a compelling case for the continuation of the development of such compounds. These include fewer adverse effects and little invasiveness, short treatment time and selectivity, and lower costs than other treatments. Other advantages include the following: it can be used in outpatient settings, can be applied multiple times, and leaves little or no scarring after healing.[33]

A PS should, ideally, be a single and pure compound that accumulates preferentially in tumors. At the same time, it should have low toxicity in the dark to minimize phototoxic side effects, and it should be rapidly eliminated from the

https://dx.doi.org/10.1021/acs.jmedchem.0c00047
J. Med. Chem. 2020, 63, 14119−14150

body.[27,34] To reach target cells, the PS needs a good balance between hydrophilicity and lipophilicity. Indeed, it must possess amphiphilicity. An ideal photosensitizing agent ought to have a high absorption peak between 600 and 800 nm (red to deep-red region). Absorption of photons at higher wavelengths (>800 nm) does not provide enough energy to excite oxygen to its singlet state and accordingly to generate sufficient ROS. These characteristics as well as others are summarized in Figure 3.

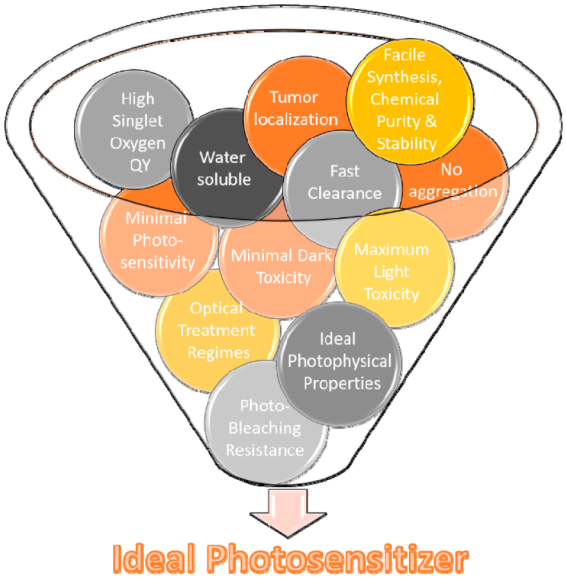

Figure 3. Ideal characteristics of photosensitizers.

In addition, a PS must have good photophysical properties, such as high quantum yields of triplet state formation, high singlet oxygen production, and an appropriate triplet lifetime. The triplet lifetime is crucial to allow the PS to interact with oxygen and other substrates in view to generate ROS.[27,34] Moreover, PSs should have good absorption between 600 and 800 nm to ensure strong light penetration into tissues. Therefore, agents absorbing strongly in the red, such as chlorins, bacteriochlorins, and phthalocyanins, are more suitable for PDT treatments. However, most known PSs do not possess all requirements. In the past few years, efforts have been focused on the development of PSs that can be activated with the light of a longer wavelength, with mild photosensitivity and high tumor specificity. Tetrapyrrole-based structures seem to gather most of these characteristics, making them the best option for PS when compared with other classes of molecules.

Many different molecular structures have been studied for PDT (Figure 4), including some natural products such as hyperacin,[35−37] curcumin,[38−41] hypocrellin[42,43] and riboflavin,[44−47] as well as synthetic dyes. When it comes to synthetic dyes, the most commonly studied are phenothiazinium salts such as Methylene Blue[48] and Toluidine Blue,[49] which have been widely studied both for antimicrobial applications[50] and, less often, anticancer activity.[51] Rose Bengal, which has a long history as a photoactive dye and has been explored for antimicrobial applications,[52] tissue bonding applications,[53] and anticancer applications is another example.[54] Squaraine and BODIPY dyes, with delocalized systems of molecular orbitals, provide good absorption in the visible range.[55]

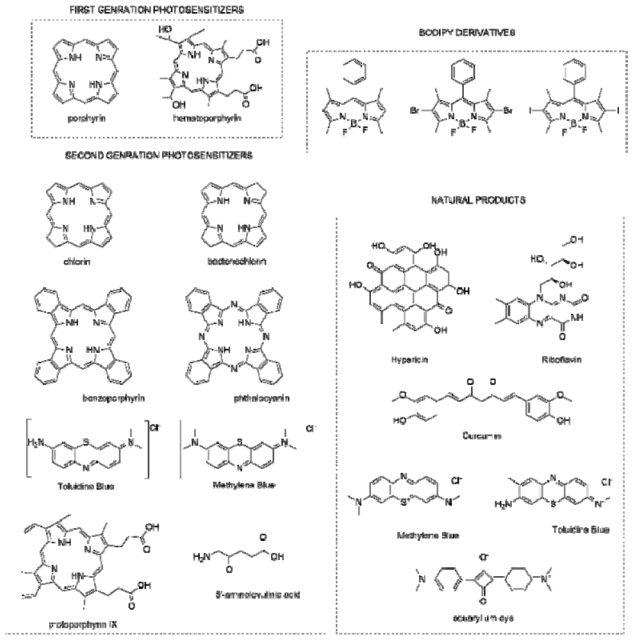

Figure 4. Structures of photosensitizers currently used in PDT.

Most BODIPY dyes have the right characteristics, such as a low dark toxicity, a good cellular uptake, a high extinction coefficient, and a low quantum yield for photobleaching, which make them good PDT agents. However, some modifications can be made to their structure in order to enhance intersystem crossing (ISC) and prevent photodamage in PDT, which is thought to occur predominantly via triplet excited states. Spin-coupling to heavy atoms ("heavy atom effect") is a common modification. Generally, the addition of heavy atoms occurs at positions that will not disrupt the planarity of the dye. An appropriate placing of heavy atoms on a BODIPY core promotes spin−orbit coupling, without any energy loss from excited states.[56] In the case of Rose Bengal, the introduction of halogens into the rings, such as bromine or iodine, seems to increase the triplet yield of the molecule by facilitating intersystem crossing. In a similar manner, the introduction of iodine into the delocalized system of squarines also increases the triplet yield.

Other synthetic dyes include phenalenones,[57] often used as a standard for the generation of $^1O_2$ and recently developed into an antimicrobial PS,[58,59] and coordinated to transition metals. These are a relatively new class of PSs. Ruthenium(II) polypyridyl complexes are perhaps the most studied,[60] although other ruthenium,[61] rhodium,[62] and cyclometalated iridium[63] complexes have also been studied. There is also evidence that luminescent platinum(II) and gold(III) complexes can act as PSs.[64] In addition to these structures, nowadays, most PSs utilized in PDT (Figure 5 and Table 1) show a tetrapyrrole structure.

It is possible to categorize the photosensitizers into three generations, especially with regards to porphyrin-based PSs. Porfimer sodium and the hematoporphyrin derivative (HpD) are known as the first generation of photosensitizers.[22,65] Porfimer sodium shows many drawbacks, such as a poor light absorption at the maximum wavelength (ε_{max} at 630 nm), a low molar extinction coefficient (~3000 M^{-1} cm^{-1}), and a slow clearance, which causes prolonged photosensitivity of the skin after treatment.[65−68]

https://dx.doi.org/10.1021/acs.jmedchem.0c00047
J. Med. Chem. 2020, 63, 14119−14150

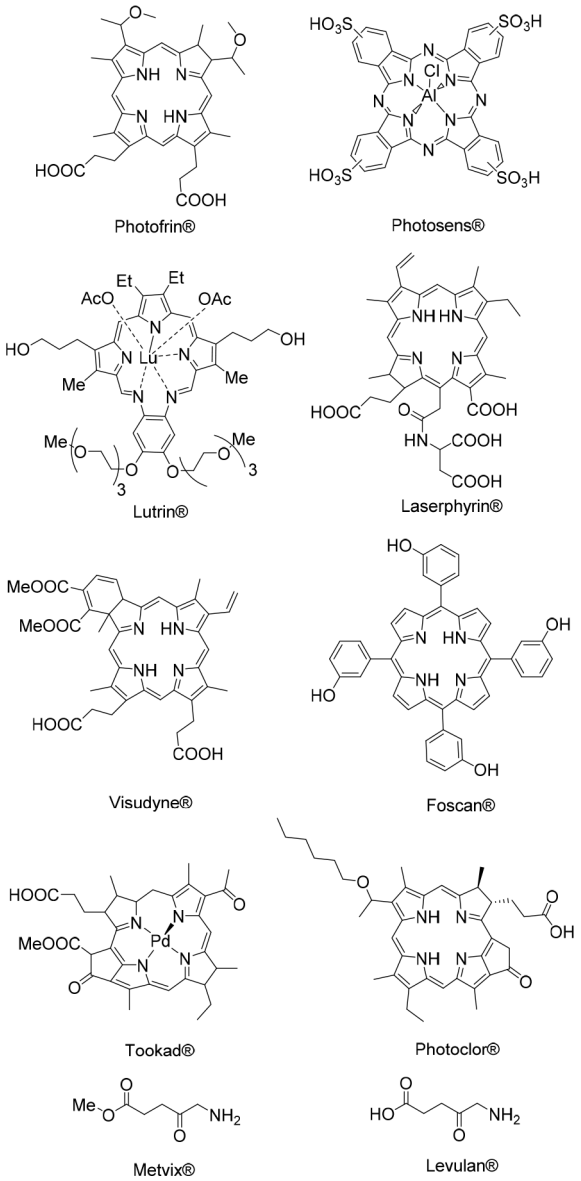

Figure 5. Most commonly used PSs in the clinic.

While a photodynamic impact can be achieved with porfimer sodium, efficiency can be improved by red-shifting the absorbance band and by increasing the absorbance at longer wavelengths. There has been a noteworthy exertion among therapeutic physicists to find second-generation PSs, and numerous compounds have been proposed as potent anticancer agents for PDT.[34] The so-called second generation of photosensitizers, which include various derivatives of porphyrins, phthalocyanines, naphthalocyanines, chlorins, and bacteriochlorins, was created from not only just the need to overcome drawbacks but also to increase the formation of singlet oxygen ($^1O_2$), through a type II process.[69,70]

When the wavelength is higher, the light penetrates through tissues deeper; therefore, PSs with strong absorbance in the deep-red region, such as chlorins, bacteriochlorins, and phthalocyanins, can have a better impact on tumors. Chlorin derivatives show an intense absorption band around 650 nm, which make them good candidates for PDT applications. These PSs with increased light penetration were classified as second-generation photosensitizers.[71]

An early example is temoporfin, which was approved in Europe in 2001. This chlorin derivative reduces the skin post-treatment photosensitivity by at least a factor of two, from 4 to 12 weeks with porfimer sodium to only 2 to 4 weeks. Moreover, because it possesses an increased light absorption at a longer wavelength (652 nm), the light dose required for treatment is reduced by a factor of 10. Although showing significant progress when compared to sodium porfimer, some other aspects needed to improve such as pharmacokinetic profiles and higher phototherapeutic indices, as well as solubility.[72] The side effects of the second generation of PSs caused by nonspecific localization, and the need for better pharmacokinetic profiles gave rise to the development of a third generation of photosensitizers: PSs with amphiphilic properties appropriate for diffusion through the lipid barrier and for endocellular localization.[73]

Therefore, to improve the efficacy of PSs in PDT, the so-called third generation of PSs must show a longer wavelength activation and a better selectivity for tumor tissues. To achieve these goals, conjugation of targeting molecules (such as antibodies) to the PS, encapsulation of a PS into carriers (such as liposomes, micelles, or nanoparticles), or functionalization with prodrugs that get activated only at the tumor site, is among the new strategies employed.[65−68] The main goals being the improvement of specificity and efficacy, reduction of off-target accumulations, and optimization of the pharmacokinetic.

In order to reduce the impact on adjacent tissues, the concept of prodrug has been evaluated. The strategy consists of the administration of a PS in an inactive form, which will become active only after reaching the target. The activation will be triggered by proteases, the pH, or another biological response. A PS producing singlet oxygen in a specific environment, acidic conditions, for example, will have a stronger impact on tumors where the pH is lower.[73] Such activatable photosensitizers combine the concept of local treatment and personalized therapy, the main objective being to display minimal phototoxicity when off-target, and high activity in the targeted tissue to increase PDT selectivity.[74] Although the strategy of activatable agents seems to be of great interest for the future of photodynamic therapy, the main strategy applied nowadays still seems to be the functionalization of these molecules through conjugation with biomolecules and carriers such as porphysomes, quantum dots, nanoparticles, and targeting moieties.

2.3. Functionalization of PSs. Incorporation of hydrophilic groups on the PS, such as HSO_3^-, COO^-, and NR_4^+, increases the water solubility, but the delivery of lipophilic PSs to target cells remains an important PDT goal.[75,76] To achieve that goal, different types of functionalization of PS can be performed, usually through the conjugation with other molecules. The choice of the conjugates is driven by the tumor microenvironment, such as hypoxia,[77] enzymes,[78] leaky vasculature,[79,80] and receptors overexpressed by cancer cells.[81,82]

Lately, certain limitations of potent PSs, such as (i) poor solubility in aqueous media, (ii) high potency for aggregations, and/or (iii) undesired interactions with proteins or biomolecules in aqueous media, in combination to the rapid advances in nanotechnology, led to the development of another round of the third generation of PSs, which are encapsulated to the nanostructure,[83−87] with the most commonly used nanoparticles being listed in Table 2.

https://dx.doi.org/10.1021/acs.jmedchem.0c00047
J. Med. Chem. 2020, 63, 14119−14150

Table 1. PSs Currently Used in Clinics or Under Clinical Trials[73]

		generic name	chemical name	excitation wavelength (nm)	application	manufacturer
clinically approved	first generation	photofrin	porfimer sodium	630	esophageal cancer, lung adenocarcinoma, endobronchial cancer	Axcan Pharma, Canada
	second generation	ameluz/ levulan	aminolevulinic acid hydrochloride	635	mild to moderate actinic keratosis	DUSA, USA
		foscan	temoporfin	652	advanced head and neck cancer	Biolitec, Germany
		laserphyrin	aspartyl chlorin	664	Early centrally located lung cancer	Meiji Seika, Japan
		metvix/ metvixia	methyl aminolevulinate	570−670	nonhyperkeratotic actinic keratosis, basal cell carcinoma	Galderma, UK
		redaporphine		749	biliary tract cancer	Luzitin, Portugal
		visudyne	verteporfin	690	age-related macular degeneration	Novartis, Switzerland
under clinical trials		antrin	motexafin lutetium	732	coronary artery disease	Pharmacyclics
		fotolon		665	nasopharyngeal sarcoma	Apocare Pharam, Germany
		photoclor		664	head and neck cancer	Rosewell Park
		photosens	sulfontaed alumunium phthalocyanines	675	age-related macular degeneration	Russia
		photrex		664	age-related macular degeneration	Miravant, USA
		radachlorin		662	skin cancer	Rada-pharma, Russia
		talaporfin	L-aspartyk chlorin e6	664	colorectal neoplasms, liver metastasis	Novartis, Switzerland
		TOOKAD	padeliporfin	762	prostate cancer	Negma-Lerads

Table 2. Clinically Approved Nanoparticles[130]

	type	agent	modality	indication	trade name
clinically approved	sulfur colloid	^{99m}Tc	SPECT	lymphoscintigraphy, bone marrow, gastrointestinal, liver, and spleen	Technecoll (US)
	albumin colloid	^{99m}Tc	SPECT	lymphoscintigraphy, inflammation imaging, melanoma, prostate	Nanocoll (EU)
	SnF_2 colloid	^{99m}Tc	SPECT	lymphoscintigraphy, gastrointestinal, liver, and spleen	Hepatate (France)
	Re_2S_7 colloid	^{99m}Tc	SPECT	lymphoscintigraphy, gastrointestinal, melanoma, prostate	Nanocis (EU)
	albumin colloid	^{99m}Tc	SPECT	lymphoscintigraphy of breast	Senti-Scint
	dextran-coated iron oxide (ferumoxide)	$Fe^{2+}\ Fe^{3+}{}_2O_4$ $(Fe^{3+}\ Fe^{2+}{}_2)O_4$	MRI	mononuclear phagocyte system imaging, cellular labeling	Feridex (US), Endorem (Britain)
	carboxydextran-coated iron oxide (ferucarbotran)	$Fe^{2+}\ Fe^{3+}{}_2O_4$ $(Fe^{3+}\ Fe^{2+}{}_2)O_4$	MRI	lymph node imaging, perfusion imaging	Sinerem (EU), Combidex (US)
	carboxydextran-coated iron oxide (ferucarbotran)	γ-Fe_2O_3	MRI	hepatocellular carcinoma, cell labeling	Resovist (US, EU), Cliavist (France)
	polyglucose sorbitol carboxymethyl ether-coated iron oxide (ferumoxytol)	γ-Fe_2O_3	MRI	iron-deficiency anemia, off-label uses in imaging	Faraheme (US)
under clinical trials	sulfur colloid	^{99m}Tc	SPECT	colon cancer	
	sulfur colloid	^{99m}Tc	SPECT	cancer	
	sulfur colloid	^{99m}Tc	SPECT	head and throat cancer	
	gold	nanoshell	photothermal	head and neck cancer	
	silica	^{124}I and Cy5	PET and optical	melanoma	
	iron oxide	ferumoxytol	MRI	glioma	
	iron oxide	ferumoxytol	MRI	pancreatic cancer	
	iron oxide	ferumoxide	MRI	inflammation	
	iron oxide	ferumoxytol	MRI	myocardial infarction	

Medicinal nanoparticles (NPs) are drug-loaded, and their overall size does not exceed the 100 nm in order to cross effectively physiological barriers *in vivo*.[91,92] Appropriate modification of NPs enables improved solubility, excess in drug loading, and to control drug release and enhancing their imaging modalities.[92−94] These interesting and sometimes unexpected properties of nanoparticles are largely due to their high surface-area-to-volume ratio. Introduction of different functional groups at the surface of NPs provide a variety of chemical properties.[91] In other words, the surface or core of the nanoparticle might be loaded with various agents, allowing the use in multiple applications simultaneously (such as imaging and therapy).[95−97] A common example of indirect PS functionalization is the usage of peptide linkages that can be cut by metalloproteinases (MMP's), which are ordinarily abundant in an assortment of tumors. Nanoparticles can likewise help in the delivery of hard-to-formulate drugs within

https://dx.doi.org/10.1021/acs.jmedchem.0c00047
J. Med. Chem. 2020, 63, 14119−14150

water-based solutions, by either protective biopolymer coating or encapsulation.[3]

Nanoparticles can also be surface-covered with polymers such as poly(lactic-*co*-glycolic corrosive) (PLGA) or polyethylene glycol (PEG) for increased tumor selectivity.[98] The surface can be decorated with drugs, pro-drugs, contrast agents, or a mixture of different elements.[99] Optimally, the monitoring of treatments (before, during, after) is conducted by the contrast agent. Nanoparticles can also be loaded with drugs or prodrugs (peripherally or internally).[99] Such theranostic nanoparticles can be tweaked to release the drug based on tumor microenvironment conditions.[99−102] Indeed, many tumors possess a poor blood vessel system, of leaky, dilated, and irregular shapes, which allow large molecules to reach the tumor.[103] Then, when inside, the lack of efficient lymphatic drainage traps the NPs in the tumor. These two phenomena are known as the enhanced permeability and retention effect (EPR).[103,104] The surface of the NPs can be functionalized with targeting agents to interact with overexpressed tumor-related receptors.[105] Targeting biomolecules can be combined so that one functional group may allow the nanoparticle internalization by endocytosis, while another functional group targets a specific receptor before drug release.[106]

Recent studies have demonstrated the possibility of using metal-based nanoparticles as photosensitizers, up-conversion tools delivery, and vehicles.[107] Moreover, metal-based NPs show good sizes and shapes to ensure prolonged activity and biodistribution. Studies dealing with nanoparticles based on molybdenum oxide, TiO_2, ZnO, and tungsten oxide as photosensitizers in PDT have been conducted in recent years.[108,109]

The first investigation of nanoscaled metal−organic frameworks (MOF) in PDT was reported by Lu et al. in 2014.[110] Their study suggests that the Hf−porphyrin nanoscale metal−organic framework (DBP−UiO) is an excellent photosensitizer in PDT treatments of resistant head and neck cancers. The DBP−UiO framework shows enhanced *in vitro* and *in vivo* PDT efficacy. Following this initial study, other applications of nanoscaled MOFs in PDT were reported.[111] MOFs have indeed become popular metal-based nanoparticles for PDT applications.

A very common conjugation of photosensitizers is with porphysomes. Porphysomes are derived from porphyrin−lipid bilayers, and they show a high static quenching effect. In addition, they have a structure and a loading capacity similar to those observed for liposomes. Most importantly, they have a high porphyrin payload that is advantageous for PDT treatment, while being biocompatible, nontoxic, and biodegradable.[112]

Jin et al. have constructed folate-porphysomes by incorporating a small percentage of folate conjugate lipids in porphysome formulation. This allowed FR-mediated cell uptake of nanoparticles, which, subsequently, resulted in a rapid disruption in cells upon activation of porphyrin fluorescence and production of ROS. The irradiation of the folate porphysomes increases folate receptor-selectivity and ultimately PDT efficacy. Once systematically administrated to FR-positive tumor-bearing mice, the folate-porphysomes were reducing the tumor size and increasing the survival rate. Furthermore, such targeting-porphysome formulation facilitates the introduction of additional targeting moieties to realize disease-specific and personalized PDT treatments.

Similarly, Lovell et al. developed porphysomes with a higher quenching capacity than the PS alone.[113] Located inside a simple bilayer, the porphyrin−lipid orientation promotes porphyrin interaction and quenching. However, after loading porphyrins into the nanocarrier, the fluorescence response was regained, thus confirming the benefit of these combinations.

Another example of a successful porphysome design was published by Philp et al., in which porphysomes were used to monitor in real time the resection of primary tumors, lymph nodes, and abdominal metastases in rabbits.[114] Another proof of the diagnostic ability of nanoparticles was reported by Ng et al., who employed bacteriopheophorbide as a fluorescent energy acceptor in a self-sensing porphysome (FRETysome).[115] Following subcutaneous injection in mice, the presence of FRETysome has permitted to image the tumor. Moreover, they observed after 24 and 48 h postinjection the persistence of nanovesicles at the tumor site.[116]

Several research groups have recently focused their interest in the functionalization of "quantum dots" QDs with PDT agents. Nanostructured semiconductor materials were first applied in heterogeneous photocatalysis in the 1980s, and their unique properties have raised attention.[88,117−120] Scientists used these nanocrystals as PSs, due to their ability to selectively transfer energy and to produce light over a broad range of wavelengths, which can be optimized to the appropriate wavelength for PS excitation.[121−125] Unlike most organic photosensitizers, QDs do not have metastable excited states, which can promote effective energy transfer, and therefore, distinct processes are expected to occur, thus yielding reactive oxygen species in a different way.[126]

Wang et al. developed a water-soluble and pH/H_2O_2 responsive silicon QDs-based nanocomplex and explored their applications in PDT.[127] Silicon is not only an outstanding semiconductor but also a promising fluorescent probe for targeting and imaging cancer cells. The developed QDs could not only deliver more photosensitizers but also image the tumor by fluorescence. *In vivo* experiments have confirmed that, under light exposure, the growth of tumor was effectively repressed.[127]

When administered individually, both PSs and QDs have advantages and limitations. Some properties such as NIR absorption, broad absorption bands, and photostability are required for PDT. Surprisingly, the actual PSs present disadvantages when compared to the unique optical properties of QDs, such as narrow absorption band, poor photostability, and visible light absorption.[128] QDs' properties such as efficient light outputs and the capacity of tuning their absorption and emission bands gave them an exceptional photoresistance. This allows light excitation for continuous ROS production either via type I or type II processes and accordingly ensures prolonged phototherapies.[129]

Nanotechnology in PDT has created new opportunities and new modalities in the field by providing efficient nanoscale PSs delivery systems. While allowing a controlled release of drug and efficient uptake by cells, their surface area can be modified with functional groups for additional chemical/biochemical properties, which together improve the treatment efficacy and minimize side effects associated with classic PDT. Moreover, it has been demonstrated that it is conceivable to have a single nanoparticle formulation conveying a lower dose of the imaging probe and a high payload of the therapeutic drug, meaning that nanocarriers can positively modulate biodistribution and pharmacokinetic profiles of the drug formula-

https://dx.doi.org/10.1021/acs.jmedchem.0c00047
J. Med. Chem. 2020, 63, 14119−14150

tions overcoming the current drawback of most molecular theranostic agents.[130−132] To date, there has been a high number of different synthetic strategies,[133] which only consolidates the potential interest in NPs, both as drug carriers and as imaging agents. Hence, many tactics have been used to incorporate PSs into polymers, gold nanoparticles, magnetic and silica nanoparticles, as well as other various delivery carriers such as liposomes, quantum dots, and so on.[134−137] These NPs show high selectivity, high efficacy, and limited side effects.[138] Currently, there are only a few nanoparticle-based theranostic platforms tested in clinical trials, but this might change in the near future.[139,140]

2.4. Active and Passive Targeting of PSs. One of the main challenges in PDT is linked to drug delivery and targeting.[84,85] An ideal PS is delivered in therapeutic concentrations to only the target cells, while healthy cells remain untouched. This basic concept ensures minimal side effects, when keeping and efficient PDT treatment.[85,133] For more than 20 years, intensive efforts have been put in the development of targeted photodynamic therapy. The subcellular localization of the PS in mitochondria, lysosomes, endoplasmic reticulum, and plasma membrane (different organelles) plays a crucial role in the cell death mechanism involved (apoptotic, necrotic, and autophagy-associated cell death). For example, the majority of the clinically approved photosensitizers, temoporfin,[138] porfimer sodium,[141] and verteporfin,[142] already partially localize to the mitochondria,[143] which is considered as one of the most pivotal subcellular organelles in eukaryotic cells.[144] Moreover, defects or dysfunctions of mitochondria are connected to cancer progression and programmed cell death. Therefore, intensive research has been done toward the development of mitochondria-targeting therapeutics and diagnosis, which can effectively overcome tumor hypoxia, evade MDR, improve photothermal cancer treatment efficiency, and so on.[145,146] A study by Sibrian-Vazquez et al. demonstrated an increased localization of guanidinium and bisguanidinium porphyrin derivatives to the mitochondria, due to the positive charge of the compounds.[147]

One of the two main approaches to accomplish tumor-targeted PDT is by covalent conjugation of the photosensitizer with targeting biomolecules (Figure 6). These include proteins (essentially antibodies and their fragments), peptides, nucleic acids, and small molecules (biotin, folic acid, gefitinib, etc.). This is called active tumor targeting and refers to specific interactions at the molecular level between the drug/nanocarrier and target cells, usually through specific recognition and ligand−receptor interactions.[148,149]

Active targeting can be further separated in vascular targeting and tumor targeting. Both can work simultaneously to achieve better therapeutic efficacy. The first aims to eradicate tumorous blood vessels, which supply nutrients and oxygen to the tumors, by facilitating the accumulation of nanoparticles in vascular tissues.[150] Tumor targeting, on the other hand, increases the accumulation and cellular uptake of nanoparticles by selecting an appropriate receptor−ligand or antigen−antibody pairing. This is one of the most important issues in active targeting. Tumor cell markers must have two defining characteristics: (1) overexpression on the surface of tumor cells while being mostly quiescent on the surface of a normal, noncancerous cell and, (2) at the same time, should be selectively identified and bound by corresponding ligands.[150] Only in this way, they can be used as sites (i.e., the receptor)

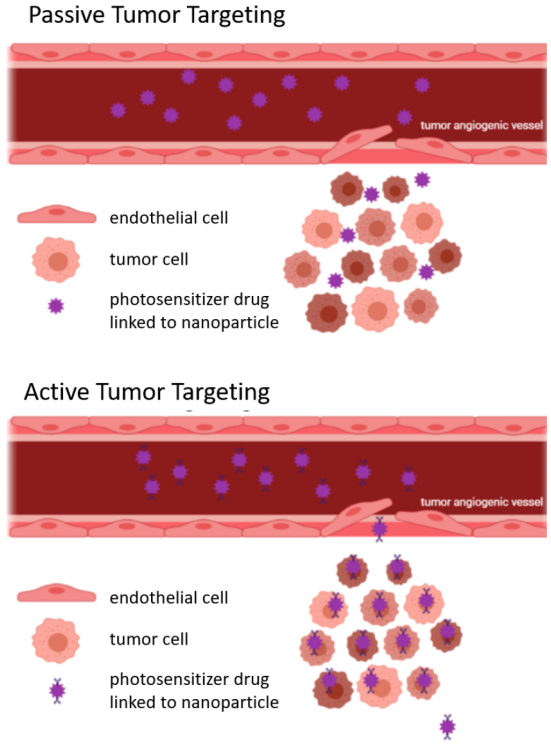

Figure 6. Two main strategies to accomplish tumor-targeted PDT.

for the targeted delivery of specific drugs (such as anticancer drugs or photosensitizers). Targeting moieties can be separated into different categories: nonprotein small molecules, receptor-specific peptides, aptamers, and a variety of proteins, such as transferrins, lectins, and antibodies.[151,152]

Several tumor cell markers have been explored for active photodynamic targeting, including transferrin receptors (TR), folic acid receptors (FR), glucose transporters, growth factor receptors, LDL receptors, integrin receptors, and insulin receptors. Other potential tumor cell markers often include glycoproteins, such as lung cancer tumor markers (i.e., CEA, Cyfra21−1, and NSE), gastrointestinal tumor markers (i.e., CEA, CA199, the CA242 group, and CA724), breast cancer markers (CA153), ovarian cancer markers (CA125), hepatocellular carcinoma markers (AFP), prostate cancer markers (PSA), and choriocarcinoma markers (HCG).[150]

Recently, for example, Kim et al. synthesized a tumor penetrating trastuzumab (Tra) derivative by chemical conjugation to chlorin e6 (Ce6).[153] Tra is a monoclonal antibody used for treating human epidermal growth factor receptor 2 (HER2) overexpressing cancers.[154] The ability of Ce6 to generate ROS and the targeting of HER2 receptors increased the internalization of the conjugated PS. In this derivative, Tra and Ce6 were linked by a maleimide-poly(ethylene glycol) spacer. A confocal microscopy study showed that the fluorescence associated with Ce6 was only detected for the HER2-positive cell lines (SK-BR-3, BT-474), thus confirming selectivity. In comparison, the Ce6-Tra conjugate compound penetrated more deeply, which can contribute to better destruction of dense tumor tissue. In this system, visualization and PDT treatment were combined.[155]

When it comes to conjugated biomolecules, several types have been investigated, including receptor-specific peptides, transferrins, antibodies, oligonucleotide aptamers, and nonprotein small molecules, which include vitamins (e.g., folic

https://dx.doi.org/10.1021/acs.jmedchem.0c00047
J. Med. Chem. 2020, 63, 14119−14150

acid, vitamin D, vitamin E, and vitamin B), retinoic acid, steroids, and other hormones. Some very effective binders include those interacting preferentially to low-density lipoprotein (LDL), suggesting that upregulated LDL receptors found on tumor cells are important.[156] Consequently, studies dealing with PSs covalently linked to molecules with affinity for neoplasia or to receptors expressed on specific tumors have been published.[157] In particular, those involving small molecular-based targeting drugs have received a great deal of attention in the design of targeted photosensitizers for cancer therapeutics.[158]

Conjugation of PSs to tumor-specific biomolecules such as monoclonal antibodies, epidermal growth factor, and small molecules (e.g., short peptides or peptidomimetics) provides another promising strategy to increase selectivity. Incorporation of functional groups to target specific receptors associated with cancer is, indeed, a common strategy to increase the efficiency of PSs (Figure 7). As mentioned before, an overexpressed receptor that has already been explored for the targeting of cancer cells is the folate receptor α.[159]

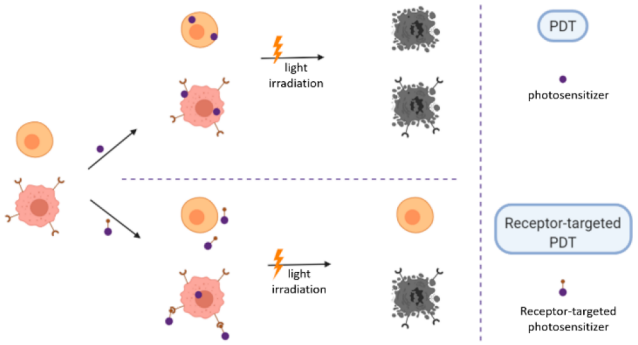

Figure 7. Receptor-targeted approach in PDT.

Another example of this kind of functionalization for targeting can be found in the work of Soukos et al., where a monoclonal antibody was conjugated to Ce6 as a tumor-specific targeting agent for imaging and therapy in a hamster cheek pouch carcinogenesis model.[9] This "photoimmunoconjugate" derivative (PIC), as it was defined, increases the specific delivery of the PS. In this study, EGFR, which is overexpressed in several human tumors, was the target. The anti-EGFR monoclonal antibody (C225) was selected and attached to Ce6. Then, the PIC was used as a diagnostic platform and monitoring tool to determine the therapeutic response. The same antibody (C225) was also conjugated to the benzoporphyrin derivative (BPD, verteporfin), thus providing another PIC derivative.[160]

Besides antibody-based PICs, small molecules and peptides can also be introduced to PSs. For example, Choi et al. introduced a membrane-penetrating arginine oligopeptide (R7) on 5-[4-carboxyphenyl]-10,15,20-triphenyl-2,3-dihydroxychlorin (TPC), in view to enhance cellular uptakes.[161] For similar reasons, new kinds of PSs with high water solubility, as well as with one or more functional groups for conjugation with biological agents, have been prepared by Li et al.[122] They have reported on the synthesis and characterization of asymmetrically substituted highly water-soluble phthalocyanines (Pc), with two different types of peripheral substituents: one reactive group for conjugation and the others for water solubility (Figure 8).

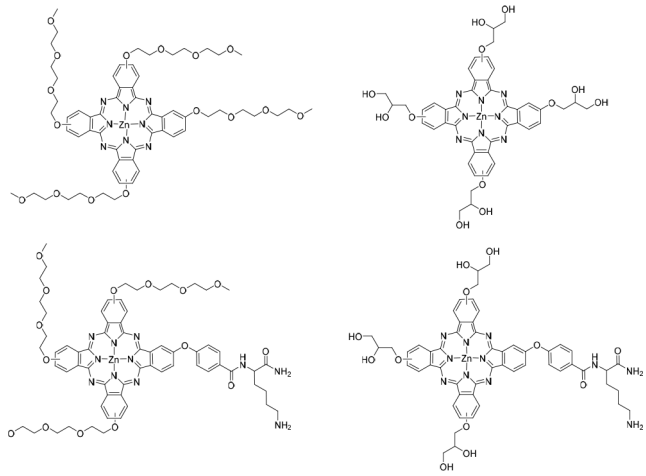

Figure 8. Structures of conjugated PSs.

Passive targeting is occasionally interpreted as physical targeting, which exploits the physiological and morphological differences between healthy and tumor tissues to achieve tumor selectivity and preferential accumulation of PSs. As mentioned previously, nanocarriers provide the potential for improvement of PS delivery to the target area to maximize PDT efficacy. Due to the uncontrolled proliferation of tumor cells, solid tumors have an abnormal tissue composition and architecture, which limit the uptake and distribution of drugs.[162] While rapid vascularization promotes fast-growing tumor sites, inflamed tissues embrace a leaky and defective architecture, thus leading to the enhanced permeability and retention (EPR) effect.[163,164] In addition, there is an accumulation of drugs due to inefficient lymphatic drainage, which make it harder for tumor sites to clear nanoparticles.[164]

Hyperproliferative tumor cells have a high metabolic rate and keep growing despite limited oxygen and nutrients. Therefore, in order to maintain its activity, tumor cells employ an enhanced level of anaerobic glycolysis, which produces a large quantity of lactic acid, resulting in intratumoral hypoxia and a lower pH environment.[165] The accumulation of PSs in tumors is known to be enhanced as its hydrophobicity increases. This is due to the fact that hydrophilic molecules are retained in the blood circulation system, while hydrophobic molecules tend to extravasate and accumulate in tumor tissues. PSs, however, generally have large π-conjugation domains for high quantum yields and effective energy absorption, which enable most classical PSs to easily aggregate in an aqueous environment. For this reason, these PSs are not suitable for intravenous administration, and further functionalization is needed, usually through the conjugation with a nanocarrier.

Since accumulation at the tumor involves a passive process requiring a long circulation half-life, the targeted delivery of PS-loaded nanocarriers is largely dependent on the biophysical and morphological properties of the nanocarrier. These properties include the material composition, morphology, hydrodynamic size, and surface charge.[166] The hydrodynamic size affects NP concentrations in the vessel, NP permeability, and clearance from the body.[167,168]

Another important factor concerning passive targeting is the surface properties. *In vivo* experiments have shown that hydrophobicity and surface charge affect the fate of nanoparticles and determines their behavior with plasma proteins, cells of the immune system, and nontargeted cells.[169]

https://dx.doi.org/10.1021/acs.jmedchem.0c00047
J. Med. Chem. 2020, 63, 14119−14150

Table 3. Commonly Used Imaging Agents

modality	agent	application
MRI	gadolinium	highlights areas of tumor or inflammation
PET/SPECT	[^{64}Cu]Cu-ATSM	identify hypoxic tissue
	[^{18}F]FDG	radioactive sugar molecule (-[^{18}F]-fluorodeoxyglucose) that shows the metabolic activity of tissues
	[^{18}F]-fluoride	imaging of new bone formation
	[^{18}F]FLT	3′-deoxy-3′-[^{18}F]-fluorothymidine allows to detect growth in the primary tumor; detect tumor response to treatment
	[^{18}F]FMISO	[^{18}F]-fluoromisonidazole is used to identify hypoxia
	[^{68}Ga]Ga(III)	attaches to areas of inflammation, such as infection; attaches to areas of rapid cell division, such as cancer.
	technetium-99m	used to radiolabel many different common radiopharmaceuticals; most used in bone and heart scans
	thallium-201	examine heart blood flow
X-ray and CT imaging	barium	contrast agent used to enhance images of the abdomen and pelvis
	gastrografin	same as barium but contains iodine instead
	iodine contrast agents	highlight blood vessels as well as the tissues of various organs; can be ionic or nonionic (less side effects)

3. IMAGING AND THERAPY TECHNIQUES IN PDT

In the medical field, approval to run clinical trials is often a limiting step, and this is also true for the implementation of molecular imaging biomarkers.[170] However, it is undeniable that molecular imaging, if the modality is chosen correctly, is more efficient in a timely and resource manner when compared to other practices such as tissue dissection and histological analysis.[171] From all of the different imaging techniques used for PDT, optical imaging is more broadly studied due to the fluorescence properties of the PSs. For this reason, we cannot exclude from this review where we will also focus on nuclear medical imaging (PET/SPECT) due to the great potentials the authors believe it holds, even though other techniques like MRI[172−175] and ultrasound[176] have also been developed and extensively studied on PDT over the past decade. A summary of the most used imaging agents currently in medicine can be found in Table 3.

In addition, PSs are fundamentally theranostic agents when used for PDT treatments, since such compounds absorb and emit light upon activation. Hence, the fluorescence property is used for imaging to monitor tumor uptake. Moreover, the PS fluorescence holds promise for fluorescence-guided resection (FGR) treatment, which is approved in Europe for both brain[177] and bladder cancers,[178] Another advantage of using PSs for FGR is that it allows a posteriori follow-up of treatments.[179] The specificity of PDT presents itself as the same molecule that may do both, the therapeutic and imaging roles.

3.1. Optical Imaging. A pivotal role has already been played by optical imaging in PDT dosimetry.[13] The presence of PSs at the targeted location before PDT treatment was used to quantitatively monitor the fluctuation of fluorescence before and after treatment, thus showing a correlation between clinical response and fluorescence.[180] This different outcome was associated with photobleaching during the production of reactive oxygen species. Zhou et al. have also observed that the response to treatment is less influenced when the light dose is adjusted to PS uptake.[181] Such studies confirm the significance of fluorescence imaging in PDT dosimetry.[179]

The fluorescence property of PSs can also serve for imaging as most PSs upon activation emit light in the visible region. Moreover, as PSs have a tendency to accumulate better in neoplastic tissues, this approach, frequently named photodynamic diagnosis (PDD), is very much appropriated for selective visualization of tumors and to outline the frontiers between cancerous and healthy tissues. The ability to precisely define tumor boundaries is a crucial step during an optimization process of a surgical intervention. At the moment, this fluorescence imaging technique constitutes the majority of the imaging applications. Ensuring a cancer-free margin around cancerous tissues is a crucial factor in avoiding recurrence. Resection of excess healthy tissue, on the other hand, can have serious and severe implications for the patient. This is one of the reasons why combining imaging and therapy is so important, and why over the past years, there has been an increasing interest in the development of innovative theranostic agents.

Therefore, the preparation of PSs with high fluorescence intensity and excellent singlet oxygen ($^1O_2$) quantum yields (QYs) is particularly needed for cancer diagnosis and PDT. In this regard, diketopyrrolopyrrole (DPP) and boron dipyrromethene (BODIPY) are two kinds of a building block with great potential for PDT. Recently, Zou et al. have linked DPP and BODIPY through a series of donor−acceptor−donor (D−A−D) linkers, thus forming a DPPBDPI structured organic photosensitizer (Figure 9).[182] The results indicate that the synergistic effect, resulting from the combination of the two photosensitizers, can simultaneously increase the fluorescence intensity by 5.0% and the $^1O_2$ QY by up to 80%.

Upon nanoprecipitation, the DPPBDPI can form uniform nanoparticles (NPs), which display not only high phototoxicity but also insignificant dark toxicity toward HeLa cells. *In vivo* fluorescence imaging shows that the DPPBDPI-NPs target tumors rapidly and inhibit tumor growth upon PDT treatment, even at reduced doses (0.5 mg kg^{-1}). The imaging and photodynamic behavior of DPPBDPI suggest a synergistic effect that can provide a novel theranostic platform for cancer diagnosis and PDT.

The high sensitivity of the method, the harmless nature of the agent, and the low cost of the procedure, makes optical imaging and detection an ideal imaging modality.[5] Among several characteristics, a potent PDD needs to have an intense absorption band in the red or the near-infrared (NIR) spectral region.[183] The optimal wavelength for PDT treatment must be a good compromise between activation and tissue penetration with low dispersion. Moreover, it should take into consideration the characteristics of the damaged tissue (location, lesion size, and accessibility). Because of these, and by utilizing near-infrared wavelengths (650−900 nm), which combine deep tissue with enough energy to excite the photosensitizer, fluorescence has ended up being an excellent asset for disease diagnostics and treatment.[184] It is easy to understand now how

https://dx.doi.org/10.1021/acs.jmedchem.0c00047
J. Med. Chem. 2020, 63, 14119−14150

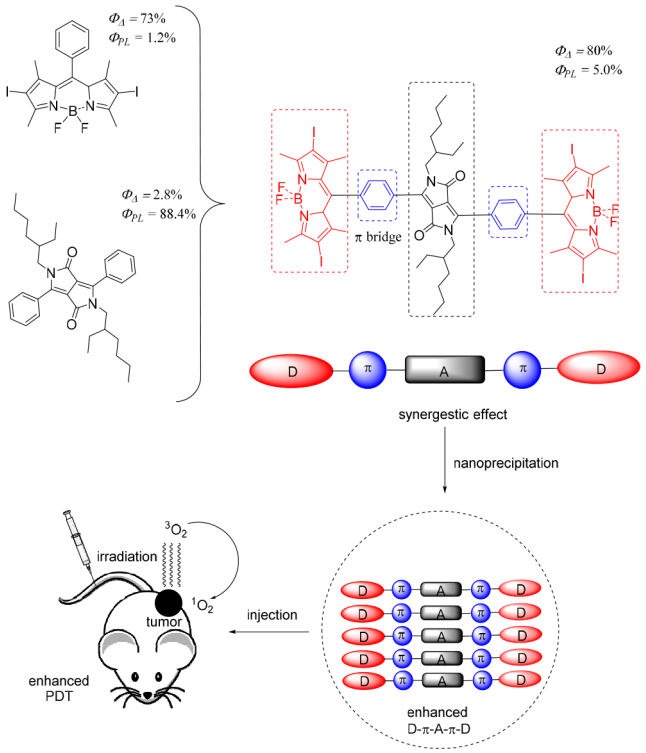

Figure 9. Illustration of a theranostic agent for PDT with a D−A−D structure with enhanced $^1O_2$, QYs, and fluorescence.

PSs are not limited exclusively to the therapeutic generation of singlet oxygen species, since numerous photosensitizers are additionally excellent fluorophores valuable for imaging, thus helping to characterize and to modify parameters amid PDT treatments. The tetrapyrrolic skeleton remains the most prominent structure for the development of photosensitizers. Tetrapyrrolic units show strong absorption in the visible region, and they possess an excellent photosensitizing ability to produce reactive oxygen species (ROS). In addition, the photophysical parameters of tetrapyrrolic units can be tuned by the insertion of metal ions or halogen atoms, like chlorine and fluorine, which induce macrocycle changes that modify the balance between fluorescence and intersystem crossing.[185−187]

The most fascinating and valuable imaging probes are photosensitizers that are nonphototoxic outside their destination and are only dynamic within the presence of a targeting molecule whereupon fluorescence and singlet oxygen production happen. Activatable photosensitizers (aPS) are perfect imaging probes since they share comparative activation mechanisms to fluorophores, and they can distinguish cancer cells from ordinary cells.[74] A few authors have researched into what they call "killer beacons" comprised of up to four modules: a fluorescent probe, a quencher, a linker, and a delivery vehicle, whose properties can be adjusted, modified, or joined to fill diverse needs (Figure 10). These beacons are based on a unique fluorescent photosensitizer linked to other functional groups. The dye should theoretically be hushed in the absence of the target, and its fluorescence re-established simply after the target is reached. To accomplish that, the PS must be linked to a quenching unit (Q) through a reasonable linker, which should keep the PS and quencher close enough to ensure fluorescence resonance energy transfer (FRET).

In another example of activatable photosensitizers, Stefflova et al. have designed and synthesized a folate receptor-targeted,

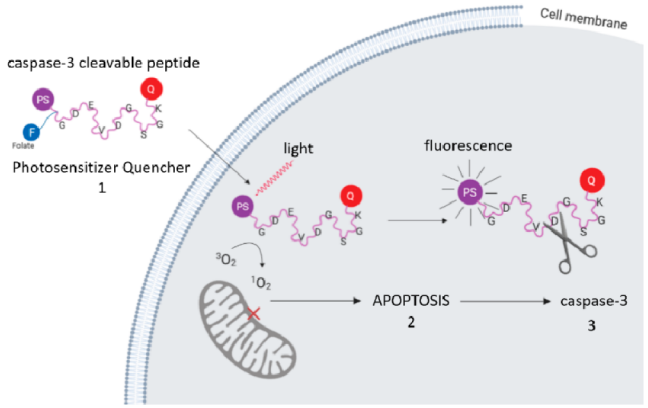

Figure 10. Principles behind a beacon system for post-PDT imaging of apoptosis.[184] The system is composed of four parts: a PS (violet dot), a folate delivery entity (blue dot), a caspase-3 cleavable linker (KGDEVDGSGK), and a quencher (red dot).

hydrophilic, and pharmaco-modulated PDT agent (Figure 11).[184] This molecule, obtained after three synthetic steps

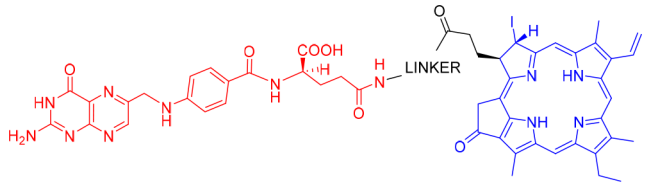

Figure 11. Pyro-GDEVDGSGK-Folate comprising three components: pyropheophorbide-a (imaging and therapeutic agent), a peptide sequence (linker), and folate (delivery vehicle).

from Spirulina algae, selectively detects and destroys cancer cells, while avoiding healthy tissues.[188] Pyropheophorbide-a (Pyro) is a fluorescent photosensitizer that can also be used for NIR imaging and PDT (over 50% quantum yield). The Photochlor derivative is in phase I/II of clinical trials. In this compound, the folate moiety serves as a guiding molecule to bring the photosensitizer to folate receptor (FR)-overexpressing cancer cells. The PS and guiding folate are linked by a short GDEVDGSGK peptide. This peptidic sequence is stable and water-soluble, thus preventing cleavage prior to reaching the target. Moreover, the length of the sequence ensures that no steric hindrance takes place. Lastly, it serves as a pharmaco-modulator for efficient delivery and reduced toxicity, and the system is easily modified to introduce other peptide sequences for different targeting.

At last, photosensitizers' efficiency can be upgraded by linking them with different particles that can deliver the entire cargo in malignant cells either nonspecifically or specifically, by focusing on "disease fingerprints". For instance, PSs linked to oil dispersions, liposomes, or hydrophilic polymers (PEG) can be internalized to disease cells through passive diffusion or phagocytosis. Such carriers help to solubilize the PS in biological media (for intravenous infusion) and, furthermore, to increase uptake and retention by tumors.[184] The bifunctional chelator approach presents itself as one of the most interesting and viable solutions for a theranostic goal, using porphyrins as the perfect building blocks since they offer both a metal isotope chelator and a targeting vector.

3.2. PET/SPECT Imaging. Two main directions can be pursued for the radiolabeling of dyes, including photo-

https://dx.doi.org/10.1021/acs.jmedchem.0c00047
J. Med. Chem. 2020, 63, 14119−14150

sensitizers: the first one focuses on hydrogen-3 and carbon-14 marking for biodistribution studies and tissue autoradiography, while the second focuses on labeling these molecules with a short half-life (the time is needed for a radioisotope to decay to its half) γ- or positron-emitting radionuclides for tumor imaging and nonintrusive quantitation of photosensitizers.[189] Nuclear medical imaging (NMI) strategies like positron emission tomography (PET) and single-photon emission computed tomography (SPECT) are interesting complementary techniques, as they provide a further tissue penetration and decreased scattering of the produced signal.

In 1951, the first radiolabeled porphyrin system was prepared, introducing copper-64 in the core of protoporphyrin IX (Scheme 1). Soon after, hydrogen-3, carbon-14, palladium-

Scheme 1. Synthesis of [^{64}Cu]CuPPIX (Protoporphyrin IX)[141]

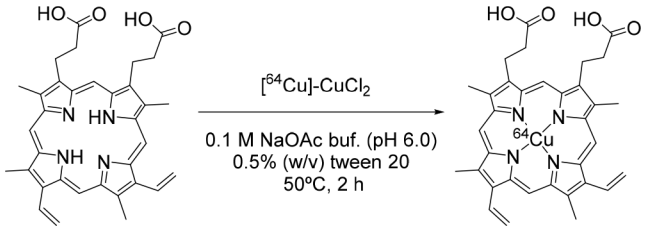

109, sulfur-35, zinc-65, cobalt-57, and iodine-125 were likewise investigated. However, they are unacceptable for *in vivo* imaging as a result of their long half-lives or powerless gamma photon energy.[190] Currently, iodine-124, copper-64, and zinc-62 are the most promising radionuclides for PET imaging in PDT.[114,190−192]

In the 1980s, it was demonstrated that the *in vivo* biodistribution and pharmacokinetics of porphyrins are not affected by chelation with copper-64 in light of the fact that the copper molecule fits into the focal point of the tetrapyrrole ring without modifying the side chains that dictate the *in vivo* conduct. This made it conceivable to exploit porphyrins' inborn capacity to chelate metals to fuse the radionuclide, taking into account the direct radiolabeling of photosensitizers with copper-64 without adjusting their conduct *in vivo*, which ultimately yields to exceptionally stable radiolabeled photonic nanoparticles.[193] Subsequently, the radiolabeling of metal complexes of porphyrins is the most encouraging strategy, the only issue being whether the metal has a radioactive species suitable for quantitative *in vivo* scanning and whether this can be exchanged with the nonradioactive species.

For nonmetallo-photosensitizers, the inclusion of the radioactive metal may change the biodistribution so that, for each metal-photosensitizer, combination biodistribution tests must be performed, normally with hydrogen-3 or carbon-14 labeling or quantitative fluorometry of excited tissues as a standard. In general, just as standard porphyrins, radiolabeled porphyrins accumulate in the tumor without changing the principle attributes of the host porphyrin molecules. Gallium-68[191] and copper-64[192,194,195] are promptly accessible and inexpensive metal isotopes, both appropriate for human PET imaging that may very well turn into the prime isotopes for radiolabeling porphyrins since complexation chemistry with the porphyrin core is quite straightforward, especially when it comes to copper-64.

While copper-64 marking has shown that, at least in animal tumor models, the fuse of this metal particle into the porphyrin ring does not significantly alter the uptake kinetics in tumors and healthy tissues. Marked differences between gallium-67 and technetium-99-labeled sulfonated phthalocyanines have shown that the metal ion modifies the dye conformation and thus may influence the molecular aggregation.[189,196] This leads to the conclusion that it is necessary to proceed with biodistribution investigations of radiolabeled analogues of photosensitizers at the beginning of *in vivo* studies.

On the other hand, the bifunctional chelator approach enables guided delivery of radioisotopes to selected cells by a kinetically and thermodynamically stable chelator conjugated to cancer-specific biomolecules such as antibodies, antibody fragments, peptides, or proteins. These systems exploit the overexpression of receptors and proteins on tumor cells. Some investigators accomplish this functionalization through the introduction of glucose and galactose moieties on the photosensitizer, thus culminating in an increased activity in tumor uptake.[190]

Since fluorine-18 is the most common radioisotope used in clinics, further research has been done regarding its potentials linkage to PSs. A dual-modality agent named [^{18}F]-PET/fluorescence, in which both the positron-emitting and fluorescence properties are combined, has been developed by Li et al.[197] They used a BF_2 unit, typically present in BODIPY dies, which can provide a [^{18}F]-radiofluorination site. Through PET imaging, they observed 2 h post-injection, an accumulation of the radiolabeled PS in the liver and kidneys, as well as in the gall bladder. Considering the lipophilicity and electronic property of the radiolabeled system, an accumulation in these organs is not surprising, as the BF_2 group possesses no targeting value.

The utilization of the fluorine-18 isotope in studies including antibodies and in photodynamic treatment (PDT) is, however, limited by its short half-life (110 min). In this regard, iodine-124 is considered a better choice for longitudinal imaging studies utilizing preclinical PET due to its half-life of 4.2 days. The labeling strategy for the iodine-124 isotope is well recognized, and it has been used in the labeling of an assortment of biologically active molecules.[198]

Developed by Roswell Park's group, the [^{124}I]-1′-3-(*m*-iodobenzylox)ethylpyropheophorbide-*a* derived from chlorophyll-*a* has demonstrated *in vivo* PET-imaging capacity.[199] As a nonradioactive analogue of chlorophyll-*a*, it shows PDT efficiency, and therefore, it is an interesting candidate for PET imaging. With great pharmacokinetic and pharmacodynamics profiles, it can be utilized for imaging (PET/fluorescence) and PDT. Curiously, when comparing to nonradioactive compounds, the postloading of the iodinated analogues in polyacrylamide-based (PAA) nanoparticles (NPs) had a striking effect in the biodistribution. In mice, the imaging and treatment agents are better taken up by tumors, with decreased uptake in different organs, particularly in the spleen (Figure 12).

Focusing on another approach, some authors have detailed the labeling of phthalocyanines (Pc) with PET isotopes for both tumor imaging and drug development studies. Phthalocyanines, which are structurally like porphyrins, are powerful PSs in their own right because of their high singlet oxygen quantum yield and high activation wavelength (600−850 nm). Van Lier et al. have demonstrated that the level of Pc sulfonation strongly affects the level of complex aggregation

https://dx.doi.org/10.1021/acs.jmedchem.0c00047
J. Med. Chem. 2020, 63, 14119−14150

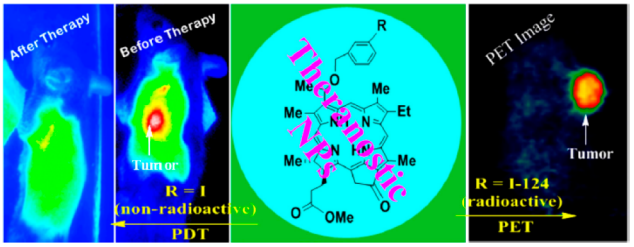

Figure 12. Multifunctional nanoplatform for cancer imaging and therapy with radiolabeled (^{124}I) chlorophyll-*a* (right) and the nonradioactive analogue (left), showing the accumulation in the tumor.[3]

and biodistribution, still conserving photosensitivity.[200] Consequently, they prepared a series of phthalocyanines with increasing sulfonate groups and radiolabeled each of them with copper-64 (Scheme 2). The tri- and tetra-sulfonated water-

Scheme 2. Synthesis of ^{64}Cu-Labeled Phthalocyanines[200]

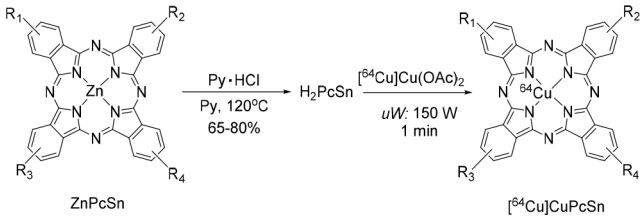

soluble phthalocyanines have shown rapid renal clearance on the EMT-6 tumor model, being both under the detection limits. Despite having a comparable excretion pathway, the disulfonated analogue showed an increased uptake in tumors, thus providing sufficient contrast for PET imaging.[199]

With imaging and treatment in mind, Liu and MacDonald have looked into the synthesis and evaluation of radiolabeled porphysomes. These nanoparticle platforms have been used as drug delivery vehicles.[98] As opposed to standard NPs, porphysomes do not require functionalization of the nanoparticle surface with metal radioisotope chelators.[98] Benzoporphyrin derivative monoacid (BPD-MA) was demonstrated to be a potent photosensitizer both *in vitro* and *in vivo*, as well as in clinical trials.[201] However, as many porphyrins exhibit a high level of lipophilicity, including BPD-MA, they have a tendency to aggregate in aqueous solution, therefore, limiting its bioavailability.[37] To circumvent this problem, porphyrins have been incorporated into liposomes for improved delivery, solubility, and efficacy.

Verteporfin, for example, has been utilized in clinical preliminaries and endorsed for clinical use, showing how liposomes have been considered as good delivery frameworks and as a feasible choice for the improvement of hydrophobic PSs.[202] A few authors extended the capacity of porphysomes by investigating the inherent capacity of the porphyrin−lipid conjugates to form steady, high-affinity complexes with copper-64, which has good attributes for nanoparticle tracking through positron emission tomography (PET).

Shi et al. prepared [^{64}Cu]-Cu(II)-labeled pyropheophorbide-α (a near-infrared fluorescent porphyrin) derivatives coupled to folic acid for improved folate receptor interceded take-up in the tumor, opting to utilize the porphyrin element in a chelating role.[192] The porphysomes, composed of lipid functionalized porphyrin units, have been labeled specifically with copper-64 with a radiochemical load of 98%. The [^{64}Cu]Cu(II)-labeled porphyrin units contribute to <5% of the porphysome molecular weight, unaffecting the nanoparticle size and photonic properties. The tumor uptake of the [^{64}Cu]Cu(II)-porphysomes was evaluated at 24 h post-injection by PET/CT (Figure 13A) and fluorescence imaging (Figure 13B,C).

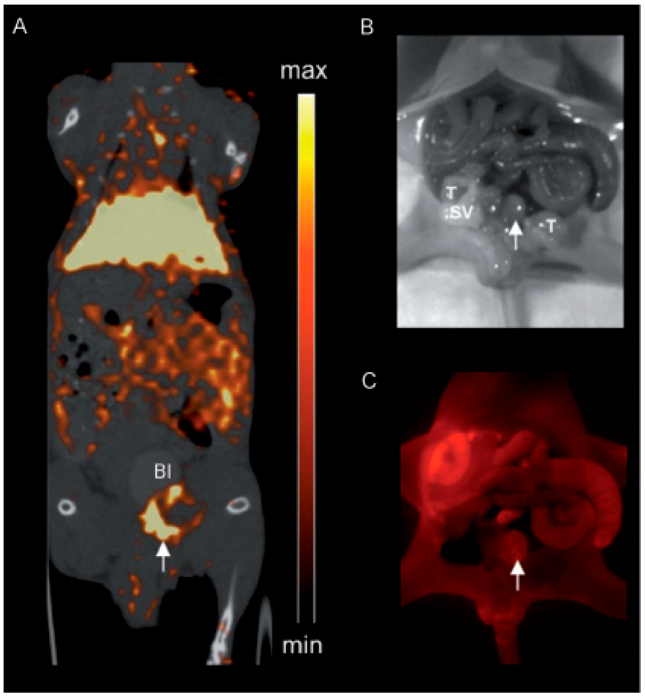

Figure 13. *In vivo* multimodal imaging of [^{64}Cu]-Cu(II)-porphysomes in an orthotropic prostate cancer model.[192]

3.3. Combination of PET/SPECT and Optical Imaging toward Multimodal Theranostic Agents. The different techniques used for imaging cancers are stand-alone techniques, and it becomes imperative to have multimodal probes, in order to progress in cancer treatments.[203−205] At the moment, our current imaging modalities are limited in what they can perform individually,[206] but by combining different techniques, new achievements are expected. In principle, multimodal imaging agents can combine magnetic resonance imaging (MRI),[175,207] fluorescence imaging,[207−209] computed tomography (CT),[175,210] positron emission tomography (PET),[208,210] and single-photon emission computed tomography (SPECT).[175,203]

Recently, the feasibility of using multimodal agents has been verified in multiple *in vitro* and *in vivo* models.[211,212] A series of multimodal probes, with magnetic elements, such as iron oxide,[213,214] or Gd(III)-based chelates,[215,216] were coupled to PS. These studies demonstrate a remarkable potential for image-guided cancer therapy. However, such hybrid materials have limited applications since they are difficult to synthesize and produce in large quantities.[210] Therefore, the extended clinical use of theranostic agents will require affordable and easy-to-make derivatives. Not all multimodality combinations are useful, but certain imaging combinations are more attractive because some possess synergistic properties, like the combination of optical fluorescence imaging and PET (OFI/PET).

https://dx.doi.org/10.1021/acs.jmedchem.0c00047
J. Med. Chem. 2020, 63, 14119−14150

As previously discussed, fluorescence is an inexpensive modality. It is easy to operate; it possesses multiplexing capacity and high spatial resolution at histologic or superficial levels. On the other hand, PET shows quantitative, noninvasive, and extremely sensitive *in vivo* imaging without depth restraint.[217,218] The molar sensitivity of OFI and PET are relatively equal and both excellent; therefore, they can be used at nontoxic tracer quantities.[217] Fluorescence contrast imaging shows a better spatial resolution than PET at the histologic and superficial levels.[219] Moreover, fluorescence probes are stable, unlike PET probes, which rapidly decay. PET, on the other hand, has a superior resolution to fluorescence imaging through deep tissues. Therefore, the OFI/PET dual modality is a promising combination in clinical preoperative PET imaging and intraoperative optical imaging-guided surgery or PDT. Among dual-modality OFI/PET probes, those containing NIR dye and especially those based on cyanine-based NIR organic dyes (Figure 14), are of particular interest due to optimal tissue penetration.[220]

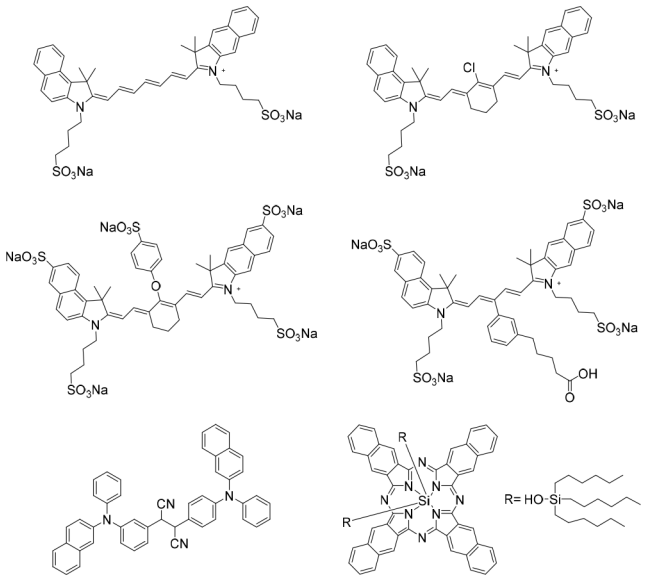

Figure 14. Structures of Cyanine-Based NIR dyes.

Not only NIR dyes should be considered, those emitting in the visible region are also suitable, as fluorescence imaging can be partially compensated by PET. Similarly, dual-modality OFI/SPECT combines SPECT's depth penetration, high sensitivity, and quantitative signals with the already mentioned advantages of OFI. The design remains very similar; however, γ-emitting radioisotopes such as technetium-99m and indium-111 are used. Indium-111 is the most common SPECT radionucleus, and it is often coupled to cyanine-based NIR fluorescent groups. Moreover, to increase the response for cancerous tissues, targeting groups are generally employed.

In view of generating a "trifunctional agent" for double-imaging (PET and fluorescence) and PDT treatment, Pandey et al. have modified the tumor-avid porphyrin (pyropheophorbide a), and reported the synthesis of a ^{124}I-labeled PS with high (>95%) radioactive specificity.[199] The half-lifetime of the nuclide allows us to perform the synthesis of the labeled PS and to accumulate in the target tissues after injection. They were the first to demonstrate that selective accumulation of porphyrin-based trifunctional agents to tumors can be achieved, thus confirming that using a single agent for imaging (PET and optical) and therapy is a promising avenue. In contrast to other studies, the different techniques are noninvasive, and the use of a single agent limits inconsistencies in the pharmacokinetic and pharmacodynamic patterns of the compound at all stages.

Another example of multiple-modality imaging with a known photosensitizer as the fluorescence probe was published by Cheng and co-workers.[221] A PEG-Ce6 nanomicelle was successfully prepared and used for OFI/PET dual-modal image-guided photodynamic cancer therapy. The presence of chlorin e6 molecules allows the PEG-Ce6 nanomicelles to work as a chelating agent for [^{64}Cu]Cu^{2+}. After internalization, PDT was carried out *in vivo* at a low irradiation rate, showing an excellent therapeutic effect on tumors. They were able to elaborate a simple approach to synthesize biocompatible multifunctional PEG-Ce6-based theranostic agents with the right properties for multimodality imaging-guided tumor therapy. The size and shape of nanoparticles and nanomicelles ensure high tumor uptake *in vivo* and partial renal clearance. These results might improve future applications and end up in clinical trials for these theranostic agents. In addition, these

Table 4. Representative Nanoparticles and their Biomedical Applications[90,291]

type of nanoparticle	possible surface modifications	imaging modality applicable	possible therapeutic strategies	synthetic protocol
quantum dots	lipids, polymer, targeting ligands or biomolecules	optical	PDT	colloidal synthesis, self-assembly, viral assembly
dendrimer	charge, polymer, targeting ligands, or biomolecules	MRI, optical	drug and gene delivery	organic chemistry techniques
liposome	charge, polymer, targeting ligands or biomolecules, viral protein coating	MRI, optical, radionuclide imaging	drug, gene and protein delivery, PDT	emulsion, polymerization
gold nanoparticle	lipids, polymeric shell, targeting ligands, or biomolecules	CT, optical	drug delivery, PTT	biological reduction, colloidal synthesis, vapor precipitation
carbon nanotube	polymeric shell, targeting ligands or biomolecules	MRI, optical, radionuclide imaging	drug delivery, PTT	arc discharge, laser ablation, vapor precipitation
mircrobubble	polymeric shell, targeting ligands or biomolecules	ultrasound	drug, gene and protein delivery	emulsion, layer-by-layer fabrication, polymerization
iron oxide	charge, dextran, lipids, polymer, targeting ligands or biomolecules	MRI	siRNA delivery, PT	coprecipitation, decomposition, microemulsion, sol−gel, thermal
micelle	charge, polymer, targeting ligands or biomolecules	MRI, optical, radionuclide imaging	drug and gene delivery	microemulsion
silica nanoparticle	charge, polymer, targeting ligands or biomolecules	MRI, optical	drug and gene delivery	chemical polymerization, microemulsion

https://dx.doi.org/10.1021/acs.jmedchem.0c00047
J. Med. Chem. 2020, 63, 14119−14150

PEG-Ce6 nanomicelles can chelate other metals (Mn^{2+} or Gd^{3+}) for additional imaging modalities, thus providing high-resolution imaging for anatomical information. Combining PET/OFI/MRI can be a winning combination since it can gather crucial information. The high sensitivity of the imaging techniques and excellent resolution of the images should help physicians to design better therapeutic approaches for cancer treatments.[221] In this regard, Li et al. acknowledged that nanotechnology is an ideal platform to combine different imaging agents into hybrid materials. Moreover, they can have a tremendous impact on tumor diagnoses.[222] Representative nanoparticles for their use as multimodal agents and their biomedical applications can be found in Table 4.

Nanoparticles are behaving differently from single molecules or bulk particles. They have properties of their own, and this can be nicely exploited in medicine. For example, nanoparticles tend to accumulate and internalize selectively to cells, being transported across membranes via transcytosis.[223] Furthermore, structural modifications of nanoparticles can be performed chemically, thus modifying not only their properties but also their biocompatibility.[224] However, to develop nanoparticles with multimodal imaging or therapeutic capacity, multiple factors need to be considered, such as toxicity, interaction with metabolites, biocompatibility, and biodegradability.[224]

Among multimodal techniques associated with nanoparticles, those involving SPECT/CT are the most common. For example, a liposomal nanocarrier incorporating technetium-99 has been developed for SPECT/CT imaging.[225] The imaging probe was used to visualize the amount of drug delivered to tumors. In addition, the therapeutic effects of this probe were determined using different tools. These probes can gather multiple information from different imaging modalities without having to inject other substances.

Overall, multimodal imaging agents should have a low toxicity and/or high biodegradability. They should have a high selectivity to target the disease. These characteristics would allow us to evaluate the efficacy of specific targeting and to determine the toxicity caused by the off-target accumulation of the multimodal imaging agent. On the other hand, there is a need to develop more efficient nanocarriers for controlling the external release of nanoparticles. Only then can this approach start to be considered for effective clinical translation and accurate diagnosis.

4. IMAGING HYPOXIA IN PDT

One of the major drawbacks in PDT is the increased oxygen needs. As mentioned earlier, oxygen consumption is predominant through the active mechanism of PDT, resulting in aggravate further the hypoxic conditions in tumors. It is well-known nowadays that tumor hypoxia can be linked to tumor aggressiveness, metastatic spread, poor tumor control, increased level of recurrence, and unfortunate therapeutic outcomes, mainly due to radiation and chemotherapy resistance.[10,226−230] Taking into account the variability of O_2 concentrations within tumors and even tumor regions, it is quite undeniable that O_2 concentrations will have an impact on PDT treatments.[231] Regrettably, solid tumors are known to show acute hypoxia due to a series of abnormal physiological variations in the tumor microenvironment including uncontrollable tumor cell proliferation, an irregular vascular system, and a deteriorating microenvironment.[232,233] The degree of hypoxia is, therefore, directly linked to cancer treatment effectiveness.[234,235]

An increasing interest in developing methods to measure tumor hypoxia has, therefore, been raised. These techniques can either be invasive (e.g., polarographic O_2 sensor) or noninvasive (e.g., molecular imaging), and they both aim at measuring the oxygen level within the tumors. Medicinal imaging (optical, MRI, PET, and SPECT) has become a useful tool to characterize the variability and magnitude of hypoxia within tumors and to help the physicians' decisions.[236] Optical imaging techniques assess the optical absorption, scattering, and fluorescence in tissues.[237] MRI techniques, based on contrast agents (endogenous or exogenous), embrace techniques such as electron paramagnetic resonance (EPR),[238] dynamic contrast MRI (DCE-MRI), magnetic resonance spectroscopy (MRS),[239] and blood oxygen-dependent level (BOLD) imaging.[240,241] However, undoubtedly, one of the most extensively investigated imaging modality toward hypoxia imaging is PET due to the various advantages discussed in the previous section and to the development of hypoxia-specific radiolabeled agents.[242−244] Since the very early stages of hypoxia research, it has been revealed that several nitroimidazoles and thiosemicarbasides can directly and reproducibly identify the absence of oxygen.[245]

In 1981, Chapman et al. pioneered the use of nitroimidazole derivatives and molecular imaging techniques to evaluate the degree of hypoxia in tumors.[237] These compounds are particularly interesting because the oxygen-binding affinity to nitroimidazoles is directly linked to cell retention and O_2 concentration (Scheme 3).[246] Following this study, hypoxia-specific agents targeting intracellular macromolecules have made possible the widespread use of PET for imaging hypoxia.

Nowadays, copper-based complexes incorporating bis(thiosemicarbazone) ligands have become the most effective class of compounds for imaging diagnostics of hypoxic tumors. The pharmacological activity and theranostic properties of these complexes have allowed the determination of the origin of hypoxia and how it is involved in tumors and heart diseases. The mechanisms by which these copper complexes (CuATSM) are hypoxia selective seem to be associated with metal coordination. The hypoxia selectivity involves intricate intracellular reduction−oxidation processes, leading to Cu(I) species, which are free from the chelated complex via redox reactions (Figure 15). In hypoxic environments, Cu(II) species are easily reduced to Cu(I) derivatives, and upon decomplexation, the Cu(I) can interact with biomolecules.[247] This phenomenon is essential for delivering free copper to cells. However, it does not guarantee a selective uptake.[248] Therefore, to increase selectivity, bis(thiosemicarbazonato) complexes as well as thiosemicarbazide analogues have been modified to better target tumors, and their responses *in vitro* have been explored worldwide.[247,249−251]

To date, only a few PET agents have been evaluated in clinical trials: [^{18}F]-fluoromisonidazole ([^{18}F]FMISO),[253,254] [^{18}F]-fluoroazomycin arabinoside ([^{18}F]FAZA),[255] and [^{64}Cu]copper-diacetyl-bis(*N*(4)-methylthiosemicarbazonato),[248,249] being the most promising ones. Although [^{18}F]FMISO is consensually known as the gold standard in clinical research for hypoxia measurement, it is considered to have low-specific tissue accumulation resulting in limited imaging contrast of hypoxic tissues compared to normoxic areas, slow nonhypoxic cellular wash out, and no specific time for image acquisition.[256,257] [^{18}F]FAZA was developed along

https://dx.doi.org/10.1021/acs.jmedchem.0c00047
J. Med. Chem. 2020, 63, 14119−14150

Scheme 3. Mechanism of Nitroimidazole Derivatives in Hypoxic Cells

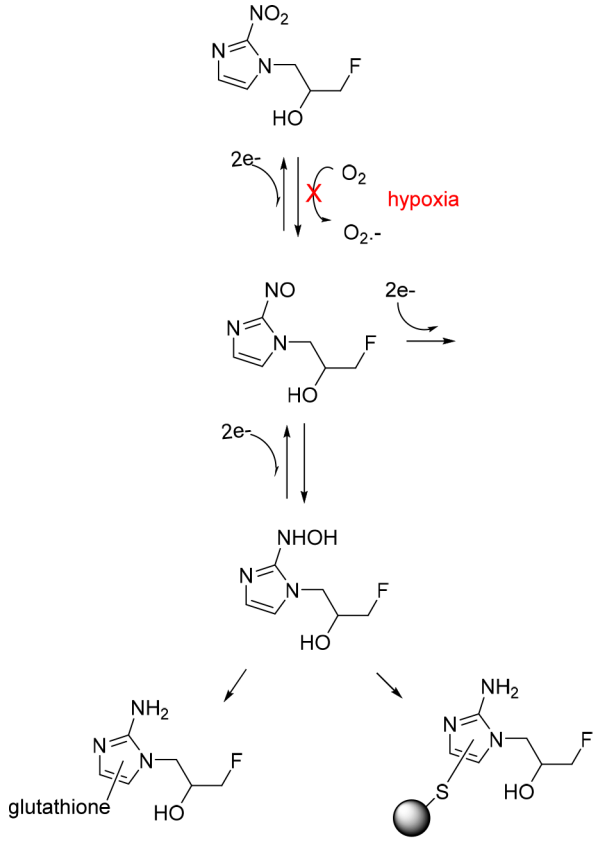

with the second-generation 2-nitroimidazoles, and while it has been denoted that it overcomes most of [^{18}F]FMISO's limitations, its intertumoral activity is lower.[254,258]

On the other side, studies suggest that [^{64}Cu]Cu(ATSM) occasionally possesses better properties,[259,260] due to its capacity to enter hypoxic cells and localize in tissues with low O_2 concentrations.[261] However, its selectivity seems to be related to the intracellular redox potential (Figure 16).[262,263] Subsequently, regardless of the collection of different tracers that are currently used for hypoxia tracing, none of them provide reproducibility across variant hypoxia subtypes, and new ones need to be developed in order to raise the sensitivity, the selectivity, and the resolution of the imaging studies.

Lately, gallium-68 (~68 min) is one of the radionuclides that has been commonly applied as a probe. These systems usually contain a nitroimidazole or a macrocyclic ligand, which is able to complex gallium-68 (for example, 1,4,7,10-tetraazacyclododecane-1,4,7,10-tetraacetic acid or 1,4,7-triazacyclononane-1,4-diacetic acid, generally alluded to as DOTA and NOTA). A variety of studies have shown improved clearance and successful hypoxia imaging compared to [^{18}F]FMISO. Recent studies have also demonstrated an affinity for the (HIF)-1 regulated carbonic anhydrase-IX receptor (CA-IX), a renowned endogenous marker of hypoxia.[264]

Hypoxia-responsive domains have been reported, and functional groups, such as nitro, quinone, transition metals, aliphatic, and aromatic N-oxides, have been identified for chemo-drug release. Such derivatives have been studied by

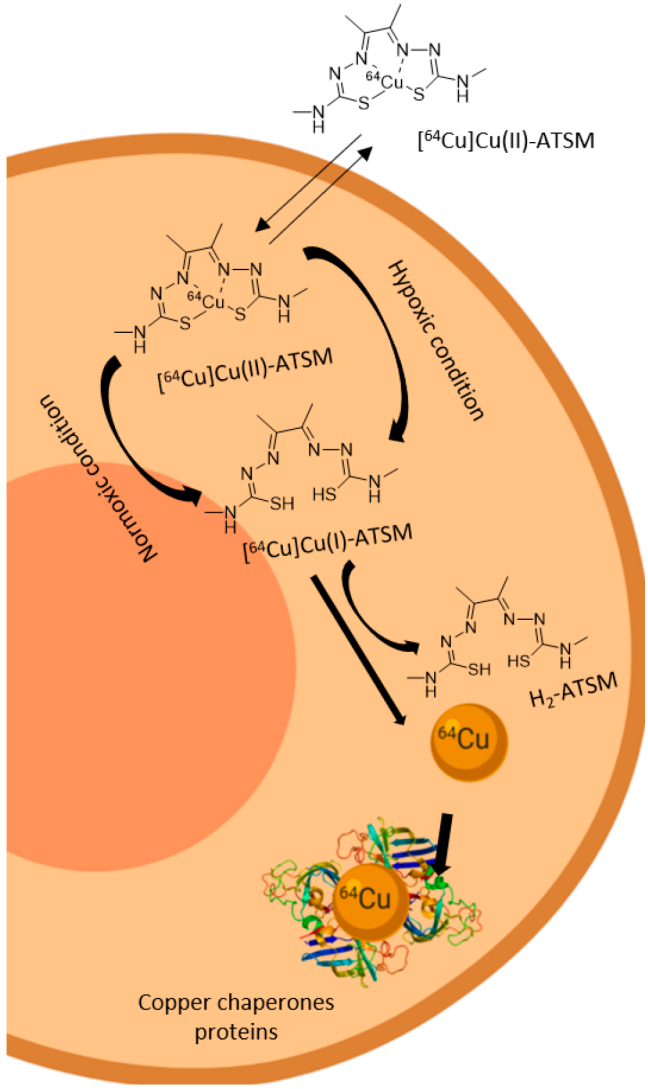

Figure 15. Proposed mechanism of hypoxic selectivity for [^{64}Cu]-CuATSM.[247,251,252]

different groups and recently added to the design of carriers for PSs and for anticancer drugs. These systems have led to the development of hypoxia-responsive nanoplatfom domains.[265,266] For instance, light-activatable nanoparticles (NPs) with nitroimidazole groups was developed by Lin et al. to selectively release drugs in hypoxic cells.[267] Furthermore, Gu's team has reported a 2-nitroimidazole (NI) conjugate linked to the dithiophene-benzotriazole polymer (NI-CP), which can encapsulate doxorubicin (DOX) via a double emulsion method, thus forming a DOX decorated polymer (DOX/NI-CP).[268] Near-infrared (NIR) light irradiation was performed after accumulation in the tumor region, showing a good production of ROS despite the hypoxic conditions. Moreover, the tumor hypoxia aggravated by the photodynamic reaction facilitated the cargo release, which turns this procedure into a self-feedback process, leading to selective drug release and an excellent therapeutic effect. This study suggests that the introduction of PSs in hypoxia-sensitive delivery carriers offers spatiotemporal control over the drug released, thus providing another type of theranostic agent.[269]

Moreover, it has been established that PDT planning might be facilitated by molecular imaging through the estimation of

https://dx.doi.org/10.1021/acs.jmedchem.0c00047
J. Med. Chem. 2020, 63, 14119−14150

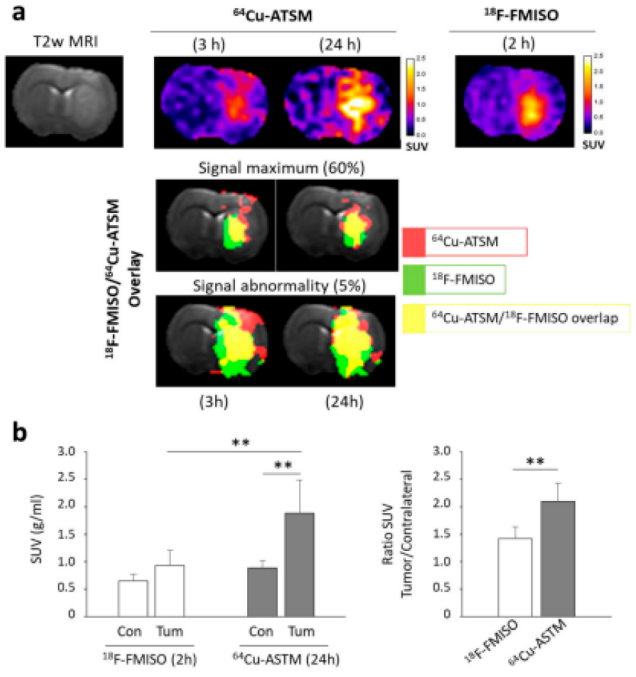

Figure 16. Studies showing the relationships between the retention of [^{18}F]FMISO and [^{64}Cu]Cu(ATSM) and hypoxia. (a) Coregistration of the [^{18}F]FMISO PET signal (2 h postinjection) with the [^{64}Cu]Cu(ATSM) PET signal (3 or 24 h postinjection. (b) [^{18}F]FMISO and [^{64}Cu]Cu(ATSM) uptake was evaluated at 2 and 24 h after radiotracer injection, respectively.[260]

the biodistribution of the PS in tumors. However, the concentration of oxygen remains crucial for PDT efficacy, and the role of imaging in this regard is often overlooked. Increasing intratumoral blood flow, using oxygen carriers, generating oxygen *in situ*, and targeting hypoxia-induced factors are some of the strategies that have, up to now, been developed to overcome tumor hypoxia. From all techniques, one, in particular, has stood out. This technique takes into consideration the existence of endogenous hydrogen peroxide (H_2O_2), which is naturally produced in cancerous cells. This approach utilizes H_2O_2 catalysts, such as catalase (CAT), to decompose H_2O_2 into O_2. Though, as an exogenous enzyme, the protease induced degradation as well as the immunogenicity of CAT, two non-negligible factors that need to be considered.[270−273]

Some authors have looked into the possibility of taking advantages of the porphyrin structure of THPP to coordinate metal ions and have come up with catalase-entrapped nanocapsules (CAT-THPP-PEG). To increase solubility, the nanocapsules are functionalized with short polyethylene glycol (PEG) chains. The enzymatic activity and stability of catalase are ensured by the CAT-THPP-PEG nanoparticles, which, after labeling with technetium-99m, can be traced by *in vivo* SPECT imaging. These nanoparticles have prolonged blood circulation and show efficient tumor retention after intravenous (iv) injection, and once located in the tumor, the catalytic activity is regained, transforming H_2O_2 to O_2. These very interesting therapeutic responses were associated with the nature of the PS (THPP) and tumor hypoxia. Moreover, in mouse tumor models, reduced immunogenicity was observed as compared to free catalase. The authors, therefore, presented an easy approach for the preparation of a unique type of enzyme entrapped theranostic nanocapsules, using PS as linkers. This, ultimately, allows for enhanced cancer therapy by modulation of tumor hypoxia via nanoparticle functionalization. The enzyme stability and reduced immunogenicity, which also enhance PDT, enable *in vivo* SPECT imaging to become an attractive cancer theranostic nanoscale platform.

5. DISCUSSION AND PERSPECTIVES

In general, standard medical protocols analyze a disease or disorder, determine its characteristics, and then apply treatments. A similar strategy is employed by the researcher when developing new drugs or new modalities of treatment.[274] Despite the predominance of this old-fashioned strategy, studies suggest that, for some diseases, another approach should be taken. Most of the modern diseases are heterogeneous in their behavior and appearance.[274] For instance, with a cancer patient, the first step is to identify the phenotype, then the heterogeneity is assessed, and finally, the stage in which the cancer has evolved is determined.[89,275] According to the stage and the characteristic of the cancer, the patient will receive a specific modality of treatment, so two patients with a similar disease may end up with different treatments.[17] The "one size fits all" approach that has been preconized for many years is not viable with cancers; the more we learn about the disease, the better we understand that a different approach is needed for developing successful treatment against cancer.[276]

The preferential localization of porphyrins in tumors, their ability to produce reactive oxygen species upon light activation, and their low toxicity have made them perfect molecules for photodynamic therapy. Moreover, the photophysical properties of porphyrins and the possibility to bind metal ions provide a unique platform for developing imaging agents. An ideal imaging agent is harmless to the body, and it possesses a fluorescence intensity above the cellular autofluorescence. These characteristics have been incorporated in recently synthesized porphyrins or porphyrin conjugates.[277] It is also important to note that porphyrin analogues, such as phthalocyanines, chlorins, and bacteriochlorins, are also good candidates for imaging, and several reviews have been written on the subject.[278,279] Although porphyrin analogues show similar behaviors and similar applications, they are often studied separately. Metalloporphyrin is another type of porphyrin derivatives that can be used as imaging agents. The introduction of metal ions in the porphyrin core modifies the photophysical property of porphyrins, and accordingly, it can improve the phototherapeutic efficacy, provide MRI contrast, and enhance Raman imaging.[280] In conclusion, metalloporphyrins own all of the essential characteristics of becoming theranostic agents.

There are, however, two main limitations of porphyrin-based imaging agents in therapy, and they come down to the synthesis and the aggregation of porphyrins. The principal strategy for the synthesis of these compounds is based on the condensation of mixed aldehydes resulting in a complex mixture of porphyrin derivatives, which are often difficult to purify and to isolate. Then, despite having pure molecules, the planar aromatic structure of porphyrins increases the probability of aggregation, a problem encountered by most researchers in the field.[281] Aggregation is not only a problem when it comes to therapy because it is usually related to low solubility, which, in the case of PDT, means worse pharmacokinetic profiles but also in imaging because aggregation usually translates into changes in the absorption

https://dx.doi.org/10.1021/acs.jmedchem.0c00047
J. Med. Chem. 2020, 63, 14119−14150

spectra.[282] In this way, having lower Soret bands would damage the pharmacodynamics of PDT as well as the imaging due to their decreased fluorescence. Therefore, many researchers have turned, as previously explained, to the solution of these problems by conjugation with nanostructures, which promise to help overcome these challenges.

On the other hand, more specific and individualized modalities of treatment are needed.[283] Diagnostic tools are vital for determining the progress of a disease in a patient, and combining diagnostic and therapeutic applications in a single molecule can, in principle, provide personalized treatments.[226] Having a single platform[99] will help doctors to apply the best treatment to individuals and, by doing so, will reduce side effects and other undesirable outcomes.[284]

The advent of novel drug delivery technologies is essentially driven by the observation that many therapeutic agents are not able to localize preferentially in target tissues and/or because of their lack of selectivity against diseased cells. Commonly, a preclinical biodistribution study leads to the quantification of the drug over time in tissues/organs. Generally, these studies are carried out *ex vivo* through time-consuming methods that required the sacrifice of many animals. These days, this can be done *in vivo* and in real time using imaging methodologies and tailored imaging probes. In a typical nanomedicine approach, the nanocarrier is loaded with both the drug and the imaging agent, an agent that can be detected by the corresponding imaging technique. Due to the good quantification properties and outstanding detection sensitivity, radioisotopes that have been broadly utilized for *ex vivo* biodistribution studies may have an interesting potential for *in vivo* applications. Kopelman et al. gave an example of such systems, in which an intricate mixture of porphyrin oligomers (porfimer sodium) and MRI contrasting agents were trapped together in a nanoparticle (Figure 17).[172] In these systems, the nanoparticles were

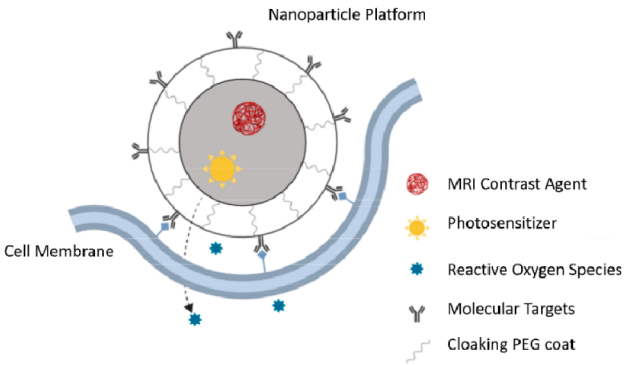

Figure 17. Schematic PAA core matrix nanoplatform with photodynamic dye, MRI contrast agent, polyethylene glycol (PEG) loading, and molecular targeting groups.[172]

functionalized at the surface with RGD targeting sequences and PEG for immune cloaking. Then, after delivery to tumors in rats, the photosensitizers were activated by light. The results show a complete necrosis of 9 L gliosarcoma tumors in rats within 5 min.[172]

As it was mentioned earlier, the effectiveness of photoinactivation can be affected due to PS aggregation.[285] Taking this into consideration, several studies have looked at different carriers to avoid aggregation, to stop degradation, and to increase uptake. For example, silica-based NPs (SiNPs) have been loaded with PSs.[286−288] In the clinical field, SiNPs are used as cell markers,[289−291] drug and gene delivery platforms,[291,292] enzyme adsorption, and immobilization agents,[293] and they are able to internalize cells.[289−291] Therefore, it made sense for them to be investigated for PDT applications. Synthetically modified SiNPs, such as ORMOSIL, mesoporous silica NPs (MSiNP), and hollow SiNPs (HSiNP), are frequently used in the clinic. These SiNPs are particularly appropriate for PDT as they show chemical inertness, and they are structurally stable. At the same time, they are resistant to pH variations and do not absorb light. However, perhaps most importantly, the functionalization of SiNPs ensures a monomeric environment to all PSs, thus avoiding aggregation phenomena. Moreover, singlet oxygen can travel through the SiNP shell.[294] Finally, the functionalization of SiNPs remains relatively easy, and the surface of SiNPs can accommodate all kinds of functional groups, including PEGs, antibodies, peptides, glycosides, and several other biomolecules.[286,295,296]

ORMOSIL functionalized NPs have shown great promises for PDT applications.[286] They have been widely studied because of their hydrophobic/hydrophilic tunability, which can ease the solubility of PSs. Accordingly, Ohulchanskyy et al. have prepared ORMOSIL NP derivatives with covalently bound PSs. The covalent attachment of the PS increases the stability and avoids leaching of the PS before reaching its target.[297] Among different systems, the iodobenzylpyropheophorbide derivative (Figure 18) was synthesized to initiate a

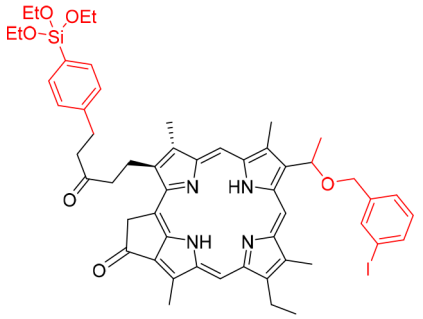

Figure 18. Iodobenzylpyropheophorbide precursor for functionalization to ORMOSIL NPs.

coprecipitation reaction, thus facilitating purification and isolation of the compound. These ORMOSIL and ORMOSIL-PS conjugates were evaluated on two tumor cell lines, Colon-26 and RIF-1. The study shows an excellent uptake by cells and that the photophysical properties of the PSs are preserved. Indeed, upon light activation, the phototoxicity of the PSs was comparable to that of the PS alone. Moreover, the authors highlighted the possibility of replacing the natural iodine of iodobenzylpyropheophorbide with a different isotope (e.g., I-124, I-125, etc.). This modification implies that the same systems can be used as contrast agents (PET/SPECT), while still having PDT effect, thus becoming theranostic agents.[297] A similar observation was made by other groups, on systems involving other PSs covalently linked or encapsulated in ORMOSIL NPs.[298]

Metal NPs are another category of NPs commonly used in PDT. Among metal-based NPs, gold NPs (AuNPs) are particularly attractive, due to their distinctive properties, which make them perfect candidates for labeling, delivery, heating, imaging, and sensing applications.[299−301] Mostly linked to their biocompatibility, precise structure, limited

https://dx.doi.org/10.1021/acs.jmedchem.0c00047
J. Med. Chem. 2020, 63, 14119−14150

surface, and optical properties, gold NPs have received a great deal of attention in PDT.[302−304] While the introduction of specific groups (thiol, amino, cyano) confer the colloidal stability,[221] the functionalization of gold NPs with lipids, proteins, oligonucleotides, or PSs can improve their biological properties (targeting, stability, selectivity).[300] In fact, the conjugation of PSs on the surface of AuNPs may produce an enhanced electromagnetic field as a result of localized surface plasmon resonance of AuNPs upon light activation and, consequently, an increase the PDT efficacy (Figure 19). This phenomenon will enhance the PS excitation rate, increase ROS production, and, ultimately, will generate an improved PDT agent.[301,302]

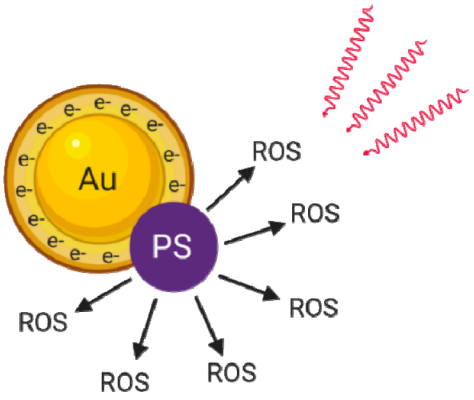

Figure 19. Cartoon illustrating the surface plasmon resonance phenomena on gold NPs.

The use of hydrophilic AuNPs as a platform to prepare multimodal systems was recently published by Penon et al.[305] The multifunctional AuNPs (PS-AuNPs-PEG-Ab) show porphyrins and PEG chains connected to an anti-erbB2 antibody. The antibody aims to target overexpressed erbB2 receptors, which are commonly found on the membrane of SK-BR-3 breast cancer cells. The different components are attached to the AuNPs via thiol groups, which have a high chemical affinity for AuNPs. These functionalized NPs are photoactive, producing $^1O_2$ and killing cells under PDT conditions. It was also demonstrated that the PS-AuNP-PEG-Ab conjugate accumulates in cells, and upon photoactivation, damage to membranes and modification to cellular morphology were detected.[305]

Like metal-based nanoparticles, nanotheranostic particles involving PDT can destroy their targets. However, to be effective, nanotheranostic particles need to reach their target, to avoid off-target phototoxicity. Therefore, it is important to monitor the localization of these particles in real time, in order to minimize side effects linked to the generation of reactive oxygen species outside the tumors.

Luckily, most photosensitizers used for PDT are also fluorescent molecules, a useful property that can be employed to localize the photosensitizer. Fluorescence spectroscopy is cheap to operate, it shows outstanding resolution in the appropriate spectral region, and it can be used in parallel to radioisotopes (PET and SPECT), thus being perfectly compatible with other techniques.[306,307] Photons released by naturally fluorescent biomolecules or from externally administered fluorescent probes can be used for imaging. However, some limitations are associated with fluorescence, including poor tissue penetration, high noise, and background from tissue scattering of photons in the visible region, autofluorescence, light absorption by proteins, and interference from water molecules.[99] Nevertheless, NIR activation can overcome these limitations in that region: tissue penetration of light is up to several centimeters, a low autofluorescence is observed, and tissue scattering is reduced to a minimum.[308,309]

Selectivity and targeting strategies are keys for fluorescence imaging and PDT. This can be achieved by passive transport, which implies the use of large molecules, such as nanoparticles. The particular size of nanoparticles increases their accumulation in tumors, and after internalization, the particles are retained (EPR effect). Peng et al. have developed multifunctional polymeric nanoparticles loaded with IR-780, which provide both NIR fluorescent dyes and photosensitizers in a large particle.[310] These micellar nanoparticles confirm that passive targeting can be accomplished with nanoparticles.

Using similar concepts, Tsai and co-workers studied the accumulation in cells of nanoparticles decorated with the photosensitizer PPIX.[311,312] They found that the pH-sensitive particles were delivering PPIX in the nucleus, while non-pH-sensitive nanoparticles were delivering PPIX in lysosomes.[313] In mice bearing A549 xenografts, the different accumulation was nicely linked to the biological activity. Indeed, the pH-sensitive nanoparticles have a stronger inhibition on tumor growth, suggesting that the localization of the photosensitizer in cells can strongly affect PDT.

Like PPIX, chlorin e6 (Ce6) is another popular photosensitizer used as a theranostic agent.[314−316] Lee et al. have developed glycol chitosan nanoparticles to transport Ce6 to cells.[317] Two transport systems were evaluated: one involving physical encapsulation and the other involving covalently linked Ce6 nanoparticles. The conjugated system showed a longer circulation time, a better-controlled release of Ce6, and a higher accumulation of the PS to tumors. The increased accumulation in tumors of mice bearing HT-29 human colon adenocarcinoma was established by NIR imaging. Then, PDT treatments on the same tumors showed severe necrosis and mass reduction of tumors.

Phthalocyanines (Pc) are also a class of molecules with significant potential as theranostic agents, given the strong absorption within the NIR window. For example, a fluorescent Pc-loaded graphene nanoplatform was used as an imaging and PDT agent on ovarian cancer cells.[318] Similarly, a biocompatible carbon nanodot loaded with zinc Pc was used for the same modalities (imaging and PDT) on HeLa cells, as well as on animal models.[319] Both examples confirm the usefulness of passive transport in view to target tumors for PDT and fluorescence imaging.

A second strategy to target tumors and add selectivity to PDT/imaging agents implies the development of activatable multifunctional agents, which can become active after responding to a biological or physical stimulus.[28] The activation can be triggered artificially (exogenous stimuli) by applying, for example, a magnetic/electrical field, ultrasound, or light. On the other hand, the activation can be triggered biologically, by physiological conditions associated with cancer (endogenous stimuli), such as the temperature, pH, or enzymatic activity.[152,320−322] Among these endogenous stimuli, pH is probably one of the most attractive targets, as tumors tend to have a mildly acidic pH.[173] Accordingly, charge-switching nanoparticles have been designed to react under acidic conditions (Figure 20). In such system, the positively charged region of the compound interacts strongly with

https://dx.doi.org/10.1021/acs.jmedchem.0c00047
J. Med. Chem. 2020, 63, 14119−14150

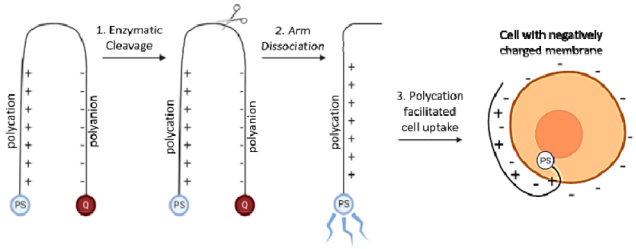

Figure 20. Mechanism of an activatable peptidic zipper-based PS.

negatively charged particles, especially those located in membranes, thus overall increasing cellular uptake.[315]

Enzymes such as matrix metalloprotease-2 that are overexpressed in tumor cells can be targeted by activatable nanoparticles.[323] Likewise, a theranostic agent with double targeting possibilities can, for example, be fluorescent and phototoxic only after being released by tumor-associated lysosomal enzyme cathepsin B. This is particularly attractive for targeting folate receptor-positive cancer cells.[324] This strategy focuses on selectivity and specificity for malignant cells, using targeted moieties that can aim specific receptors found on the surface of biomolecules and inside cells. One frequently mentioned group is the RGD peptide (tripeptide Arg-Gly-Asp), which can target the integrin avb3 receptors that are overexpressed in several tumor types. RGD conjugates loaded in ICG nanoparticles showed promises for FGS in liver resection.[221] Conjugation of (i) RGD peptides for improved tumor targeting, (ii) temoporfin as a photosensitizer, and (iii) with fluorescent dye molecules for improved contrast has been performed.[325] An *in vivo* study has confirmed the dual modalities of these systems, fluorescence imaging and PDT.

Folic acid (FA) is another functional group that can be used to target specific receptors. Folate receptors are upregulated in ovarian, lung, brain, and breast cancers, thus making folate conjugates good candidates for increasing selectivity.[326] Wang et al. reported a nanoparticle that incorporates fluorescence imaging, PDT, and FA targeting ability.[327] Later on, a highly biocompatible carbon nanodot was synthesized, which incorporates the same modalities. Biological studies showed that the functionalized carbon nanodot increases fluorescence and has PDT effects *in vitro* and in mice.[319] More recently, FA-coupled nanoprobes loaded with Ce6 were synthesized, and after a series of *in vitro* and *in vivo* experiments to access specificity, efficacy, and safety, the multifunctional theranostic agent ability was demonstrated.

Radionuclide imaging is another strategy that combines high sensitivity and unlimited tissue penetration. It can be associated with imaging to monitor disease development. Usually, the half-life of the selected PET isotope matches the time necessary for imaging,[328,329] with the necessity of producing a high signal-to-background ratio at a target localization. For tumor imaging, copper-64 or zirconium-89 are normally used with systemic injection of an intact antibody to maximize the tumor-to-background ratio. Fluorine-18 is also a good radioisotope, which is already used in the clinic ([^{18}F]FDG). However, ^{18}F radiochemistry can be hard to manipulate at the radiochemical level, and ^{18}F radiochemistry involved a covalent bond.[330−333] DOTA, on the other hand, involves coordination chemistry, and it is quite easy to use the same platform for different radionuclides and different imaging techniques, for example, copper-64 and gallium-68 for PET, indium-111 for SPECT, and yttrium-90 for radiotherapy. The versatility of DOTA provides an ideal system, where different imaging techniques can be applied to a single platform.

Another significant consideration when selecting a PET radionuclide is the time frame associated with the targeted biological event. In other words, the half-life of the positron-emitting radionuclide must fit with the biological event; otherwise, the results may be misleading and the imaging may not provide answers. For example, copper-64 possesses a half-life of 12.7 h, ideal for tracking monoclonal antibodies over a period of 48 h, while fluoride-18 with a half-life of 110 min can be used to trace fast clearance molecules.[334] Therefore, radioisotopes such as carbon-11, fluoride-18, copper-64, bromide-76, technetium-99m, indium-111, and yttrium-90 have been utilized along with various copolymers, in view to develop robust nanodelivery systems.[335−337]

If we take into consideration the already mentioned impact of hypoxia on tumor progression, metastatic spread, absence of tumor control, amplified recurrence phenomena, and poor therapeutic outcome, then imaging hypoxia is a step forward. As opposed to other noninvasive techniques, PET imaging offers specificity for the detection of hypoxic tissues. In this regard, the first compounds to address the imaging of hypoxia tissues were developed in the early 1980s.[338] They consist of 2-nitroimidazole derivatives linked to multiple PET tracers (Figure 21).

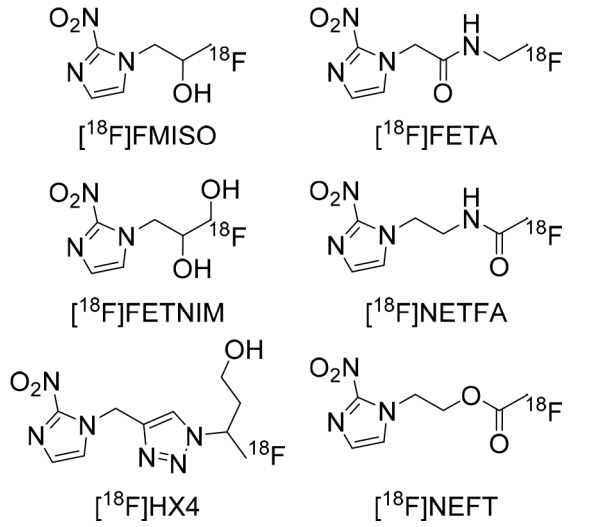

Figure 21. Structures of known [^{18}F]-based 2-nitroimidazole derivatives.

The main idea behind these [^{18}F]-based 2-nitroimidazole derivatives is to have a stable compound showing high specificity for imaging hypoxia without the inconsistent correlation that is often associated with other imaging techniques like PET with [^{18}F]-fluorodeoxyglucose ([^{18}F]FDG). The most common PET tracer for hypoxia imaging is the fluorinated nitroimidazole derivative [^{18}F]-fluoromisonidazole ([^{18}F]FMISO).[338,339] Like other compounds in the nitroimidazole family, [^{18}F]FMISO can diffuse passively through cell membranes due to its lipophilicity. Then, after internalization, the compound is reduced into R-NO$_2$ radicals by the nitroreductase enzyme (NTR). This process remains reversible, meaning the tracer will only stay in the cell under hypoxic conditions; otherwise, in the presence of oxygen, the tracer is released. As mentioned, in the absence of

https://dx.doi.org/10.1021/acs.jmedchem.0c00047
J. Med. Chem. 2020, 63, 14119−14150

oxygen (pO_2 < 10 mmHg), the reduction process is much slower. Consequently, the increasing production of R-NHOH derivatives that bind directly to intracellular molecules ensures that the level of tracers inside cells is high.[340−343] However, the main drawbacks of [^{18}F]FMISO include the fact that passive transport requires 2−4 h after intravenous injection for [^{18}F]FMISO to accumulate to hypoxic tissues[344,345] and that, despite this uptake period, tracer accumulation remains low.[344,346]

Alternatively, among the non-nitroimidazole compounds, radioactive copper (copper-60, -61, -62, -64) labeled with diacetyl-bis(*N*4-methylthiosemicarbazone) [^{64}Cu]CuATSM) is another promising PET radiopharmaceutical for hypoxia imaging. First studied in 1997, the compound has shown suitability for the detection of hypoxia in living tissues.[250] However, the mechanism of uptake remains unclear. Nevertheless, it is known that [^{64}Cu]CuATSM is a neutral lipophilic molecule, which is easily crossing membranes by passive diffusion.[340] Fujibayashi et al. suggested that, after internalization, the accumulation in tumor cells mainly depends on the cytosolic/microsomal bioreduction process.[347] The bivalent [^{64}Cu]Cu(II)-ATSM, once inside cells, undergoes a thiol reduction and is converted to the less stable Cu(I) complex [^{64}Cu]Cu(I)-ATSM.[348] In hypoxic conditions, this complex is progressively dissociated into H_2-ATSM and free Cu(I), which can rapidly coordinate to proteins.[250,347−349]

It is, therefore, plausible that copper itself plays a major role in the [^{64}Cu]CuATSM entrapment. In order to verify this hypothesis, Hueting et al. analyzed the *in vitro* and *in vivo* distribution of [^{64}Cu]CuATSM and [^{64}Cu]CuOAc in animal models (EMT6 and CaNT).[248] The study shows that both copper tracers accumulate in similar fashion in tissues, confirming that copper metabolism takes part in the activity of [^{64}Cu]CuATSM.

Hypoxia for cancer patients is very important, and the development of prognostic biomarkers for hypoxia can make a huge difference in the success or failure of a treatment. Additionally, identifying hypoxia *in vivo* without any intrusive intervention may facilitate its use in the clinic. Nonetheless, determining the best tracer for this purpose remains difficult. While some data suggest that [^{18}F]FMISO is an excellent candidate, a suboptimal imaging limitation remains. On the other hand, high PET image quality favored the use of [^{64}Cu]CuATSM. Besides, when directly compared to the principal 2-nitroimidazole family representative ([^{18}F]-FMISO), [^{64}Cu]CuATSM uptake is significantly better in hypoxic tissues than in other areas, and it reaches its target more rapidly (10−15 min versus 2−4 h).[259] It is clear that these achievements are important and can potentially generate better theranostic-PDT agents.

Even though the outlook for imaging seems encouraging, obstacles remain high for commercial applications. In fact, both imaging agent development and standard drug discovery and development share much in common, especially those binding to a specific target *in vivo*. Both must overcome several challenges when it comes to factors such as target authentication, identification of the best possible candidate, showing high affinity and selectivity, as well as good clearance, and low toxicity.[350]

The impact of a therapeutic intervention is difficult to evaluate in cancer treatment, which makes the validation of molecular imaging biomarkers difficult when compared to existing surrogate markers. A quantitative assessment through imaging can help to determine the real impact of a new treatment (complete or partial response), and it can provide information on the progression of the disease.[351] PET/CT and other hybrid imaging modalities, by overlaying different images, allow the determination of the therapeutic effect with PET and the size of the tumor with CT.[352]

Another challenge is the need to understand the drug's mechanism of action when integrating PET or SPECT into clinical research. For example, [^{18}F]FDG PET may help to identify downstream effects at an early stage of cancer development, even before tumor shrinkage. Routine clinical use of [^{18}F]FDG PET involves static imaging 2 h post-injection, which can be useful if we only want the localization of tumors and metastases. On the other hand, if we are intent to perform dynamic imaging, the recollection of PET data from the initial injection of [^{18}F]FDG will give direct access to pharmacokinetics and pharmacodynamics information on the tracer, which can be very important for better understanding how drugs and therapies work in real time.[353] This example illustrates the careful planning and deep understanding that is required of all of the processes involved when trying to perform the imaging of cancer and how they can limit or help each other.

We can, by this, conclude that the similarities between the processes of developing therapeutic drugs and diagnostic agents make their simultaneous development into theranostic agents even more challenging. At the same time, technologies and development from one domain can accelerate the development processes of the other (PET microdosing, for example). Finally, the development of new drugs incorporating tracers and imaging biomarkers can also contribute to the emergence of theranostic agents.[350]

6. OUR CONTRIBUTIONS

As it can be understood from this review, there is an urgent need for new drugs and practices to treat cancer. Photodynamic therapy (PDT) imposes itself as one of the most preponderant voices to answer this demand. With the combination of a photosensitizer, light, and oxygen, PDT achieves a unique selectivity by the production of localized reactive oxygen species inside tumor cells, which leads to their destruction with limited side effects.[354] Our approach aims to use cellulose nanocrystals to transport and deliver radiolabeled photoresponsive molecules to biological targets and create new theranostic agents.

In order to achieve our goal of using these cellulose-metal-porphyrin assemblies and to trace them using SPECT imaging, several steps have been taken so far. First, we have prepared and characterized CNCs[355] as well as photoresponsive molecules through stoichiometric quantities of aldehydes and pyrrole in propionic acid (Scheme 4).[356] Then metalla-assemblies were obtained using inorganic metalla-clips under a well-developed methodology.[357] The last step was to load these metalla-assemblies to nanocrystals by dissolution in methanol, adding them dropwise to the CNC solution and leaving it to react for 24 h.[355] Derivatives of the 5,10,15,20-tetra(4-pyridyl)-21*H*,23*H*-porphine were chosen as photoresponsive molecules, due to their ability to simultaneously be linked to the cellulose nanocrystals (CNC) and coordinated to ruthenium. Even though different grafting methods were explored, the best results were achieved through the covalent amide binding of the photosensitizer and the CNC.

https://dx.doi.org/10.1021/acs.jmedchem.0c00047
J. Med. Chem. 2020, 63, 14119−14150

Scheme 4. Synthesis of Cellulose-Metallo-Porphyrin Theranostic Agents

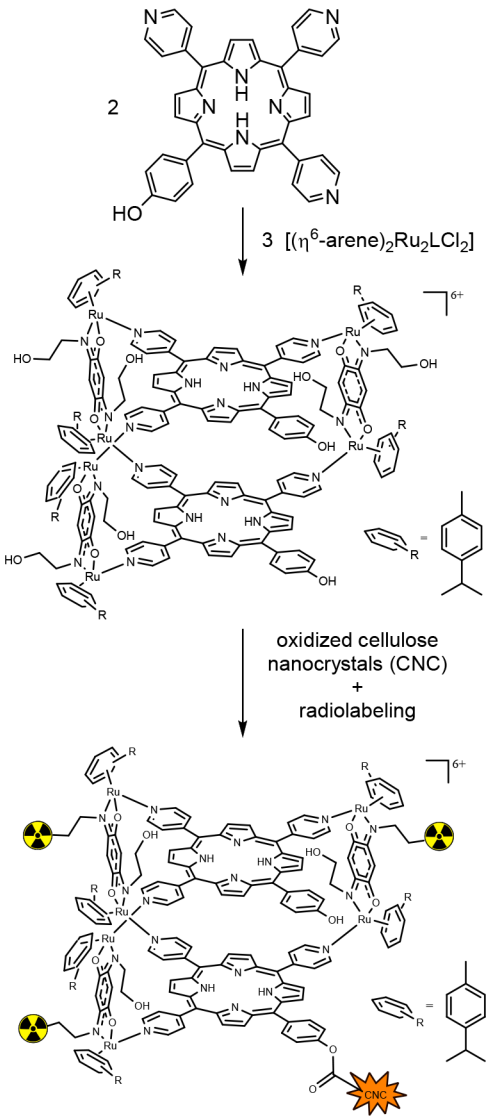

Labeling of CNC with the nonradioactive metallic isotope has also been explored, and the radiolabeling experiments will follow shortly. A full set of *in vitro* assays with the nonradioactive derivatives will be performed to determine the IC_{50} and the influence of the cage and CNC to cells. Following the *in vitro* study, *in vivo* imaging will be conducted, and the data will be processed and statistically analyzed.

Our preliminary results are very promising regarding the synthesis of a multimodal agent that combines a photosensitizer for PDT treatment and a radioactive agent for imaging (before, during, and after the process), thus aiming to develop an innovative theranostic agent. The conjugation with cellulose nanocrystals and coordination to inorganic entities intend to ameliorate their delivery, solubility, and metabolism.

7. CONCLUSIONS

The importance of PDT in the treatment of cancers as well as nononcological diseases is growing rapidly. However, despite increasing reports showing the benefits of PDT over traditional treatments, extensive use in the clinics remains to be seen. This limited utilization of PDT in the clinics is due to different factors, some linked to the pharmaceutical formulations of PDT agents (solubility, administration, aggregation, selectivity) and some to the technology involved (instrument, light source, etc.).

For more than 20 years, researchers have focused on developing safer and more effective PDT agents not only to cure cancers but also to be used in many other domains.[358] During that period, the clinical success of PDT for the treatment of head and neck cancers is undeniable, showing an increased survival rate of patients with such cancers, as well as an improved quality of life. Similarly, the cure of some early stage tumors, precancerous lesions, and nonmelanoma skin cancers has been enormously effective.[7] In addition, the association of PDT to NPs technology has offered new solutions and new perspectives to further develop the field of photodynamic therapy.

Photodynamic treatment (PDT) is and should be considered a therapy with promising outcomes for the treatment of different diseases, the most studied one being cancer. This treatment depends on the impacts of light conveyed to photosensitized cells. Therefore, adding molecular imaging to PDT treatment is crucial and keeps on expanding, from disease detection, treatment planning, to real-time monitoring and its outcome evaluation. While there has been impressive progress over the past decade, to be successful in the clinic, numerous technical difficulties must be investigated and ameliorated, for example, the requirement of imaging probes to precisely recognize the spatial and temporal occurrence of specific cell death processes. As cancer is proliferating fast, innovative diagnostic and therapeutic strategies are imperative for early detection and precision treatment. In addition, to optimize the therapeutic outcome of PDT, an evaluation of the local microenvironment before treatment is essential. For example, as photosensitizers (PSs) need oxygen to operate, the presence or absence of O_2 is crucial for the production of toxic reactive oxygen species (ROS), according to PDT treatment. Therefore, without specific information on local O_2 concentrations during PDT treatments, the effectiveness of treatments can fluctuate greatly. Moreover, due to O_2 consumption during PDT treatments, the oxygen level needs to be continuously maintained to ensure efficacy. Thus, measuring O_2 levels in real time during PDT treatments has become one of the main challenges for the future of PDT.

So far, multiple sensors have been used to monitor O_2 concentrations in biological media, thus providing convenient imaging tools for refining cancer diagnosis and improving therapeutic efficiency. However, the combination of an imaging agent with a photosensitizer to generate a theranostic O_2 sensory platform for image-guided PDT has been rarely reported.[359] In the clinic, PET imaging has become one of the most effective tools to visualize tumor hypoxia in patients. It has been used clinically on various cancer types with different radiotracers. It is now well-documented; PET imaging can increase treatment response and optimize radiotherapy plans. OFI and PET as double-modality contrasting agents have proven to be an excellent combination. The OFI/PET systems show low toxicity, and they possess high spatial and long temporal resolutions.[206]

In summary, multimodal imaging presents itself as a powerful tool to make an accurate picture of diseased sites. The accumulation and retention of nanoparticles in real time can be quantified by PET imaging, while OFI imaging can

https://dx.doi.org/10.1021/acs.jmedchem.0c00047
J. Med. Chem. 2020, 63, 14119−14150

provide other information at a cellular/molecular level. Together, they can validate and optimize treatments without being too expensive. Therefore, the emergence of integrated diagnostic and therapeutic agents in a single system is a valuable strategy to develop new therapeutic combinations in PDT.

AUTHOR INFORMATION

Corresponding Authors

Bruno Therrien − *Institute of Chemistry, University of Neuchatel, CH-2000 Neuchatel, Switzerland;* orcid.org/0000-0002-0388-2745; Email: bruno.therrien@unine.ch

George Loudos − *BioEmission Technology Solutions, 11472 Athens, Greece*; Email: george@bioemtech.com

Authors

João C. S. Simões − *Institute of Chemistry, University of Neuchatel, CH-2000 Neuchatel, Switzerland; BioEmission Technology Solutions, 11472 Athens, Greece*

Sophia Sarpaki − *BioEmission Technology Solutions, 11472 Athens, Greece*

Panagiotis Papadimitroulas − *BioEmission Technology Solutions, 11472 Athens, Greece*

Complete contact information is available at: https://pubs.acs.org/10.1021/acs.jmedchem.0c00047

Author Contributions

The manuscript was written through contributions of all authors. All authors have given approval to the final version of the manuscript.

Funding

This project has received financial support from the European Union's Horizon 2020 research and innovation program under the Marie Sklodowska-Curie grant agreement no. 764837.

Notes

The authors declare no competing financial interest.

Biographies

João C. S. Simões was born in Coimbra, Portugal. He concluded his Bachelor's in 2016 and Master's in 2018, both at the University of Coimbra in Medicinal Chemistry. His Master's thesis consisted of "Novel Ring-Fused Chlorins as Promising PDT Agents against Cancer". Currently, he is an Early Stage Researcher within the POLYTHEA project, in a Marie Curie Innovative Training Network, which aims for the design, photo-optimization, and biological evaluation of photosensitizers for human health and food security applications.

Sophia Sarpaki is a radiopharmaceutical chemist and obtained her Ph.D. diploma from the Chemistry Department of Bath University, on "Investigations into the Radiochemistry of Gallium- and Fluorine-Containing Compounds for Molecular Imaging Applications". She holds the FELASSA certification for small animal handling. She works as a researcher and project manager on research preclinical imaging projects at BIOEMETCH. Her expertise lies in developing radiolabeling protocols for small molecules, biomolecules, and nanostructures, executing their necessary chemical analysis and performing their *in vivo* evaluation. Her scientific interest has a strong focus on cancer research, but she is also involved with projects related to cardiovascular diseases and stem cell therapy. She has participated in a variety of international research projects under the framework of EuroNanoMed, H2020, and ERC.

Panagiotis Papadimitroulas is cofounder and Project Director of BIOEMTECH (www.bioemtech.com) since 2013. He holds a Ph.D. in Medical Physics (2015) awarded by the University of Patras. He has extensive expertise in the evaluation and optimization of clinical and preclinical dosimetry protocols, in Monte Carlo simulations, image processing tools, and advanced computational models. Since 2019, he gained a Post-Doc Research Grant from the State Scholarships Foundation (IKY). He authored 2 chapter books related to internal dosimetry and computational tools, 18 publications in peer-review journals, and more than 60 announcements in international/national conferences. He has participated in more than 15 international and national research projects under the framework of FP7, COST, H2020, ERANET, NSRF. Since 2017, he is an official member of the OpenGATE collaboration.

Bruno Therrien is an Associate professor at the University of Neuchatel, Switzerland. He studied chemistry at the University of Montreal and obtained his Ph.D. in 1998 from the University of Bern, Switzerland. After his Ph.D., he undertook several postdoctoral positions (Weizmann Institute, Massey University, Tokyo University), before returning to Switzerland. His main research interests are supramolecular chemistry and the biological applications of metalla-assemblies.

George Loudos is an Assistant Professor at the University of West Attica Athens and CEO and cofounder of BIOEMTECH. He has participated as a coordinator or partner in more than 15 EU projects, as well as two National Excellence grants and several smaller national and other projects. He has published over 120 articles in international journals and has >250 publications in conference proceedings and ∼1350 citations. He has given 60 invited lectures and holds one patent. He has been the organizer of many international conferences, workshops, and training schools. His research interests are focused on molecular imaging of nanoparticles and other biomolecules using nuclear medicine techniques, medical instrumentation, and he strongly supports interdisciplinary cooperation and education in the field of nanomedicine and molecular imaging.

ABBREVIATIONS USED

AFP, hepatocellular carcinoma markers; aPS, activatable photosensitizer; Arg, arginine; Asp, aspartate; AuNPs, gold nanoaprticles; BODIPY, boron-dipyrromethene; BOLD, blood oxygen-dependent level; BP, benzoporphyrin derivative; BPD-MA, benzoporphyrin derivative monoacid; C225, EGFR antibody; CA125, ovarian cancer marker; CA153, breast tumor marker; CA199, gastrointestinal tumor marker; CA242, gastrointestinal tumor marker; CA724, gastrointestinal tumor marker; CA-IX, (HIF)-1 regulated carbonic anhydrase-IX receptor; CAT, catalase; Ce6, chlorin e6; CEA, lung cancer tumor marker; CNC, cellulose nanocrystals; CT, computer tomography; Cu-ATSM, Diacetylbis(*N*(4)-methylthiosemicarbazonato) copper(II); Cyfra21−1, lung cancer tumor marker; DBP-UiO, Hf−porphyrin nanoscale metal−organic framework; DLI, drug to light interval; DOTA, 1,4,7,10-tetraazacyclododecane-1,4,7,10-tetraacetic acid; DOX, doxorubicin; DPP, diketopyrrolopyrrole; EGFR, epidermal growth factor receptor; EPR, enhanced permeability and a retention effect; FA, folic acid; FGR, fluorescence-guided resection; FMISO, fluoromisonidazole; FR, folate receptors; FRET, fluorescence resonance energy transfer; GLUT, glucose transporters; Gly, glycine; HCG, choriocarcinoma marker; HeLa, immortal cell line derived from cervical cancer cells; HIF, hypoxia-inducible factors; HpD, hematoporphyrin derivative; HSiNP, hollow SiNPs; ICG, indocyanine green;

https://dx.doi.org/10.1021/acs.jmedchem.0c00047
J. Med. Chem. 2020, 63, 14119−14150

ISC, intersystem crossing; LDL, low density lipoprotein; MDR, multidrug resistance; MOF, metal−organic frameworks; MRI, magnetic resonance imaging; MSiNP, metal SiNPs; NI, nitrimidazole; NI-CP, (NI)-conjugated dithiophene-benzotriazole-containing polymer; NIR, near-infrared; NMI, nuclear medical imaging; NOTA, 1,4,7-triazacyclononane-1,4-diacetic acid; NP, nanoparticle; NSE, lung cancer tumor marker; OFI, optical fluorescence imaging; PAA, polyacrylamide; Pc, phthalocyanine; PDD, photodynamic diagnosis; PDT, photodynamic therapy; PEG, polyethylene glycol; PET, positron emission tomography; PIC, photimmunoconjugate; PLGA, poly(lactic-*co*-glycolic acid; PPIX, protoporphyrin IX; PS, photosensitizer; PSA, prostate cancer marker; Q, quencher particle; QD, quantum dots; QY, quantum yield; RGD, arginylglycylaspartic acid; ROS, reactive oxygen species; SiNP, silica nanoparticles; SK-BR-3, human breast cancer cell line; SPECT, single-photon emission computed tomography; THPP, tris(3-hydroxypropyl)phosphine; TPC, 5-[4carboxyphenyl]-10,15,20-triphenyl-2,3-dihydroxychlorin; TR, transferrin receptor.

REFERENCES

(1) McGuire, S. World Cancer Report 2014. *Adv. Nutr.* **2016**, *7*, 418−419.

(2) Jin, G.; He, R.; Liu, Q.; Dong, Y.; Lin, M.; Li, W.; Xu, F. Theranostics of Triple-Negative Breast Cancer Based on Conjugated Polymer Nanoparticles. *ACS Appl. Mater. Interfaces* **2018**, *10*, 10634−10646.

(3) Srivatsan, A.; Missert, J. R.; Upadhyay, S. K.; Pandey, R. K. Porphyrin-Based Photosensitizers and the Corresponding Multifunctional Nanoplatforms for Cancer-Imaging and Phototherapy. *J. Porphyrins Phthalocyanines* **2015**, *19*, 109−134.

(4) Evans, C. L.; Rizvi, I.; Hasan, T.; Boer, J. F. de. Vitro Ovarian Tumor Growth and Treatment Response Dynamics Visualized With Time-Lapse OCT Imaging. *Opt. Express* **2009**, *17*, 8892.

(5) Georgakoudi, I.; Solban, N.; Novak, J.; Rice, W. L.; Wei, X.; Hasan, T.; Lin, C. P. In Vivo Flow Cytometry: A New Method for Enumerating Circulating Cancer Cells. *Cancer Res.* **2004**, *64*, 5044−5047.

(6) Solban, N.; Pal, S. K.; Alok, S. K.; Sung, C. K.; Hasan, T. Mechanistic Investigation and Implications of Photodynamic Therapy Induction of Vascular Endothelial Growth Factor in Prostate Cancer. *Cancer Res.* **2006**, *66*, 5633−5640.

(7) Abrahamse, H.; Hamblin, M. R. New Photosensitizers for Photodynamic Therapy. *Biochem. J.* **2016**, *473*, 347−364.

(8) Gibbs-Strauss, S. L. Noninvasive Measurement of Aminolevulinic Acid-Induced Protoporphyrin IX Fluorescence Allowing Detection of Murine Glioma in Vivo. *J. Biomed. Opt.* **2009**, *14*, 014007.

(9) Soukos, N. S.; Hamblin, M. R.; Keel, S.; Fabian, R. L.; Deutsch, T. F.; Hasan, T. Epidermal Growth Factor Receptor-Targeted Immunophotodiagnosis and Photoimmunotherapy of Oral Precancer in Vivo. *Cancer Res.* **2001**, *61*, 4490−4496.

(10) Zheng, X.; Sallum, U. W.; Verma, S.; Athar, H.; Evans, C. L.; Hasan, T. Exploiting a Bacterial Drug-Resistance Mechanism: A Light-Activated Construct for the Destruction of MRSA. *Angew. Chem., Int. Ed.* **2009**, *48*, 2148−2151.

(11) Zhong, W.; Celli, J. P.; Rizvi, I.; Mai, Z.; Spring, B. Q.; Yun, S. H.; Hasan, T. In Vivo High-Resolution Fluorescence Microendoscopy for Ovarian Cancer Detection and Treatment Monitoring. *Br. J. Cancer* **2009**, *101*, 2015−2022.

(12) Li, Y.; Wang, J.; Zhang, X.; Guo, W.; Li, F.; Yu, M.; Kong, X.; Wu, W.; Hong, Z. Highly Water-Soluble and Tumor-Targeted Photosensitizers for Photodynamic Therapy. *Org. Biomol. Chem.* **2015**, *13*, 7681−7694.

(13) Celli, J. P.; Spring, B. Q.; Rizvi, I.; Evans, C. L.; Samkoe, K. S.; Verma, S.; Pogue, B. W.; Hasan, T. Imaging and Photodynamic Therapy: Mechanisms, Monitoring, and Optimization. *Chem. Rev.* **2010**, *110*, 2795−2838.

(14) Kharroubi Lakouas, D.; Huglo, D.; Mordon, S.; Vermandel, M. Nuclear Medicine for Photodynamic Therapy in Cancer: Planning, Monitoring and Nuclear PDT. *Photodiagn. Photodyn. Ther.* **2017**, *18*, 236−243.

(15) Jokerst, J. V.; Lobovkina, T.; Zare, R. N.; Gambhir, S. S. Nanoparticle PEGylation for Imaging and Therapy. *Nanomedicine* **2011**, *6*, 715−728.

(16) Crawley, N.; Thompson, M.; Romaschin, A. Theranostics in the Growing Field of Personalized Medicine: An Analytical Chemistry Perspective. *Anal. Chem.* **2014**, *86*, 130−160.

(17) Kelkar, S. S.; Reineke, T. M. Theranostics: Combining Imaging and Therapy. *Bioconjugate Chem.* **2011**, *22*, 1879−1903.

(18) Terreno, E.; Uggeri, F.; Aime, S. Image Guided Therapy: The Advent of Theranostic Agents. *J. Controlled Release* **2012**, *161*, 328−337.

(19) Yoon, H. Y.; Jeon, S.; You, D. G.; Park, J. H.; Kwon, I. C.; Koo, H.; Kim, K. Inorganic Nanoparticles for Image-Guided Therapy. *Bioconjugate Chem.* **2017**, *28*, 124−134.

(20) Jenni, S.; Sour, A. Molecular Theranostic Agents for Photodynamic Therapy (PDT) and Magnetic Resonance Imaging (MRI). *Inorganics* **2019**, *7*, 10.

(21) Dougherty, T. J. Hematoporphyrin Derivative for Detection and Treatment of Cancer. *J. Surg. Oncol.* **1980**, *15*, 209−210.

(22) Allison, R. R. Photodynamic Therapy: Oncologic Horizons. *Future Oncol.* **2014**, *10*, 123−142.

(23) Calin, M. A.; Parasca, S. V. Photodynamic Therapy in Oncology. *J. Optoelectron. Adv. Mater.* **2006**, *8*, 1173−1179.

(24) Verma, S.; Watt, G. M.; Mai, Z.; Hasan, T. Strategies for Enhanced Photodynamic Therapy Effects. *Photochem. Photobiol.* **2007**, *83*, 996−1005.

(25) Spring, B. Q.; Abu-Yousif, A. O.; Palanisami, A.; Rizvi, I.; Zheng, X.; Mai, Z.; Anbil, S.; Sears, R. B.; Mensah, L. B.; Goldschmidt, R.; Erdem, S. S.; Oliva, E.; Hasan, T. Selective Treatment and Monitoring of Disseminated Cancer Micrometastases in Vivo Using Dual-Function, Activatable Immunoconjugates. *Proc. Natl. Acad. Sci. U. S. A.* **2014**, *111*, E933−E942.

(26) Chilakamarthi, U.; Giribabu, L. Photodynamic Therapy: Past, Present and Future. *Chem. Rec.* **2017**, *17*, 775−802.

(27) Juarranz, Á.; Jaén, P.; Sanz-Rodríguez, F.; Cuevas, J.; González, S. Photodynamic Therapy of Cancer. Basic Principles and Applications. *Clin. Transl. Oncol.* **2008**, *10*, 148−154.

(28) Huang, P.; Lin, J.; Wang, S.; Zhou, Z.; Li, Z.; Wang, Z.; Zhang, C.; Yue, X.; Niu, G.; Yang, M.; Cui, D.; Chen, X. Photosensitizer-Conjugated Silica-Coated Gold Nanoclusters for Fluorescence Imaging-Guided Photodynamic Therapy. *Biomaterials* **2013**, *34*, 4643−4654.

(29) Chen, R.; Zhang, L.; Gao, J.; Wu, W.; Hu, Y.; Jiang, X. Chemiluminescent Nanomicelles for Imaging Hydrogen Peroxide and Self-Therapy in Photodynamic Therapy. *J. Biomed. Biotechnol.* **2011**, *2011*, 1.

(30) Iranifam, M. Analytical Applications of Chemiluminescence Methods for Cancer Detection and Therapy. *TrAC, Trends Anal. Chem.* **2014**, *59*, 156−183.

(31) Laptev, R.; Nisnevitch, M.; Siboni, G.; Malik, Z.; Firer, M. A. Intracellular Chemiluminescence Activates Targeted Photodynamic Destruction of Leukaemic Cells. *Br. J. Cancer* **2006**, *95*, 189−196.

(32) Theodossiou, T.; Hothersall, J. S.; Woods, E. A.; Okkenhaug, K.; Jacobson, J.; MacRobert, A. J. Firefly Luciferin-Activated Rose Bengal: In Vitro Photodynamic Therapy by Intracellular Chemiluminescence in Transgenic NIH 3T3 Cells. *Cancer Res.* **2003**, *63*, 1818−1821.

(33) Calixto, G.; Bernegossi, J.; de Freitas, L.; Fontana, C.; Chorilli, M. Nanotechnology-Based Drug Delivery Systems for Photodynamic Therapy of Cancer: A Review. *Molecules* **2016**, *21*, 342.

(34) Agostinis, P.; Berg, K.; Cengel, K. A.; Foster, T. H.; Girotti, A. W.; Gollnick, S. O.; Hahn, S. M.; Hamblin, M. R.; Juzeniene, A.; Kessel, D.; Korbelik, M.; Moan, J.; Mroz, P.; Nowis, D.; Piette, J.;

https://dx.doi.org/10.1021/acs.jmedchem.0c00047
J. Med. Chem. 2020, 63, 14119−14150

Wilson, B. C.; Golab, J. Photodynamic Therapy of Cancer: An Update. *Ca-Cancer J. Clin.* **2011**, *61*, 250−281.
(35) Zheng, Y.; Yin, G.; Le, V.; Zhang, A.; Lu, Y.; Yang, M.; Fei, Z.; Liu, J. Hypericin-Based Photodynamic Therapy Induces a Tumor-Specific Immune Response and an Effective DC-Based Cancer Immunotherapy. *Biochem. Pharmacol.* **2014**, 1.
(36) Theodossiou, T. A.; Hothersall, J. S.; De Witte, P. A.; Pantos, A.; Agostinis, P. The Multifaceted Photocytotoxic Profile of Hypericin. *Mol. Pharmaceutics* **2009**, *6*, 1775−1789.
(37) Liu, X.; Jiang, C.; Li, Y.; Liu, W.; Yao, N.; Gao, M.; Ji, Y.; Huang, D.; Yin, Z.; Sun, Z.; Ni, Y.; Zhang, J. Evaluation of Hypericin: Effect of Aggregation on Targeting Biodistribution. *J. Pharm. Sci.* **2015**, *104*, 215−222.
(38) Ghosh, S.; Banerjee, S.; Sil, P. C. The Beneficial Role of Curcumin on Inflammation, Diabetes and Neurodegenerative Disease: A Recent Update. *Food Chem. Toxicol.* **2015**, *83*, 111−124.
(39) Wikene, K. O.; Hegge, A. B.; Bruzell, E.; Tonnesen, H. H. Formulation and Characterization of Lyophilized Curcumin Solid Dispersions for Antimicrobial Photodynamic Therapy (Apdt): Studies on Curcumin and Curcuminoids LII. *Drug Dev. Ind. Pharm.* **2015**, *41*, 969−977.
(40) Bernd, A. Visible Light And/Or UVA Offer a Strong Amplification of the Anti-Tumor Effect of Curcumin. *Phytochem. Rev.* **2014**, *13*, 183−189.
(41) Leite, D. P. V.; Paolillo, F. R.; Parmesano, T. N.; Fontana, C. R.; Bagnato, V. S. Effects of Photodynamic Therapy With Blue Light and Curcumin as Mouth Rinse for Oral Disinfection: A Randomized Controlled Trial. *Photomed. Laser Surg.* **2014**, *32*, 627−632.
(42) Li, T.; Hou, X.; Deng, H.; Zhao, J.; Huang, N.; Zeng, J.; Chen, H.; Gu, Y. Liposomal Hypocrellin B as a Potential Photosensitizer for Age-Related Macular Degeneration: Pharmacokinetics, Photodynamic Efficacy, and Skin Phototoxicity in Vivo. *Photochem. Photobiol. Sci.* **2015**, *14*, 972−981.
(43) Zhenjun, D.; Lown, J. W. Hypocrellins and Their Use in Photosensitization. *Photochem. Photobiol.* **1990**, *52*, 609−616.
(44) Makdoumi, K.; Bäckman, A.; Mortensen, J.; Crafoord, S. Evaluation of Antibacterial Efficacy of Photo-Activated Riboflavin Using Ultraviolet Light (UVA). *Graefe's Arch. Clin. Exp. Ophthalmol.* **2010**, *248*, 207−212.
(45) Ettinger, A.; Miklauz, M. M.; Bihm, D. J.; Maldonado-Codina, G.; Goodrich, R. P. Preparation of Cryoprecipitate from Riboflavin and UV Light-Treated Plasma. *Transfus. Apher. Sci.* **2012**, *46*, 153−158.
(46) Papaioannou, L.; Miligkos, M.; Papathanassiou, M. Corneal Collagen Cross-Linking for Infectious Keratitis: A Systematic Review and Meta-Analysis. *Cornea* **2016**, *35*, 62−71.
(47) Maisch, T.; Eichner, A.; Späth, A.; Gollmer, A.; König, B.; Regensburger, J.; Bäumler, W. Fast and Effective Photodynamic Inactivation of Multiresistant Bacteria by Cationic Riboflavin Derivatives. *PLoS One* **2014**, *9*, e111792.
(48) Wainwright, M.; Crossley, K. B. Methylene Blue - a Therapeutic Dye for All Seasons? *J. Chemother.* **2002**, *14*, 431−443.
(49) Tseng, S. P.; Hung, W. C.; Chen, H. J.; Lin, Y. T.; Jiang, H. S.; Chiu, H. C.; Hsueh, P. R.; Teng, L. J.; Tsai, J. C. Effects of Toluidine Blue O (Tbo)-Photodynamic Inactivation on Community-Associated Methicillin-Resistant Staphylococcus Aureus Isolates. *J. Microbiol. Immunol. Infect.* **2017**, *50*, 46−54.
(50) Tardivo, J. P.; Adami, F.; Correa, J. A.; Pinhal, M. A. S.; Baptista, M. S. A Clinical Trial Testing the Efficacy of PDT in Preventing Amputation in Diabetic Patients. *Photodiagn. Photodyn. Ther.* **2014**, *11*, 342−350.
(51) Graciano, T. B.; Coutinho, T. S.; Cressoni, C. B.; Freitas, C. de P.; Pierre, M. B. R.; de Lima Pereira, S. A.; Shimano, M. M.; Cristina da Cunha Frange, R.; Garcia, M. T. J. Using Chitosan Gels as a Toluidine Blue O Delivery System for Photodynamic Therapy of Buccal Cancer: In Vitro and in Vivo Studies. *Photodiagn. Photodyn. Ther.* **2015**, *12*, 98−107.
(52) Costa, A. C. B. P.; Rasteiro, V. M. C.; Pereira, C. A.; Rossoni, R. D.; Junqueira, J. C.; Jorge, A. O. C. The Effects of Rose Bengal- and Erythrosine-Mediated Photodynamic Therapy on Candida Albicans. *Mycoses* **2012**, *55*, 56−63.
(53) Xu, N.; Yao, M.; Farinelli, W.; Hajjarian, Z.; Wang, Y.; Redmond, R. W.; Kochevar, I. E. Light-Activated Sealing of Skin Wounds. *Lasers Surg. Med.* **2015**, *47*, 17−29.
(54) Panzarini, E.; Inguscio, V.; Fimia, G. M.; Dini, L. Rose Bengal Acetate PhotoDynamic Therapy (RBAc-PDT) Induces Exposure and Release of Damage-Associated Molecular Patterns (DAMPs) in Human HeLa Cells. *PLoS One* **2014**, *9*, e105778.
(55) Boens, N.; Leen, V.; Dehaen, W. Fluorescent Indicators Based on Bodipy. *Chem. Soc. Rev.* **2012**, *41*, 1130−1172.
(56) Kamkaew, A.; Lim, S. H.; Lee, H. B.; Kiew, L. V.; Chung, L. Y.; Burgess, K. BODIPY Dyes in Photodynamic Therapy. *Chem. Soc. Rev.* **2013**, *42*, 77−88.
(57) Segado, M.; Reguero, M. Mechanism of the Photochemical Process of Singlet Oxygen Production by Phenalenone. *Phys. Chem. Chem. Phys.* **2011**, *13*, 4138.
(58) Cieplik, F.; Späth, A.; Regensburger, J.; Gollmer, A.; Tabenski, L.; Hiller, K. A.; Bäumler, W.; Maisch, T.; Schmalz, G. Photodynamic Biofilm Inactivation by SAPYR - an Exclusive Singlet Oxygen Photosensitizer. *Free Radical Biol. Med.* **2013**, *65*, 477−487.
(59) Späth, A.; Leibl, C.; Cieplik, F.; Lehner, K.; Regensburger, J.; Hiller, K. A.; Bäumler, W.; Schmalz, G.; Maisch, T. Improving Photodynamic Inactivation of Bacteria in Dentistry: Highly Effective and Fast Killing of Oral Key Pathogens With Novel Tooth-Colored Type-II Photosensitizers. *J. Med. Chem.* **2014**, *57*, 5157−5168.
(60) Gill, M. R.; Thomas, J. A. Ruthenium(II) Polypyridyl Complexes and DNA - From Structural Probes to Cellular Imaging and Therapeutics. *Chem. Soc. Rev.* **2012**, *41*, 3179−3192.
(61) Fong, J.; Kasimova, K.; Arenas, Y.; Kaspler, P.; Lazic, S.; Mandel, A.; Lilge, L. A Novel Class of Ruthenium-Based Photosensitizers Effectively Kills In Vitro Cancer Cells and In Vivo Tumors. *Photochem. Photobiol. Sci.* **2015**, *14*, 2014−2023.
(62) Angeles-Boza, A. M.; Bradley, P. M.; Fu, P. K. L.; Wicke, S. E.; Bacsa, J.; Dunbar, K. R.; Turro, C. Dna Binding and Photocleavage in Vitro by New Dirhodium(II) Dppz Complexes: Correlation to Cytotoxicity and Photocytotoxicity. *Inorg. Chem.* **2004**, *43*, 8510−8519.
(63) Li, Y.; Tan, C.-P.; Zhang, W.; He, L.; Ji, L.-N.; Mao, Z.-W. Phosphorescent Iridium(III)-Bis-N-Heterocyclic Carbene Complexes as Mitochondria-Targeted Theranostic and Photodynamic Anticancer Agents. *Biomaterials* **2015**, *39*, 95−104.
(64) To, W. P.; Zou, T.; Sun, R. W. Y.; Che, C. M. Light-Induced Catalytic and Cytotoxic Properties of Phosphorescent Transition Metal Compounds with a D8 Electronic Configuration. *Philos. Trans. R. Soc., A* **2013**, *371*, 20120126.
(65) Senge, M. O. MTHPC - A Drug on Its Way from Second to Third Generation Photosensitizer? *Photodiagnosis Photodyn. Photodiagn. Photodyn. Ther.* **2012**, *9*, 170−179.
(66) Anand, S.; Ortel, B. J.; Pereira, S. P.; Hasan, T.; Maytin, E. V. Biomodulatory Approaches to Photodynamic Therapy for Solid Tumors. *Cancer Lett.* **2012**, *326*, 8−16.
(67) Byrne, A. T.; O'Connor, A. E.; Hall, M.; Murtagh, J.; O'Neill, K.; Curran, K. M.; Mongrain, K.; Rousseau, J. A.; Lecomte, R.; McGee, S.; Callanan, J. J.; O'Shea, D. F.; Gallagher, W. M. Vascular-Targeted Photodynamic Therapy With BF2-Chelated Tetraaryl-Azadipyrromethene Agents: A Multi-Modality Molecular Imaging Approach to Therapeutic Assessment. *Br. J. Cancer* **2009**, *101*, 1565−1573.
(68) Huang, Z.; Xu, H.; Meyers, A. D.; Musani, A. I.; Wang, L.; Tagg, R.; Barqawi, A. B.; Chen, Y. K. Photodynamic Therapy for Treatment of Solid Tumors - Potential and Technical Challenges. *Technol. Cancer Res. Treat.* **2008**, *7* (4), 309−320.
(69) Foote, C. S. Mechanisms of Photosensitized Oxidation. *Science* **1968**, *162*, 963−970.
(70) Ormond, A. B.; Freeman, H. S. Dye Sensitizers for Photodynamic Therapy. *Materials* **2013**, *6*, 817−840.
(71) Pereira, N. A. M.; Serra, A. C.; Pinho e Melo, T. M. V. D. Novel Approach to Chlorins and Bacteriochlorins: [8π+2π] Cycloaddition

https://dx.doi.org/10.1021/acs.jmedchem.0c00047
J. Med. Chem. 2020, 63, 14119−14150

of Diazafulvenium Methides with Porphyrins. *Eur. J. Org. Chem.* **2010**, *2010*, 6539−6543.
(72) Forouzanfar, M. H.; et al. Global, Regional, and National Comparative Risk Assessment of 79 Behavioural, Environmental and Occupational, and Metabolic Risks or Clusters of Risks in 188 Countries, 1990−2013: A Systematic Analysis for the Global Burden of Disease Study 2013. *Lancet* **2015**, *386*, 2287−2323.
(73) Baskaran, R.; Lee, J.; Yang, S.-G. Clinical Development of Photodynamic Agents and Therapeutic Applications. *Biomater. Res.* **2018**, *22*, 1.
(74) Lovell, J. F.; Liu, T. W. B.; Chen, J.; Zheng, G. Activatable Photosensitizers for Imaging and Therapy. *Chem. Rev.* **2010**, *110*, 2839−2857.
(75) Derycke, A. S. L.; De Witte, P. A. M. Liposomes for Photodynamic Therapy. *Adv. Drug Delivery Rev.* **2004**, *56*, 17−30.
(76) Postigo, F.; Mora, M.; De Madariaga, M. A.; Nonell, S.; Sagristá, M. L. Incorporation of Hydrophobic Porphyrins Into Liposomes: Characterization and Structural Requirements. *Int. J. Pharm.* **2004**, *278*, 239−254.
(77) Park, W.; Park, S.-J.; Cho, S.; Shin, H.; Jung, Y.-S.; Lee, B.; Na, K.; Kim, D.-H. Intermolecular Structural Change for Thermoswitchable Polymeric Photosensitizer. *J. Am. Chem. Soc.* **2016**, *138*, 10734−10737.
(78) Lee, C. S.; Na, K. Photochemically Triggered Cytosolic Drug Delivery Using PH-Responsive Hyaluronic Acid Nanoparticles for Light-Induced Cancer Therapy. *Biomacromolecules* **2014**, *15*, 4228−4238.
(79) Kim, K.; Lee, C. S.; Na, K. Light-Controlled Reactive Oxygen Species (ROS)-Producible Polymeric Micelles with Simultaneous Drug-Release Triggering and Endo/Lysosomal Escape. *Chem. Commun.* **2016**, *52*, 2839−2842.
(80) Park, S.; Park, W.; Na, K. Tumor Intracellular-Environment Responsive Materials Shielded Nano-Complexes for Highly Efficient Light-Triggered Gene Delivery without Cargo Gene Damage. *Adv. Funct. Mater.* **2015**, *25*, 3472−3482.
(81) Jo, Y.-u.; Lee, C. B.; Bae, S. K.; Na, K. Acetylated Hyaluronic Acid-Poly(L-Lactic Acid) Conjugate Nanoparticles for Inhibition of Doxorubicinol Production from Doxorubicin. *Macromol. Res.* **2020**, *28*, 67−73.
(82) Kim, J.; Kim, K. S.; Park, S. J.; Na, K. Vitamin Bc-Bearing Hydrophilic Photosensitizer Conjugate for Photodynamic Cancer Theranostics. *Macromol. Biosci.* **2015**, *15*, 1081−1090.
(83) Temizel, E.; Sagir, T.; Ayan, E.; Isik, S.; Ozturk, R. Delivery of Lipophilic Porphyrin by Liposome Vehicles: Preparation and Photodynamic Therapy Activity Against Cancer Cell Lines. *Photodiagn. Photodyn. Ther.* **2014**, *11*, 537−545.
(84) Master, A.; Livingston, M.; Sen Gupta, A. Photodynamic Nanomedicine in the Treatment of Solid Tumors: Perspectives and Challenges. *J. Controlled Release* **2013**, *168*, 88−102.
(85) Ogawara, K. I.; Higaki, K. Nanoparticle-Based Photodynamic Therapy: Current Status and Future Application to Improve Outcomes of Cancer Treatment. *Chem. Pharm. Bull.* **2017**, *65*, 637−641.
(86) Tada, D. B.; Baptista, M. S. Photosensitizing Nanoparticles and the Modulation of ROS Generation. *Front. Chem.* **2015**, *3*, 33.
(87) Konan, Y. N.; Gurny, R.; Allémann, E. State of the Art in the Delivery of Photosensitizers for Photodynamic Therapy. *J. Photochem. Photobiol., B* **2002**, *66*, 89−106.
(88) Paszko, E.; Ehrhardt, C.; Senge, M. O.; Kelleher, D. P.; Reynolds, J. V. Nanodrug Applications in Photodynamic Therapy. *Photodiagn. Photodyn. Ther.* **2011**, *8*, 14−29.
(89) Sumer, B.; Gao, J. Theranostic Nanomedicine for Cancer. *Nanomedicine* **2008**, *3*, 137−140.
(90) Koning, Gerben A.; Krijger, Gerard C. Targeted Multifunctional Lipid-Based Nanocarriers for Image-Guided Drug Delivery. *Anti-Cancer Agents Med. Chem.* **2007**, *7*, 425−440.
(91) Batista, C. A. S.; Larson, R. G.; Kotov, N. A. Nonadditivity of Nanoparticle Interactions. *Science* **2015**, *350*, 1242477.
(92) Gmeiner, W. H.; Ghosh, S. Nanotechnology for Cancer Treatment. *Nanotechnol. Rev.* **2014**, *3*, 111−122.
(93) Elias, D. R.; Poloukhtine, A.; Popik, V.; Tsourkas, A. Effect of Ligand Density, Receptor Density, and Nanoparticle Size on Cell Targeting. *Nanomedicine* **2013**, *9*, 194−201.
(94) Sarpaki, S. *Investigations into the Radiochemistry of Gallium- and Fluorine-Containing Compounds for Molecular Imaging Applications*, Ph.D. Thesis, University of Bath: England, 2018.
(95) Liu, T. W.; MacDonald, T. D.; Jin, C. S.; Gold, J. M.; Bristow, R. G.; Wilson, B. C.; Zheng, G. Inherently Multimodal Nanoparticle-Driven Tracking and Real-Time Delineation of Orthotopic Prostate Tumors and Micrometastases. *ACS Nano* **2013**, *7*, 4221−4232.
(96) Mitchell, N.; Kalber, T. L.; Cooper, M. S.; Sunassee, K.; Chalker, S. L.; Shaw, K. P.; Ordidge, K. L.; Badar, A.; Janes, S. M.; Blower, P. J.; Lythgoe, M. F.; Hailes, H. C.; Tabor, A. B. Incorporation of Paramagnetic, Fluorescent and PET/SPECT Contrast Agents Into Liposomes for Multimodal Imaging. *Biomaterials* **2013**, *34*, 1179−1192.
(97) Zhang, R.; Huang, M.; Zhou, M.; Wen, X.; Huang, Q.; Li, C. Annexin A5-Functionalized Nanoparticle for Multimodal Imaging of Cell Death. *Mol. Imaging* **2013**, *12*, 7290.2012.00032.
(98) Liu, T. W.; MacDonald, T. D.; Shi, J.; Wilson, B. C.; Zheng, G. Intrinsically Copper-64-Labeled Organic Nanoparticles as Radiotracers. *Angew. Chem., Int. Ed.* **2012**, *51*, 13128−13131.
(99) Janib, S. M.; Moses, A. S.; MacKay, J. A. Imaging and Drug Delivery Using Theranostic Nanoparticles. *Adv. Drug Delivery Rev.* **2010**, *62*, 1052−1063.
(100) McCarthy, J. R.; Weissleder, R. Multifunctional Magnetic Nanoparticles for Targeted Imaging and Therapy. *Adv. Drug Delivery Rev.* **2008**, *60*, 1241−1251.
(101) McCarthy, J. R. The Future of Theranostic Nanoagents. *Nanomedicine* **2009**, *4*, 693−695.
(102) Summer, D.; Grossrubatscher, L.; Petrik, M.; Michalcikova, T.; Novy, Z.; Rangger, C.; Klingler, M.; Haas, H.; Kaeopookum, P.; Von Guggenberg, E.; Haubner, R.; Decristoforo, C. Developing Targeted Hybrid Imaging Probes by Chelator Scaffolding. *Bioconjugate Chem.* **2017**, *28*, 1722−1733.
(103) Iyer, A. K.; Greish, K.; Seki, T.; Okazaki, S.; Fang, J.; Takeshita, K.; Maeda, H. Polymeric Micelles of Zinc Protoporphyrin for Tumor Targeted Delivery Based on EPR Effect and Singlet Oxygen Generation. *J. Drug Target.* **2007**, *15*, 496−506.
(104) Maeda, H.; Greish, K.; Fang, J. The EPR Effect and Polymeric Drugs: A Paradigm Shift for Cancer Chemotherapy in the 21st Century. *Adv. Polym. Sci.* **2005**, *193*, 103−121.
(105) Cai, W.; Chen, X. Multimodality Molecular Imaging of Tumor Angiogenesis. *J. Nucl. Med.* **2008**, *49*, 113−128.
(106) Haglund, E.; Seale-Goldsmith, M. M.; Leary, J. F. Design of Multifunctional Nanomedical Systems. *Ann. Biomed. Eng.* **2009**, *37*, 2048−2063.
(107) Svenskaya, Y.; Parakhonskiy, B.; Haase, A.; Atkin, V.; Lukyanets, E.; Gorin, D.; Antolini, R. Anticancer Drug Delivery System Based on Calcium Carbonate Particles Loaded with a Photosensitizer. *Biophys. Chem.* **2013**, *182*, 11−15.
(108) Cheng, L.; Wang, C.; Feng, L.; Yang, K.; Liu, Z. Functional Nanomaterials for Phototherapies of Cancer. *Chem. Rev.* **2014**, *114*, 10869−10939.
(109) Ding, D.; Guo, W.; Guo, C.; Sun, J.; Zheng, N.; Wang, F.; Yan, M.; Liu, S. MoO3-X Quantum Dots for Photoacoustic Imaging Guided Photothermal/Photodynamic Cancer Treatment. *Nanoscale* **2017**, *9*, 2020−2029.
(110) Lu, K.; He, C.; Lin, W. Nanoscale Metal-Organic Framework for Highly Effective Photodynamic Therapy of Resistant Head and Neck Cancer. *J. Am. Chem. Soc.* **2014**, *136*, 16712−16715.
(111) Liu, J.; Yang, Y.; Zhu, W.; Yi, X.; Dong, Z.; Xu, X.; Chen, M.; Yang, K.; Lu, G.; Jiang, L.; Liu, Z. Nanoscale Metal-Organic Frameworks for Combined Photodynamic & Radiation Therapy in Cancer Treatment. *Biomaterials* **2016**, *97*, 1−9.
(112) Sansaloni-Pastor, S.; Bouilloux, J.; Lange, N. The Dark Side: Photosensitizer Prodrugs. *Pharmaceuticals* **2019**, *12* (4), 148.

https://dx.doi.org/10.1021/acs.jmedchem.0c00047
J. Med. Chem. 2020, 63, 14119−14150

(113) Lovell, J. F.; Jin, C. S.; Huynh, E.; Jin, H.; Kim, C.; Rubinstein, J. L.; Chan, W. C. W.; Cao, W.; Wang, L. V.; Zheng, G. Porphysome Nanovesicles Generated by Porphyrin Bilayers for Use as Multimodal Biophotonic Contrast Agents. *Nat. Mater.* **2011**, *10*, 324−332.
(114) Waghorn, P. A. Radiolabelled Porphyrins in Nuclear Medicine. *J. Labelled Compd. Radiopharm.* **2014**, *57*, 304−309.
(115) Ng, K. K.; Takada, M.; Jin, C. C. S.; Zheng, G. Self-Sensing Porphysomes for Fluorescence-Guided Photothermal Therapy. *Bioconjugate Chem.* **2015**, *26*, 345−351.
(116) Allison, R. R.; Bagnato, V. S.; Sibata, C. H. Future of Oncologic Photodynamic Therapy. *Future Oncol.* **2010**, *6*, 929−940.
(117) Wieder, M. E.; Hone, D. C.; Cook, M. J.; Handsley, M. M.; Gavrilovic, J.; Russell, D. A. Intracellular Photodynamic Therapy With Photosensitizer-Nanoparticle Conjugates: Cancer Therapy Using a 'Trojan Horse.'. *Photochem. Photobiol. Sci.* **2006**, *5*, 727−734.
(118) Samia, A. C. S.; Chen, X.; Burda, C. Semiconductor Quantum Dots for Photodynamic Therapy. *J. Am. Chem. Soc.* **2003**, *125*, 15736−15737.
(119) Jaiswal, J. K.; Mattoussi, H.; Mauro, J. M.; Simon, S. M. Long-Term Multiple Color Imaging of Live Cells Using Quantum Dot Bioconjugates. *Nat. Biotechnol.* **2003**, *21*, 47−51.
(120) Lira, R. B.; Seabra, M. A. B. L.; Matos, A. L. L.; Vasconcelos, J. V.; Bezerra, D. P.; De Paula, E.; Santos, B. S.; Fontes, A. Studies on Intracellular Delivery of Carboxyl-Coated CdTe Quantum Dots Mediated by Fusogenic Liposomes. *J. Mater. Chem. B* **2013**, *1*, 4297−4305.
(121) Jhonsi, M. A.; Renganathan, R. Investigations on the Photoinduced Interaction of Water Soluble Thioglycolic Acid (TGA) Capped CdTe Quantum Dots with Certain Porphyrins. *J. Colloid Interface Sci.* **2010**, *344*, 596−602.
(122) Li, L.; Zhao, J. F.; Won, N.; Jin, H.; Kim, S.; Chen, J. Y. Quantum Dot - Aluminum Phthalocyanine Conjugates Perform Photodynamic Reactions to Kill Cancer Cells via Fluorescence Resonance Energy Transfer (FRET). *Nanoscale Res. Lett.* **2012**, *7*, 386.
(123) Rakovich, A.; Savateeva, D.; Rakovich, T.; Donegan, J. F.; Rakovich, Y. P.; Kelly, V.; Lesnyak, V.; Eychmüller, A. CdTe Quantum Dot/Dye Hybrid System as Photosensitizer for Photodynamic Therapy. *Nanoscale Res. Lett.* **2010**, *5*, 753−760.
(124) Tsay, J. M.; Trzoss, M.; Shi, L.; Kong, X.; Selke, M.; Jung, M. E.; Weiss, S. Singlet Oxygen Production by Peptide-Coated Quantum Dot-Photosensitizer Conjugates. *J. Am. Chem. Soc.* **2007**, *129*, 6865−6871.
(125) Wen, Y. N.; Song, W. S.; An, L. M.; Liu, Y. Q.; Wang, Y. H.; Yang, Y. Q. Activation of Porphyrin Photosensitizers by Semiconductor Quantum Dots via Two-Photon Excitation. *Appl. Phys. Lett.* **2009**, *95*, 143702.
(126) Chen, J. Y.; Lee, Y. M.; Zhao, D.; Mak, N. K.; Wong, R. N. S.; Chan, W. H.; Cheung, N. H. Quantum Dot-Mediated Photoproduction of Reactive Oxygen Species for Cancer Cell Annihilation. *Photochem. Photobiol.* **2010**, *86*, 431−437.
(127) Wang, R. gui; Zhao, M. yao; Deng, D.; Ye, X.; Zhang, F.; Chen, H.; Kong, J. lie An Intelligent and Biocompatible Photosensitizer Conjugated Silicon Quantum Dots-MnO2 Nanosystem for Fluorescence Imaging-Guided Efficient Photodynamic Therapy. *J. Mater. Chem. B* **2018**, *6*, 4592−4601.
(128) Biju, V.; Itoh, T.; Ishikawa, M. Delivering Quantum Dots to Cells: Bioconjugated Quantum Dots for Targeted and Nonspecific Extracellular and Intracellular Imaging. *Chem. Soc. Rev.* **2010**, *39*, 3031−3056.
(129) Viana, O. S.; Ribeiro, M. S.; Fontes, A.; Santos, B. S. Quantum Dots in Photodynamic Therapy. In *Oxidative Stress in Applied Basic Research and Clinical Practice*; Springer International Publishing: Switzerland, 2016; pp 525−539.
(130) Din, F. U.; Aman, W.; Ullah, I.; Qureshi, O. S.; Mustapha, O.; Shafique, S.; Zeb, A. Effective Use of Nanocarriers as Drug Delivery Systems for the Treatment of Selected Tumors. *Int. J. Nanomed.* **2017**, *12*, 7291−7309.
(131) Lombardo, D.; Kiselev, M. A.; Caccamo, M. T. Smart Nanoparticles for Drug Delivery Application: Development of Versatile Nanocarrier Platforms in Biotechnology and Nanomedicine. *J. Nanomater.* **2019**, *2019*, 1.
(132) Singh, R.; Lillard, J. W. Nanoparticle-Based Targeted Drug Delivery. *Exp. Mol. Pathol.* **2009**, *86*, 215−223.
(133) Gupta, A.; Avci, P.; Sadasivam, M.; Chandran, R.; Parizotto, N.; Vecchio, D.; de Melo, W. C. M. A.; Dai, T.; Chiang, L. Y.; Hamblin, M. R. Shining Light on Nanotechnology to Help Repair and Regeneration. *Biotechnol. Adv.* **2013**, *31*, 607−631.
(134) Bechet, D.; Couleaud, P.; Frochot, C.; Viriot, M. L.; Guillemin, F.; Barberi-Heyob, M. Nanoparticles as Vehicles for Delivery of Photodynamic Therapy Agents. *Trends Biotechnol.* **2008**, *26*, 612−621.
(135) Huang, P.; Li, Z.; Lin, J.; Yang, D.; Gao, G.; Xu, C.; Bao, L.; Zhang, C.; Wang, K.; Song, H. Photosensitizer-Conjugated Magnetic Nanoparticles for in Vivo Simultaneous Magnetofluorescent Imaging and Targeting Therapy. *Biomaterials* **2011**, *32*, 3447−3458.
(136) Sun, Y.; Chen, Z. L.; Yang, X. X.; Huang, P.; Zhou, X. P.; Du, X. X. Magnetic Chitosan Nanoparticles as a Drug Delivery System for Targeting Photodynamic Therapy. *Nanotechnology* **2009**, *20*, 135102.
(137) Wang, S.; Gao, R.; Zhou, F.; Selke, M. Nanomaterials and Singlet Oxygen Photosensitizers: Potential Applications in Photodynamic Therapy. *J. Mater. Chem.* **2004**, *14*, 487−493.
(138) Huang, P.; Xu, C.; Lin, J.; Wang, C.; Wang, X.; Zhang, C.; Zhou, X.; Guo, S.; Cui, D. Folic Acid-Conjugated Graphene Oxide Loaded With Photosensitizers for Targeting Photodynamic Therapy. *Theranostics* **2011**, *1*, 2240−250.
(139) Tomao, S. Albumin-Bound Formulation of Paclitaxel (Abraxane Abi-007) in the Treatment of Breast Cancer. *Int. J. Nanomed.* **2009**, *4*, 99−105.
(140) Malam, Y.; Loizidou, M.; Seifalian, A. M. Liposomes and Nanoparticles: Nanosized Vehicles for Drug Delivery in Cancer. *Trends Pharmacol. Sci.* **2009**, *30*, 592−599.
(141) Wilson, B. C.; Olivo, M.; Singh, G. Subcellular Localization of Photofrin and Aminolevulinic Acid and Photodynamic Cross-Resistance in Vitro in Radiation-Induced Fibrosarcoma Cells Sensitive or Resistant to Photofrin-Mediated Photodynamic Therapy. *Photochem. Photobiol.* **1997**, *65*, 166−176.
(142) Celli, J. P.; Solban, N.; Liang, A.; Pereira, S. P.; Hasan, T. Verteporfin-Based Photodynamic Therapy Overcomes Gemcitabine Insensitivity in a Panel of Pancreatic Cancer Cell Lines. *Lasers Surg. Med.* **2011**, *43*, 565−574.
(143) Mahalingam, S. M.; Ordaz, J. D.; Low, P. S. Targeting of a Photosensitizer to the Mitochondrion Enhances the Potency of Photodynamic Therapy. *ACS Omega* **2018**, *3*, 6066−6074.
(144) Zielonka, J.; Joseph, J.; Sikora, A.; Hardy, M.; Ouari, O.; Vasquez-Vivar, J.; Cheng, G.; Lopez, M.; Kalyanaraman, B. Mitochondria-Targeted Triphenylphosphonium-Based Compounds: Syntheses, Mechanisms of Action, and Therapeutic and Diagnostic Applications. *Chem. Rev.* **2017**, *117*, 10043−10120.
(145) Wang, H.; Gao, Z.; Liu, X.; Agarwal, P.; Zhao, S.; Conroy, D. W.; Ji, G.; Yu, J.; Jaroniec, C. P.; Liu, Z.; Lu, X.; Li, X.; He, X. Targeted Production of Reactive Oxygen Species in Mitochondria to Overcome Cancer Drug Resistance. *Nat. Commun.* **2018**, *9*, 1−16.
(146) Zhao, X.; Huang, Y.; Yuan, G.; Zuo, K.; Huang, Y.; Chen, J.; Li, J.; Xue, J. A Novel Tumor and Mitochondria Dual-Targeted Photosensitizer Showing Ultra-Efficient Photodynamic Anticancer Activities. *Chem. Commun.* **2019**, *55*, 866−869.
(147) Sibrian-Vazquez, M.; Nesterova, I. V.; Jensen, T. J.; Vicente, M. G. H. Mitochondria Targeting by Guanidine- and Biguanidine-Porphyrin Photosensitizers. *Bioconjugate Chem.* **2008**, *19*, 705−713.
(148) Canal, F.; Vicent, M. J.; Pasut, G.; Schiavon, O. Relevance of Folic Acid/Polymer Ratio in Targeted PEG-Epirubicin Conjugates. *J. Controlled Release* **2010**, *146*, 388−399.
(149) Farokhzad, O. C.; Langer, R. Impact of Nanotechnology on Drug Delivery. *ACS Nano* **2009**, *3*, 16−20.
(150) Lin, L.; Xiong, L.; Wen, Y.; Lei, S.; Deng, X.; Liu, Z.; Chen, W.; Miao, X. Active Targeting of Nano-Photosensitizer Delivery

Systems for Photodynamic Therapy of Cancer Stem Cells. *J. Biomed. Nanotechnol.* **2015**, *11*, 531−554.
(151) Chen, L.; Miao, W.; Tang, X.; Zhang, H.; Wang, S.; Luo, F.; Yan, J. Inhibitory Effect of Neuropilin-1 Monoclonal Antibody (NRP-1 MAB) on Glioma Tumor in Mice. *J. Biomed. Nanotechnol.* **2013**, *9*, 551−558.
(152) Zhang, Z.; Sun, Q.; Zhong, J.; Yang, Q.; Li, H.; Cheng, D.; Liang, B.; Shuai, X. Magnetic Resonance Imaging-Visible and PH-Sensitive Polymeric Micelles for Tumor Targeted Drug Delivery. *J. Biomed. Nanotechnol.* **2014**, *10*, 216−226.
(153) Kim, K. S.; Kim, J.; Kim, D. H.; Hwang, H. S.; Na, K. Multifunctional Trastuzumab-Chlorin E6 Conjugate for the Treatment of HER2-Positive Human Breast Cancer. *Biomater. Sci.* **2018**, *6*, 1217−1226.
(154) Mitri, Z.; Constantine, T.; O'Regan, R. The HER2 Receptor in Breast Cancer: Pathophysiology, Clinical Use, and New Advances in Therapy. *Chemother. Res. Pract.* **2012**, *2012*, 1−7.
(155) Kim, J.; Jo, Y. um; Na, K. Photodynamic Therapy with Smart Nanomedicine. *Arch. Pharmacal Res.* **2020**, *43*, 22−31.
(156) Kessel, D. The Role of Low-Density Lipoprotein in the Biodistribution of Photosensitizing Agents. *J. Photochem. Photobiol., B* **1992**, *14*, 261−262.
(157) Sibani, S. A.; McCarron, P. A.; Woolfson, A. D.; Donnelly, R. F. Photosensitiser Delivery for Photodynamic Therapy. Part 2: Systemic Carrier Platforms. *Expert Opin. Drug Delivery* **2008**, *5*, 1241−1254.
(158) Ke, M.-R.; Yeung, S.-L.; Ng, D. K. P.; Fong, W.-P.; Lo, P.-C. Preparation and In Vitro Photodynamic Activities of Folate-Conjugated Distyryl Boron Dipyrromethene Based Photosensitizers. *J. Med. Chem.* **2013**, *56*, 8475−8483.
(159) Cheung, A.; Bax, H. J.; Josephs, D. H.; Ilieva, K. M.; Pellizzari, G.; Opzoomer, J.; Bloomfield, J.; Fittall, M.; Grigoriadis, A.; Figini, M.; Canevari, S.; Spicer, J. F.; Tutt, A. N.; Karagiannis, S. N. Targeting Folate Receptor Alpha for Cancer Treatment. *Oncotarget* **2016**, *7*, 52553−52574.
(160) Savellano, M. D.; Hasan, T. Photochemical Targeting of Epidermal Growth Factor Receptor: A Mechanistic Study. *Clin. Cancer Res.* **2005**, *11*, 1658−1668.
(161) Choi, Y.; McCarthy, J. R.; Weissleder, R.; Tung, C. H. Conjugation of a Photosensitizer to an Oligoarginine-Based Cell-Penetrating Peptide Increases the Efficacy of Photodynamic Therapy. *ChemMedChem* **2006**, *1*, 458−463.
(162) Minchinton, A. I.; Tannock, I. F. Drug Penetration in Solid Tumours. *Nat. Rev. Cancer* **2006**, *6*, 583−592.
(163) Greish, K. Enhanced Permeability and Retention (Epr) Effect for Anticancer Nanomedicine Drug Targeting. *Methods Mol. Biol.* **2010**, *624*, 25−37.
(164) McNeil, S. E. Nanotechnology for the Biologist. *J. Leukocyte Biol.* **2005**, *78*, 585−594.
(165) Tanaka, M.; Kataoka, H.; Yano, S.; Ohi, H.; Moriwaki, K.; Akashi, H.; Taguchi, T.; Hayashi, N.; Hamano, S.; Mori, Y.; Kubota, E.; Tanida, S.; Joh, T. Antitumor Effects in Gastrointestinal Stromal Tumors Using Photodynamic Therapy With a Novel Glucose-Conjugated Chlorin. *Mol. Cancer Ther.* **2014**, *13*, 767−775.
(166) Jain, R. K. Delivery of Molecular and Cellular Medicine to Solid Tumors. *Adv. Drug Delivery Rev.* **2001**, *46*, 149−168.
(167) Decuzzi, P.; Causa, F.; Ferrari, M.; Netti, P. A. The Effective Dispersion of Nanovectors Within the Tumor Microvasculature. *Ann. Biomed. Eng.* **2006**, *34*, 633−641.
(168) Decuzzi, P.; Lee, S.; Bhushan, B.; Ferrari, M. A Theoretical Model for the Margination of Particles Within Blood Vessels. *Ann. Biomed. Eng.* **2005**, *33*, 179−190.
(169) Brigger, I.; Dubernet, C.; Couvreur, P. Nanoparticles in Cancer Therapy and Diagnosis. *Adv. Drug Delivery Rev.* **2002**, *54*, 631−651.
(170) Higgins, L. J.; Pomper, M. G. The Evolution of Imaging in Cancer: Current State and Future Challenges. *Semin. Oncol.* **2011**, *38*, 3−15.
(171) Rudin, M.; Rausch, M.; Stoeckli, M. Molecular Imaging in Drug Discovery and Development: Potential and Limitations of Nonnuclear Methods. *Mol. Imaging Biol.* **2005**, *7*, 5−13.
(172) Kopelman, R.; Lee Koo, Y. E.; Philbert, M.; Moffat, B. A.; Ramachandra Reddy, G.; McConville, P.; Hall, D. E.; Chenevert, T. L.; Bhojani, M. S.; Buck, S. M.; Rehemtulla, A.; Ross, B. D. Multifunctional Nanoparticle Platforms for in Vivo MRI Enhancement and Photodynamic Therapy of a Rat Brain Cancer. *J. Magn. Magn. Mater.* **2005**, *293*, 404−410.
(173) Abouelmagd, S. A.; Hyun, H.; Yeo, Y. Extracellularly Activatable Nanocarriers for Drug Delivery to Tumors. *Expert Opin. Drug Delivery* **2014**, *11*, 1601−1618.
(174) Misri, R.; Meier, D.; Yung, A. C.; Kozlowski, P.; Häfeli, U. O. Development and Evaluation of a Dual-Modality (MRI/SPECT) Molecular Imaging Bioprobe. *Nanomedicine* **2012**, *8*, 1007−1016.
(175) Yim, H.; Seo, S.; Na, K. MRI Contrast Agent-Based Multifunctional Materials: Diagnosis and Therapy. *J. Nanomater.* **2011**, *2011*, 1.
(176) Jerjes, W.; Upile, T.; Hamdoon, Z.; Nhembe, F.; Bhandari, R.; Mackay, S.; Shah, P.; Mosse, C. A.; AS Brookes, J.; Morley, S.; Hopper, C. Ultrasound-Guided Photodynamic Therapy for Deep Seated Pathologies: Prospective Study. *Lasers Surg. Med.* **2009**, *41*, 612−621.
(177) Eljamel, M. S.; Goodman, C.; Moseley, H. ALA and Photofrin Fluorescence-Guided Resection and Repetitive PDT in Glioblastoma Multiforme: A Single Centre Phase III Randomised Controlled Trial. *Lasers Med. Sci.* **2008**, *23*, 361−367.
(178) Mark, J. R.; Gelpi-Hammerschmidt, F.; Trabulsi, E. J.; Gomella, L. G. Blue Light Cystoscopy for Detection and Treatment of Non-Muscle Invasive Bladder Cancer. *Can. J. Urol.* **2012**, *19*, 6227−6231.
(179) Mallidi, S.; Spring, B. Q.; Chang, S.; Vakoc, B.; Hasan, T. Optical Imaging, Photodynamic Therapy and Optically Triggered Combination Treatments. *Cancer J. (Philadelphia, PA, U. S.)* **2015**, *21*, 194−205.
(180) Mallidi, S.; Anbil, S.; Lee, S.; Manstein, D.; Elrington, S.; Kositratna, G.; Schoenfeld, D.; Pogue, B.; Davis, S. J.; Hasan, T. Photosensitizer Fluorescence and Singlet Oxygen Luminescence as Dosimetric Predictors of Topical 5-Aminolevulinic Acid Photodynamic Therapy Nduced Clinical Erythema. *J. Biomed. Opt.* **2014**, *19*, 028001.
(181) Zhou, X.; Pogue, B. W.; Chen, B.; Demidenko, E.; Joshi, R.; Hoopes, J.; Hasan, T. Pretreatment Photosensitizer Dosimetry Reduces Variation in Tumor Response. *Int. J. Radiat. Oncol., Biol., Phys.* **2006**, *64*, 1211−1220.
(182) Zou, J.; Yin, Z.; Wang, P.; Chen, D.; Shao, J.; Zhang, Q.; Sun, L.; Huang, W.; Dong, X. Photosensitizer Synergistic Effects: D-A-D Structured Organic Molecule With Enhanced Fluorescence and Singlet Oxygen Quantum Yield for Photodynamic Therapy. *Chem. Sci.* **2018**, *9*, 2188−2194.
(183) Pereira, N. A. M.; Laranjo, M.; Casalta-Lopes, J.; Serra, A. C.; Piñeiro, M.; Pina, J.; Seixas de Melo, J. S.; Senge, M. O.; Botelho, M. F.; Martelo, L.; Burrows, H. D.; Pinho E Melo, T. M. V. D. Platinum(II) Ring-Fused Chlorins as Near-Infrared Emitting Oxygen Sensors and Photodynamic Agents. *ACS Med. Chem. Lett.* **2017**, *8*, 310−315.
(184) Stefflova, K.; Chen, J.; Zheng, G. Using Molecular Beacons for Cancer Imaging and Treatment. *Front. Biosci., Landmark Ed.* **2007**, *12*, 4709−4721.
(185) Pineiro, M.; Pereira, M. M.; Rocha Gonsalves, A. M. D. A.; Arnaut, L. G.; Formosinho, S. J. Singlet Oxygen Quantum Yields From Halogenated Chlorins: Potential New Photodynamic Therapy Agents. *J. Photochem. Photobiol., A* **2001**, *138*, 147−157.
(186) Serra, A.; Pineiro, M.; Santos, C. I.; Rocha Gonsalves, A. M. D. A.; Abrantes, M.; Laranjo, M.; Botelho, M. F. In Vitro Photodynamic Activity of 5,15-Bis(3-Hydroxyphenyl)Porphyrin and Its Halogenated Derivatives Against Cancer Cells. *Photochem. Photobiol.* **2010**, *86*, 206−212.

https://dx.doi.org/10.1021/acs.jmedchem.0c00047
J. Med. Chem. 2020, 63, 14119−14150

(187) Serra, A. C.; Pineiro, M.; Rocha Gonsalves, A. M. d. A.; Abrantes, M.; Laranjo, M.; Santos, A. C.; Botelho, M. F. Halogen Atom Effect on Photophysical and Photodynamic Characteristics of Derivatives of 5,10,15,20-Tetrakis(3-Hydroxyphenyl)Porphyrin. *J. Photochem. Photobiol., B* **2008**, *92*, 59−65.
(188) Stefflova, K.; Li, H.; Chen, J.; Zheng, G. Peptide-Based Pharmacomodulation of a Cancer-Targeted Optical Imaging and Photodynamic Therapy Agent. *Bioconjugate Chem.* **2007**, *18*, 379−388.
(189) Wilson, B. C.; Van Lier, J. E. Radiolabelled Photosensitizers for Tumour Imaging and Photodynamic Therapy. *J. Photochem. Photobiol., B* **1989**, *3*, 459.
(190) Pandey, S. K.; Sajjad, M.; Chen, Y.; Zheng, X.; Yao, R.; Missert, J. R.; Batt, C.; Nabi, H. A.; Oseroff, A. R.; Pandey, R. K. Comparative Positron-Emission Tomography (PET) Imaging and Phototherapeutic Potential of 1 24i- Labeled Methyl- 3-(1'-Iodobenzyloxyethyl) Pyropheophorbide-A vs the Corresponding Glucose and Galactose Conjugates. *J. Med. Chem.* **2009**, *52*, 445−455.
(191) Fazaeli, Y.; Jalilian, A. R.; Amini, M. M.; Ardaneh, K.; Rahiminejad, A.; Bolourinovin, F.; Moradkhani, S.; Majdabadi, A. Development of a ^{68}Ga-Fluorinated Porphyrin Complex as a Possible PET Imaging Agent. *Nucl. Med. Mol. Imaging* **2012**, *46*, 20−26.
(192) Shi, J.; Liu, T. W. B.; Chen, J.; Green, D.; Jaffray, D.; Wilson, B. C.; Wang, F.; Zheng, G. Transforming a Targeted Porphyrin Theranostic Agent into a PET Imaging Probe for Cancer. *Theranostics* **2011**, *1*, 363−370.
(193) Tamura, K.; Kurihara, H.; Yonemori, K.; Tsuda, H.; Suzuki, J.; Kono, Y.; Honda, N.; Kodaira, M.; Yamamoto, H.; Yunokawa, M.; Shimizu, C.; Hasegawa, K.; Kanayama, Y.; Nozaki, S.; Kinoshita, T.; Wada, Y.; Tazawa, S.; Takahashi, K.; Watanabe, Y.; Fujiwara, Y. ^{64}Cu-DOTA-Trastuzumab PET Imaging in Patients with HER2-Positive Breast Cancer. *J. Nucl. Med.* **2013**, *54*, 1869−1875.
(194) Aguilar-Ortíz, E.; Jalilian, A. R.; Ávila-Rodríguez, M. A. Porphyrins as Ligands for 64Copper: Background and Trends. *MedChemComm* **2018**, *9*, 1577−1588.
(195) Moran, M.; MacDonald, T.; Liu, T.; Forbes, J.; Zhen, G.; Valliant, J. Copper-64-Labeled Porphysomes for PET Imaging. *J. Nucl. Med.* **2014**, *55*, 1016.
(196) Rousseau, J.; Ali, H.; Lamoureux, G.; Lebel, E.; Van Lier, J. E. Synthesis, Tissue Distribution and Tumor Uptake of 99mTc- and 67Ga- Tetrasulfophthalocyanine. *Int. J. Appl. Radiat. Isot.* **1985**, *36*, 709−716.
(197) Li, Z.; Lin, T. P.; Liu, S.; Huang, C. W.; Hudnall, T. W.; Gabbaï, F. P.; Conti, P. S. Rapid Aqueous [18F]-Labeling of a BODIPY Dye for Positron Emission Tomography/Fluorescence Dual Modality Imaging. *Chem. Commun.* **2011**, *47*, 9324−9326.
(198) Pandey, R. K.; Goswami, L. N.; Chen, Y.; Gryshuk, A.; Missert, J. R.; Oseroff, A.; Dougherty, T. J. Nature: A Rich Source for Developing Multifunctional Agents. Tumor-Imaging and Photodynamic Therapy. *Lasers Surg. Med.* **2006**, *38*, 445−467.
(199) Pandey, S. K.; Gryshuk, A. L.; Sajjad, M.; Zheng, X.; Chen, Y.; Abouzeid, M. M.; Morgan, J.; Charamisinau, I.; Nabi, H. A.; Oseroff, A.; Pandey, R. K. Multimodality Agents for Tumor Imaging (Pet, Fluorescence) and Photodynamic Therapy. A Possible "See and Treat" Approach. *J. Med. Chem.* **2005**, *48*, 6286−6295.
(200) Edrei, R.; Gottfried, V.; van Lier, J. E.; Kimel, S. Sulfonated Phthalocyanines: Photophysical Properties, in Vitro Cell Uptake and Structure-Activity Relationships. *J. Porphyrins Phthalocyanines* **1998**, *2*, 191−199.
(201) Chan, W. M.; Lim, T. H.; Pece, A.; Silva, R.; Yoshimura, N. Verteporfin PDT for Non-Standard Indications-A Review of Current Literature. *Graefe's Arch. Clin. Exp. Ophthalmol.* **2010**, *248*, 613−626.
(202) Skupin-Mrugalska, P.; Piskorz, J.; Goslinski, T.; Mielcarek, J.; Konopka, K.; Düzgüneş, N. Current Status of Liposomal Porphyrinoid Photosensitizers. *Drug Discovery Today* **2013**, *18*, 776−784.
(203) Yuzhakova, D. V.; Lermontova, S. A.; Grigoryev, I. S.; Muravieva, M. S.; Gavrina, A. I.; Shirmanova, M. V.; Balalaeva, I. V.; Klapshina, L. G.; Zagaynova, E. V. In Vivo Multimodal Tumor Imaging and Photodynamic Therapy With Novel Theranostic Agents Based on the Porphyrazine Framework-Chelated Gadolinium (III) Cation. *Biochim. Biophys. Acta, Gen. Subj.* **2017**, *1861*, 3120−3130.
(204) Lim, E. K.; Kim, T.; Paik, S.; Haam, S.; Huh, Y. M.; Lee, K. Nanomaterials for Theranostics: Recent Advances and Future Challenges. *Chem. Rev.* **2015**, *115*, 327−394.
(205) Louie, A. Multimodality Imaging Probes: Design and Challenges. *Chem. Rev.* **2010**, *110*, 3146−3195.
(206) Edwards, W. B.; Xu, B.; Akers, W.; Cheney, P. P.; Liang, K.; Rogers, B. E.; Anderson, C. J.; Achilefu, S. Agonist - Antagonist Dilemma in Molecular Imaging: Evaluation of a Monomolecular Multimodal Imaging Agent for the Somatostatin Receptor. *Bioconjugate Chem.* **2008**, *19*, 192−200.
(207) Walia, S.; Acharya, A. Silica Micro/Nanospheres for Theranostics: From Bimodal MRI and Fluorescent Imaging Probes to Cancer Therapy. Beilstein. *Beilstein J. Nanotechnol.* **2015**, *6*, 546−558.
(208) Pandey, S. K.; Kaur, J.; Easwaramoorthy, B.; Shah, A.; Coleman, R.; Mukherjee, J. Multimodality Imaging Probe for Positron Emission Tomography and Fluorescence Imaging Studies. *Mol. Imaging* **2014**, *13*, 1−7.
(209) Wolfbeis, O. S. An Overview of Nanoparticles Commonly Used in Fluorescent Bioimaging. *Chem. Soc. Rev.* **2015**, *44*, 4743−4768.
(210) Thomas, R.; Park, I. K.; Jeong, Y. Y. Magnetic Iron Oxide Nanoparticles for Multimodal Imaging and Therapy of Cancer. *Int. J. Mol. Sci.* **2013**, *14*, 15910−15930.
(211) Vanderesse, D. B. Innovations of Photodynamic Therapy for Brain Tumors: Potential of Multifunctional Nanoparticles. *J. Carcinog. Mutagen.* **2014**, *8*, 8.
(212) Glasgow, M. D. K.; Chougule, M. B. Recent Developments in Active Tumor Targeted Multifunctional Nanoparticles for Combination Chemotherapy in Cancer Treatment and Imaging. *J. Biomed. Nanotechnol.* **2015**, *11*, 1859−1898.
(213) Nafiujjaman, M.; Revuri, V.; Nurunnabi, M.; Jae Cho, K.; Lee, Y. K. Photosensitizer Conjugated Iron Oxide Nanoparticles for Simultaneous in Vitro Magneto-Fluorescent Imaging Guided Photodynamic Therapy. *Chem. Commun.* **2015**, *51*, 5687−5690.
(214) Wang, D.; Fei, B.; Halig, L. V.; Qin, X.; Hu, Z.; Xu, H.; Wang, Y. A.; Chen, Z.; Kim, S.; Shin, D. M.; Chen, Z. Targeted Iron-Oxide Nanoparticle for Photodynamic Therapy and Imaging of Head and Neck Cancer. *ACS Nano* **2014**, *8*, 6620−6632.
(215) Luo, J.; Chen, L. F.; Hu, P.; Chen, Z. N. Tetranuclear Gadolinium(III) Porphyrin Complex as a Theranostic Agent for Multimodal Imaging and Photodynamic Therapy. *Inorg. Chem.* **2014**, *53*, 4184−4191.
(216) Spernyak, J. A.; White, W. H.; Ethirajan, M.; Patel, N. J.; Goswami, L.; Chen, Y.; Turowski, S.; Missert, J. R.; Batt, C.; Mazurchuk, R.; Pandey, R. K. Hexylether Derivative of Pyropheophorbide-a (HPPH) on Conjugating with 3 Gadolinium(III) Aminobenzyldiethylenetriaminepentaacetic Acid Shows Potential for In Vivo Tumor Imaging (MR, Fluorescence) and Photodynamic Therapy. *Bioconjugate Chem.* **2010**, *21*, 828−835.
(217) An, F. F.; Chan, M.; Kommidi, H.; Ting, R. Dual PET and Near-Infrared Fluorescence Imaging Probes as Tools for Imaging in Oncology. *AJR, Am. J. Roentgenol.* **2016**, *207*, 266−273.
(218) Seibold, U.; Wängler, B.; Schirrmacher, R.; Wängler, C. Bimodal Imaging Probes for Combined PET and OI: Recent Developments and Future Directions for Hybrid Agent Development. *BioMed Res. Int.* **2014**, *16*, 1.
(219) Nguyen, Q. T.; Tsien, R. Y. Fluorescence-Guided Surgery with Live Molecular Navigation-A New Cutting Edge. *Nat. Rev. Cancer* **2013**, *13*, 653−662.
(220) Ghosh, S. C.; Azhdarinia, A. Advances in the Development of Multimodal Imaging Agents for Nuclear/Near-Infrared Fluorescence Imaging. *Curr. Med. Chem.* **2015**, *22*, 3390−3404.
(221) Zeng, C.; Shang, W.; Wang, K.; Chi, C.; Jia, X.; Fang, C.; Yang, D.; Ye, J.; Fang, C.; Tian, J. Intraoperative Identification of Liver Cancer Microfoci Using a Targeted Near-Infrared Fluorescent Probe for Imaging-Guided Surgery. *Sci. Rep.* **2016**, *6*, 21959.

https://dx.doi.org/10.1021/acs.jmedchem.0c00047
J. Med. Chem. 2020, 63, 14119−14150

(222) Li, X.; Zhang, X.-N.; Li, X.-D.; Chang, J.; Li, X.; Zhang, X.-N.; Li, X.-D.; Chang, J. Multimodality Imaging in Nanomedicine and Nanotheranostics. *Cancer Biol. Med.* **2016**, *13*, 339−348.
(223) Durnev, A. D. Toxicology of Nanoparticles. Bull. *Bull. Exp. Biol. Med.* **2008**, *145*, 72−74.
(224) Liu, Z.; Kiessling, F.; Gätjens, J. Advanced Nanomaterials in Multimodal Imaging: Design, Functionalization, and Biomedical Applications. *J. Nanomater.* **2010**, *2010*, 1.
(225) Head, H. W.; Dodd, G. D.; Bao, A.; Soundararajan, A.; Garcia-Rojas, X.; Prihoda, T. J.; McManus, L. M.; Goins, B. A.; Santoyo, C. A.; Phillips, W. T. Combination Radiofrequency Ablation and Intravenous Radiolabeled Liposomal Doxorubicin: Imaging and Quantification of Increased Drug Delivery to Tumors. *Radiology* **2010**, *255*, 405−414.
(226) Ljungkvist, A. S. E.; Bussink, J.; Kaanders, J. H. A. M.; van der Kogel, A. J. Dynamics of Tumor Hypoxia Measured with Bioreductive Hypoxic Cell Markers. *Radiat. Res.* **2007**, *167*, 127−145.
(227) Vaupel, P.; Mayer, A. Hypoxia in Cancer: Significance and Impact on Clinical Outcome. *Cancer Metastasis Rev.* **2007**, *26*, 225−239.
(228) Brown, J. M. Tumor Hypoxia, Drug Resistance, and Metastases. *J. Natl. Cancer Inst.* **1990**, *82*, 338−339.
(229) Challapalli, A.; Carroll, L.; Aboagye, E. O. Molecular Mechanisms of Hypoxia in Cancer. *Clin. Transl. Imaging* **2017**, *5*, 225−253.
(230) Dewhirst, M. W.; Cao, Y.; Moeller, B. Cycling Hypoxia and Free Radicals Regulate Angiogenesis and Radiotherapy Response. *Nat. Rev. Cancer* **2008**, *8*, 425−437.
(231) Kushibiki, T.; Hirasawa, T.; Okawa, S.; Ishihara, M. Responses of Cancer Cells Induced by Photodynamic Therapy. *J. Healthc. Eng.* **2013**, *4*, 87−108.
(232) Li, S.; Meng, W.; Guan, Z.; Guo, Y.; Han, X. The Hypoxia-Related Signaling Pathways of Vasculogenic Mimicry in Tumor Treatment. *Biomed. Pharmacother.* **2016**, *80*, 127−135.
(233) Yao, J.; Feng, J.; Gao, X.; Wei, D.; Kang, T.; Zhu, Q.; Jiang, T.; Wei, X.; Chen, J. Neovasculature and Circulating Tumor Cells Dual-Targeting Nanoparticles for the Treatment of the Highly-Invasive Breast Cancer. *Biomaterials* **2017**, *113*, 1−17.
(234) Gray, L. H.; Conger, A. D.; Ebert, M.; Hornsey, S.; Scott, O. C. The Concentration of Oxygen Dissolved in Tissues at the Time of Irradiation as a Factor in Radiotherapy. *Br. J. Radiol.* **1953**, *26*, 638−648.
(235) Mottram, J. C. A. Factor of Importance in the Radio Sensitivity of Tumours. *Br. J. Radiol.* **1936**, *9*, 606−614.
(236) Arbeit, J. M.; Brown, J. M.; Chao, K. S. C.; Chapman, J. D.; Eckelman, W. C.; Fyles, A. W.; Giaccia, A. J.; Hill, R. P.; Koch, C. J.; Krishna, M. C.; Krohn, K. A.; Lewis, J. S.; Mason, R. P.; Melillo, G.; Padhani, A. R.; Powis, G.; Rajendran, J. G.; Reba, R.; Robinson, S. P.; Semenza, G. L.; Swartz, H. M.; Vaupel, P.; Yang, D.; Tatum, J. L. Hypoxia: Importance in Tumor Biology, Noninvasive Measurement by Imaging, and Value of Its Measurement in the Management of Cancer Therapy. *Int. J. Radiat. Biol.* **2006**, *82*, 699−757.
(237) Chapman, J. D.; Franko, A. J.; Sharplin, J. A Marker for Hypoxic Cells in Tumours with Potential Clinical Applicability. *Br. J. Cancer* **1981**, *43*, 546−550.
(238) Gallez, B.; Baudelet, C.; Jordan, B. F. Assessment of Tumor Oxygenation by Electron Paramagnetic Resonance: Principles and Applications. *NMR Biomed.* **2004**, *17*, 240−262.
(239) Kwock, L.; Gill, M.; McMurry, H. L.; Beckman, W.; Raleigh, J. A.; Joseph, A. P. Evaluation of a Fluorinated 2-Nitroimidazole Binding to Hypoxic Cells in Tumor-Bearing Rats by ^{19}F Magnetic Resonance Spectroscopy and Immunohistochemistry. *Radiat. Res.* **1992**, *129*, 71.
(240) Dunn, J. F.; O'Hara, J. A.; Zaim-Wadghiri, Y.; Lei, H.; Meyerand, M. E.; Grinberg, O. Y.; Hou, H.; Hoopes, P. J.; Demidenko, E.; Swartz, H. M. Changes in Oxygenation of Intracranial Tumors With Carbogen: A BOLD MRI and EPR Oximetry Study. *J. Magn. Reson. Imaging* **2002**, *16*, 511−521.
(241) Landuyt, W.; Hermans, R.; Bosmans, H.; Sunaert, S.; Beatse, E.; Farina, D.; Meijerink, M.; Zhang, H.; Bogaert, W.; Lambin, P.; Marchal, G. BOLD Contrast FMRI of Whole Rodent Tumour During Air or Carbogen Breathing Using Echo-Planar Imaging at 1.5 T. *Eur. Radiol.* **2001**, *11*, 2332−2340.
(242) Kelada, O. J.; Carlson, D. J. Molecular Imaging of Tumor Hypoxia with Positron Emission Tomography. *Radiat. Res.* **2014**, *181*, 335−349.
(243) Vaupel, P. Tumor Microenvironmental Physiology and Its Implications for Radiation Oncology. *Semin. Radiat. Oncol.* **2004**, *14*, 198−206.
(244) Mees, G.; Dierckx, R.; Vangestel, C.; Van De Wiele, C. Molecular Imaging of Hypoxia with Radiolabelled Agents. *Eur. J. Nucl. Med. Mol. Imaging* **2009**, *36*, 1674−1686.
(245) Lee, S. T.; Scott, A. M. Hypoxia Positron Emission Tomography Imaging With ^{18}F-Fluoromisonidazole. *Semin. Nucl. Med.* **2007**, *37*, 451−461.
(246) Koh, W. J.; Griffin, T. W.; Rasfy, J. S.; Laramore, G. E. Positron Emission Tomography: A New Tool for Characterization of Malignant Disease and Selection of Therapy. *Acta Oncol.* **1994**, *33*, 323−327.
(247) Cortezon-Tamarit, F.; Sarpaki, S.; Calatayud, D. G.; Mirabello, V.; Pascu, S. I. Applications of "Hot" and "Cold" Bis-(Thiosemicarbazonato) Metal Complexes in Multimodal Imaging. *Chem. Rec.* **2016**, *16*, 1380−1397.
(248) Hueting, R.; Kersemans, V.; Cornelissen, B.; Tredwell, M.; Hussien, K.; Christlieb, M.; Gee, A. D.; Passchier, J.; Smart, S. C.; Dilworth, J. R.; Gouverneur, V.; Muschel, R. J. A Comparison of the Behavior of ^{64}Cu-Acetate and ^{64}Cu-ATSM in Vitro and in Vivo. *J. Nucl. Med.* **2014**, *55*, 128−134.
(249) Holland, J. P.; Aigbirhio, F. I.; Betts, H. M.; Bonnitcha, P. D.; Burke, P.; Christlieb, M.; Churchill, G. C.; Cowley, A. R.; Dilworth, J. R.; Donnelly, P. S.; Green, J. C.; Peach, J. M.; Vasudevan, S. R.; Warren, J. E. Functionalized Bis(Thiosemicarbazonato) Complexes of Zinc and Copper: Synthetic Platforms Toward Site-Specific Radiopharmaceuticals. *Inorg. Chem.* **2007**, *46*, 465−485.
(250) Fujibayashi, Y.; Taniuchi, H.; Yonekura, Y.; Ohtani, H.; Konishi, J.; Yokoyama, A. Copper-62-ATSM: A New Hypoxia Imaging Agent with High Membrane Permeability and Low Redox Potential. *J. Nucl. Med.* **1997**, *38*, 1155−1160.
(251) Sarpaki, S.; Cortezon-Tamarit, F.; De Aguiar, S. R. M. M.; Exner, R. M.; Divall, D.; Arrowsmith, R. L.; Ge, H.; Palomares, F. J.; Carroll, L.; Calatayud, D. G.; Paisey, S. J.; Aboagye, E. O.; Pascu, S. I. Radio- and Nano-Chemistry of Aqueous Ga(III) Ions Anchored onto Graphene Oxide-Modified Complexes. *Nanoscale* **2020**, *12*, 6603−6608.
(252) Alam, I.; Arrowsmith, R.; Cortezon-Tamarit, F.; Tyman, F.; Kociok-Köhn, G.; Botchway, S.; Dilworth, J.; Carroll, L.; Aboagye, E.; Pascu, S. Microwave Gallium-68 Radiochemistry for Kinetically Stable Bis(Thiosemicarbazone) Complexes: Structural Investigations and Cellular Uptake Under Hypoxia. *Dalt. Trans.* **2016**, *45*, 144−155.
(253) Mirabello, V.; Cortezon-Tamarit, F.; Pascu, S. I. Oxygen Sensing, Hypoxia Tracing and in Vivo Imaging with Functional Metalloprobes for the Early Detection of Non-Communicable Diseases. *Front. Chem.* **2018**, *6*, 27.
(254) Schwartz, J.; Grkovski, M.; Rimner, A.; Schöder, H.; Zanzonico, P. B.; Carlin, S. D.; Staton, K. D.; Humm, J. L.; Nehmeh, S. A. Pharmacokinetic Analysis of Dynamic ^{18}F-Fluoromisonidazole Pet Data in Non-Small Cell Lung Cancer. *J. Nucl. Med.* **2017**, *58*, 911−919.
(255) Beck, R.; Röper, B.; Carlsen, J. M.; Huisman, M. C.; Lebschi, J. A.; Andratschke, N.; Picchio, M.; Souvatzoglou, M.; Machulla, M. J.; Piert, M. Pretreatment ^{18}F-Faza Pet Predicts Success of Hypoxia-Directed Radiochemotherapy Using Tirapazamine. *J. Nucl. Med.* **2007**, *48*, 973−980.
(256) Michalski, M. H.; Chen, X. Molecular Imaging in Cancer Treatment. *Eur. J. Nucl. Med. Mol. Imaging* **2011**, *38*, 358−377.
(257) Bonnitcha, P.; Grieve, S.; Figtree, G. Clinical Imaging of Hypoxia: Current Status and Future Directions. *Free Radical Biol. Med.* **2018**, *126*, 296−312.

https://dx.doi.org/10.1021/acs.jmedchem.0c00047
J. Med. Chem. 2020, 63, 14119−14150

(258) Carlin, S.; Zhang, H.; Reese, M.; Ramos, N. N.; Chen, Q.; Ricketts, S. A. A Comparison of the Imaging Characteristics and Microregional Distribution of 4 Hypoxia PET Tracers. *J. Nucl. Med.* **2014**, *55*, 515−521.
(259) Lewis, J.; McCarthy, D.; McCarthy, T.; Fujibayashi, Y.; Welch, M. Evaluation of ^{64}Cu-ATSM In Vitro and In Vivo in a Hypoxic Tumor Model. *J. Nucl. Med.* **1999**, *40*, 177−183.
(260) Pérès, E. A.; Toutain, J.; Paty, L. P.; Divoux, D.; Ibazizène, M.; Guillouet, S.; Barré, L.; Vidal, A.; Cherel, M.; Bourgeois, M.; Bernaudin, M.; Valable, S. ^{64}Cu-Atsm/^{64}Cu-Cl2 and Their Relationship to Hypoxia in Glioblastoma: A Preclinical Study. *EJNMMI Res.* **2019**, *9*, 114.
(261) Lewis, J. S.; Sharp, T. L.; Laforest, R.; Fujibayashi, Y.; Welch, M. J. Tumor Uptake of Copper-Diacetyl-Bis(N4-Methylthiosemicarbazone): Effect of Changes in Tissue Oxygenation. *J. Nucl. Med.* **2001**, *42*, 655−661.
(262) Colombié, M.; Gouard, S.; Frindel, M.; Vidal, A.; Chérel, M.; Kraeber-Bodéré, F.; Rousseau, C.; Bourgeois, M. Focus on the Controversial Aspects of ^{64}Cu-ATSM in Tumoral Hypoxia Mapping by Pet Imaging. *Front. Med.* **2015**, *2*, 58.
(263) Yuan, H.; Schroeder, T.; Bowsher, J. E.; Hedlund, L. W.; Wong, T.; Dewhirst, M. W. Intertumoral Differences in Hypoxia Selectivity of the PET Imaging Agent ^{64}Cu(II)-Diacetyl-Bis(N4-Methylthiosemicarbazone). *J. Nucl. Med.* **2006**, *47*, 989−998.
(264) Supuran, C. T. Carbonic Anhydrase Inhibition and the Management of Hypoxic Tumors. *Metabolites* **2017**, *7*, 48.
(265) Park, W.; Bae, B. Chan; Na, K. A Highly Tumor-Specific Light-Triggerable Drug Carrier Responds to Hypoxic Tumor Conditions for Effective Tumor Treatment. *Biomaterials* **2016**, *77*, 227−234.
(266) Wilson, W. R.; Hay, M. P. Targeting Hypoxia in Cancer Therapy. *Nat. Rev. Cancer* **2011**, *11*, 393−410.
(267) Lin, Q.; Bao, C.; Yang, Y.; Liang, Q.; Zhang, D.; Cheng, S.; Zhu, L. Highly Discriminating Photorelease of Anticancer Drugs Based on Hypoxia Activatable Phototrigger Conjugated Chitosan Nanoparticles. *Adv. Mater.* **2013**, *25*, 1981−1986.
(268) Qian, C.; Yu, J.; Chen, Y.; Hu, Q.; Xiao, X.; Sun, W.; Wang, C.; Feng, P.; Shen, Q. D.; Gu, Z. Light-Activated Hypoxia-Responsive Nanocarriers for Enhanced Anticancer Therapy. *Adv. Mater.* **2016**, *28*, 3313−3320.
(269) Mitton, D.; Ackroyd, R. A Brief Overview of Photodynamic Therapy in Europe. *Photodiagn. Photodyn. Ther.* **2008**, *5*, 103−111.
(270) Floeth, F. W.; Sabel, M.; Ewelt, C.; Stummer, W.; Felsberg, J.; Reifenberger, G.; Steiger, H. J.; Stoffels, G.; Coenen, H. H.; Langen, K. J. Comparison of ^{18}F-FET PET and 5-ALA Fluorescence in Cerebral Gliomas. *Eur. J. Nucl. Med. Mol. Imaging* **2011**, *38*, 731−741.
(271) Quirk, B. J.; Brandal, G.; Donlon, S.; Vera, J. C.; Mang, T. S.; Foy, A. B.; Lew, S. M.; Girotti, A. W.; Jogal, S.; LaViolette, P. S.; Connelly, J. M.; Whelan, H. T. Photodynamic Therapy (PDT) for Malignant Brain Tumors - Where Do We Stand? *Photodiagn. Photodyn. Ther.* **2015**, *12*, 530−544.
(272) Suzuki, H. I.; Katsura, A.; Matsuyama, H.; Miyazono, K. MicroRNA Regulons in Tumor Microenvironment. *Oncogene* **2015**, *34*, 3085−3094.
(273) Waghorn, P. A.; Jones, M. W.; Theobald, M. B. M.; Arrowsmith, R. L.; Pascu, S. I.; Botchway, S. W.; Faulkner, S.; Dilworth, J. R. Shining Light on the Stability of Metal Thiosemicarbazonate Complexes in Living Cells by FLIM. *Chem. Sci.* **2013**, *4*, 1430−1441.
(274) Nie, S.; Xing, Y.; Kim, G. J.; Simons, J. W. Nanotechnology Applications in Cancer. *Annu. Rev. Biomed. Eng.* **2007**, *9*, 257−288.
(275) McCarthy, J. R. Multifunctional Agents for Concurrent Imaging and Therapy in Cardiovascular Disease. *Adv. Drug Delivery Rev.* **2010**, *62*, 1023−1030.
(276) Warenius, H. M. Technological Challenges of Theranostics in Oncology. *Expert Opin. Med. Diagn.* **2009**, *3*, 381−393.
(277) Habermeyer, B.; Guilard, R. Some Activities of Porphychem Illustrated by the Applications of Porphyrinoids in PDT, PIT and PDI. *Photochem. Photobiol. Sci.* **2018**, *17*, 1675−1690.
(278) Singh, S.; Aggarwal, A.; Bhupathiraju, N. V. S. D. K.; Arianna, G.; Tiwari, K.; Drain, C. M. Glycosylated Porphyrins, Phthalocyanines, and Other Porphyrinoids for Diagnostics and Therapeutics. *Chem. Rev.* **2015**, *115*, 10261−10306.
(279) Zhang, Y.; Lovell, J. F. Recent Applications of Phthalocyanines and Naphthalocyanines for Imaging and Therapy. *Wiley Interdiscip. Rev. Nanomed. Nanobiotechnol.* **2017**, *9*, e1420.
(280) Shao, S.; Rajendiran, V.; Lovell, J. F. Metalloporphyrin Nanoparticles: Coordinating Diverse Theranostic Functions. *Coord. Chem. Rev.* **2019**, *379*, 99−120.
(281) Tsolekile, N.; Nelana, S.; Oluwafemi, O. S. Porphyrin as Diagnostic and Therapeutic Agent. *Molecules* **2019**, *24*, 2669.
(282) Pucelik, B.; Paczyński, R.; Dubin, G.; Pereira, M. M.; Arnaut, L. G.; Dąbrowski, J. M. Properties of Halogenated and Sulfonated Porphyrins Relevant for the Selection of Photosensitizers in Anticancer and Antimicrobial Therapies. *PLoS One* **2017**, *12*, e0185984.
(283) Xie, J.; Lee, S.; Chen, X. Nanoparticle-Based Theranostic Agents. *Adv. Drug Delivery Rev.* **2010**, *62*, 1064−1079.
(284) Lammers, T.; Kiessling, F.; Hennink, W. E.; Storm, G. Nanotheranostics and Image-Guided Drug Delivery: Current Concepts and Future Directions. *Mol. Pharmaceutics* **2010**, *7*, 1899−1912.
(285) Darwent, J. R.; McCubbin, I.; Phillips, D. Excited Singlet and Triplet State Electron-Transfer Reactions of Aluminium(III) Sulphonated Phthalocyanine. *J. Chem. Soc., Faraday Trans. 2* **1982**, *78*, 347−357.
(286) Couleaud, P.; Morosini, V.; Frochot, C.; Richeter, S.; Raehm, L.; Durand, J. O. Silica-Based Nanoparticles for Photodynamic Therapy Applications. *Nanoscale* **2010**, *2*, 1083−1095.
(287) Oluwole, D. O.; Nyokong, T. Photophysicochemical Behaviour of Metallophthalocyanines When Doped onto Silica Nanoparticles. *Dyes Pigm.* **2017**, *136*, 262−272.
(288) Tang, L.; Cheng, J. Nonporous Silica Nanoparticles for Nanomedicine Application. *Nano Today* **2013**, *8*, 290−312.
(289) Huang, D.; Hung, Y.; Ko, B.; Hsu, S.; Chen, W.; Chien, C.; Tsai, C.; Kuo, C.; Kang, J.; Yang, C.; Mou, C.; Chen, Y. Highly Efficient Cellular Labeling of Mesoporous Nanoparticles in Human Mesenchymal Stem Cells: Implication for Stem Cell Tracking. *FASEB J.* **2005**, *19*, 2014−2016.
(290) Lin, Y. S.; Wu, S. H.; Hung, Y.; Chou, Y. H.; Chang, C.; Lin, M. L.; Tsai, C. P.; Mou, C. Y. Multifunctional Composite Nanoparticles: Magnetic, Luminescent, and Mesoporous. *Chem. Mater.* **2006**, *18*, 5170−5172.
(291) Slowing, I. I.; Vivero-Escoto, J. L.; Wu, C. W.; Lin, V. S. Y. Mesoporous Silica Nanoparticles as Controlled Release Drug Delivery and Gene Transfection Carriers. *Adv. Drug Delivery Rev.* **2008**, *60*, 1278−1288.
(292) Tsai, C. P.; Hung, Y.; Chou, Y. H.; Huang, D. M.; Hsiao, J. K.; Chang, C.; Chen, Y. C.; Mou, C. Y. High-Contrast Paramagnetic Fluorescent Mesoporous Silica Nanorods as a Multifunctional Cell-Imaging Probe. *Small* **2008**, *4*, 186−191.
(293) Popat, A.; Hartono, S. B.; Stahr, F.; Liu, J.; Qiao, S. Z.; Lu, G. Q. Mesoporous Silica Nanoparticles for Bioadsorption, Enzyme Immobilisation, and Delivery Carriers. *Nanoscale* **2011**, *3*, 2801−2818.
(294) Chouikrat, R.; Seve, A.; Vanderesse, R.; Benachour, H.; Barberi-Heyob, M.; Richeter, S.; Raehm, L.; Durand, J.-O.; Verelst, M.; Frochot, C. Non Polymeric Nanoparticles for Photodynamic Therapy Applications: Recent Developments. *Curr. Med. Chem.* **2012**, *19*, 781−792.
(295) Lucky, S. S.; Soo, K. C.; Zhang, Y. Nanoparticles in Photodynamic Therapy. *Chem. Rev.* **2015**, *115*, 1990−2042.
(296) Piao, Y.; Burns, A.; Kim, J.; Wiesner, U.; Hyeon, T. Designed Fabrication of Silica-Based Nanostructured Particle Systems for Nanomedicine Applications. *Adv. Funct. Mater.* **2008**, *18*, 3745−3758.
(297) Ohulchanskyy, T. Y.; Roy, I.; Goswami, L. N.; Chen, Y.; Bergey, E. J.; Pandey, R. K.; Oseroff, A. R.; Prasad, P. N. Organically Modified Silica Nanoparticles With Covalently Incorporated Photo-

https://dx.doi.org/10.1021/acs.jmedchem.0c00047
J. Med. Chem. 2020, 63, 14119−14150

sensitizer for Photodynamic Therapy of Cancer. *Nano Lett.* **2007**, *7*, 2835−2842.
(298) Tang, W.; Xu, H.; Kopelman, R.; A. Philbert, M. Photodynamic Characterization and In Vitro Application of Methylene Blue-Containing Nanoparticle Platforms. *Photochem. Photobiol.* **2005**, *81*, 242.
(299) Biju, V. Chemical Modifications and Bioconjugate Reactions of Nanomaterials for Sensing, Imaging, Drug Delivery and Therapy. *Chem. Soc. Rev.* **2014**, *43*, 744−764.
(300) Castilho, M. L.; Vieira, L. S.; Campos, A. P. C.; Achete, C. A.; Cardoso, M. A. G.; Raniero, L. The Efficiency Analysis of Gold Nanoprobes by FT-IR Spectroscopy Applied to the Non-Cross-Linking Colorimetric Detection of Paracoccidioides Brasiliensis. *Sens. Actuators, B* **2015**, *215*, 258−265.
(301) Khaing Oo, M. K.; Yang, Y.; Hu, Y.; Gomez, M.; Du, H.; Wang, H. Gold Nanoparticle-Enhanced and Size-Dependent Generation of Reactive Oxygen Species from Protoporphyrin IX. *ACS Nano* **2012**, *6*, 1939−1947.
(302) Amini, S. M.; Kharrazi, S.; Hadizadeh, M.; Fateh, M.; Saber, R. Effect of Gold Nanoparticles on Photodynamic Efficiency of 5-Aminolevolenic Acid Photosensitiser in Epidermal Carcinoma Cell Line: An In Vitro Study. *IET Nanobiotechnol.* **2013**, *7*, 151−156.
(303) Pasparakis, G. Light-Induced Generation of Singlet Oxygen by Naked Gold Nanoparticles and Its Implications to Cancer Cell Phototherapy. *Small* **2013**, *9*, 4130−4134.
(304) Sherwani, M. A.; Tufail, S.; Khan, A. A.; Owais, M. Gold Nanoparticle-Photosensitizer Conjugate Based Photodynamic Inactivation of Biofilm Producing Cells: Potential for Treatment of C. Albicans Infection in BALB/c Mice. *PLoS One* **2015**, *10*, e0131684.
(305) Penon, O.; Marín, M. J.; Russell, D. A.; Pérez-García, L. Water Soluble, Multifunctional Antibody-Porphyrin Gold Nanoparticles for Targeted Photodynamic Therapy. *J. Colloid Interface Sci.* **2017**, *496*, 100−110.
(306) Basu, S.; Alavi, A. SPECT-CT and PET-CT in Oncology - An Overview. *Curr. Med. Imaging Rev.* **2011**, *7*, 202−209.
(307) Chopra, A.; Shan, L.; Eckelman, W. C.; Leung, K.; Menkens, A. E. Important Parameters to Consider for the Characterization of PET and SPECT Imaging Probes. *Nucl. Med. Biol.* **2011**, *38*, 1079−1084.
(308) Frangioni, J. V. In Vivo Near-Infrared Fluorescence Imaging. *Curr. Opin. Chem. Biol.* **2003**, *7*, 626−634.
(309) Ntziachristos, V.; Bremer, C.; Weissleder, R. Fluorescence Imaging With Near-Infrared Light: New Technological Advances That Enable in Vivo Molecular Imaging. *Eur. Radiol.* **2003**, *13*, 195−208.
(310) Peng, C.-L.; Shih, Y.-H.; Lee, P.-C.; Hsieh, T. M.-H.; Luo, T.-Y.; Shieh, M.-J. Multimodal Image-Guided Photothermal Therapy Mediated by ^{188}Re-Labeled Micelles Containing a Cyanine-Type Photosensitizer. *ACS Nano* **2011**, *5*, 5594−5607.
(311) Shen, X.; Li, L.; Wu, H.; Yao, S. Q.; Xu, Q. H. Photosensitizer-Doped Conjugated Polymer Nanoparticles for Simultaneous Two-Photon Imaging and Two-Photon Photodynamic Therapy in Living Cells. *Nanoscale* **2011**, *3*, 5140−5146.
(312) Tian, J.; Ding, L.; Xu, H. J.; Shen, Z.; Ju, H.; Jia, L.; Bao, L.; Yu, J. S. Cell-Specific and PH-Activatable Rubyrin-Loaded Nanoparticles for Highly Selective Near-Infrared Photodynamic Therapy Against Cancer. *J. Am. Chem. Soc.* **2013**, *135*, 18850−18858.
(313) Tsai, H. C.; Tsai, C. H.; Lin, S. Y.; Jhang, C. R.; Chiang, Y. S.; Hsiue, G. H. Stimulated Release of Photosensitizers from Graft and Diblock Micelles for Photodynamic Therapy. *Biomaterials* **2012**, *33*, 1827−1837.
(314) Kim, H.; Mun, S.; Choi, Y. Photosensitizer-Conjugated Polymeric Nanoparticles for Redox-Responsive Fluorescence Imaging and Photodynamic Therapy. *J. Mater. Chem. B* **2013**, *1*, 429−431.
(315) Wang, C.; Cheng, L.; Liu, Y.; Wang, X.; Ma, X.; Deng, Z.; Li, Y.; Liu, Z. Imaging-Guided PH-Sensitive Photodynamic Therapy Using Charge Reversible Upconversion Nanoparticles Under Near -Infrared Light. *Adv. Funct. Mater.* **2013**, *23*, 3077−3086.
(316) Yoon, H. Y.; Koo, H.; Choi, K. Y.; Lee, S. J.; Kim, K.; Kwon, I. C.; Leary, J. F.; Park, K.; Yuk, S. H.; Park, J. H.; Choi, K. Tumor-Targeting Hyaluronic Acid Nanoparticles for Photodynamic Imaging and Therapy. *Biomaterials* **2012**, *33*, 3980−3989.
(317) Lee, S. J.; Koo, H.; Jeong, H.; Huh, M. S.; Choi, Y.; Jeong, S. Y.; Byun, Y.; Choi, K.; Kim, K.; Kwon, I. C. Comparative Study of Photosensitizer Loaded and Conjugated Glycol Chitosan Nanoparticles for Cancer Therapy. *J. Controlled Release* **2011**, *152*, 21−29.
(318) Taratula, O.; Patel, M.; Schumann, C.; Naleway, M. A.; Pang, A. J.; He, H.; Taratula, O. Phthalocyanine-Loaded Graphene Nanoplatform for Imaging-Guided Combinatorial Phototherapy. *Int. J. Nanomed.* **2015**, *10*, 2347−2362.
(319) Choi, Y.; Kim, S.; Choi, M.-H.; Ryoo, S.-R.; Park, J.; Min, D.-H.; Kim, B.-S. Photodynamic Therapy: Highly Biocompatible Carbon Nanodots for Simultaneous Bioimaging and Targeted Photodynamic Therapy In Vitro and In Vivo. *Adv. Funct. Mater.* **2014**, *24*, 5774−5774A.
(320) Koo, H.; Lee, H.; Lee, S.; Min, K. H.; Kim, M. S.; Lee, D. S.; Choi, Y.; Kwon, I. C.; Kim, K.; Jeong, S. Y. In Vivo Tumor Diagnosis and Photodynamic Therapy via Tumoral PH-Responsive Polymeric Micelles. *Chem. Commun.* **2010**, *46*, 5668−5670.
(321) Lovell, J. F.; Jin, C. S.; Huynh, E.; MacDonald, T. D.; Cao, W.; Zheng, G. Enzymatic Regioselection for the Synthesis and Biodegradation of Porphysome Nanovesicles. *Angew. Chem., Int. Ed.* **2012**, *51*, 2429−2433.
(322) Yi, X. M.; Wang, F. L.; Qin, W. J.; Yang, X. J.; Yuan, J. L. Near-Infrared Fluorescent Probes in Cancer Imaging and Therapy: An Emerging Field. *Int. J. Nanomed.* **2014**, *9*, 1347−1365.
(323) Hu, J. J.; Liu, L. H.; Li, Z. Y.; Zhuo, R. X.; Zhang, X. Z. MMP-Responsive Theranostic Nanoplatform Based on Mesoporous Silica Nanoparticles for Tumor Imaging and Targeted Drug Delivery. *J. Mater. Chem. B* **2016**, *4*, 1932−1940.
(324) Kim, J.; Tung, C. H.; Choi, Y. Smart Dual-Functional Warhead for Folate Receptor-Specific Activatable Imaging and Photodynamic Therapy. *Chem. Commun.* **2014**, *50*, 10600−10603.
(325) Haedicke, K.; Kozlova, D.; Gräfe, S.; Teichgräber, U.; Epple, M.; Hilger, I. Multifunctional Calcium Phosphate Nanoparticles for Combining Near-Infrared Fluorescence Imaging and Photodynamic Therapy. *Acta Biomater.* **2015**, *14*, 197−207.
(326) Schneider, R.; Schmitt, F.; Frochot, C.; Fort, Y.; Lourette, N.; Guillemin, F.; Müller, J. F.; Barberi-Heyob, M. Design, Synthesis, and Biological Evaluation of Folic Acid Targeted Tetraphenylporphyrin as Novel Photosensitizers for Selective Photodynamic Therapy. *Bioorg. Med. Chem.* **2005**, *13*, 2799−2808.
(327) Wang, F.; Chen, X.; Zhao, Z.; Tang, S.; Huang, X.; Lin, C.; Cai, C.; Zheng, N. Synthesis of Magnetic, Fluorescent and Mesoporous Core-Shell-Structured Nanoparticles for Imaging, Targeting and Photodynamic Therapy. *J. Mater. Chem.* **2011**, *21*, 11244−11252.
(328) Kenanova, V.; Wu, A. M. Tailoring Antibodies for Radionuclide Delivery. *Expert Opin. Drug Delivery* **2006**, *3*, 53−70.
(329) Vieira, P.; Rajewsky, K. The Half-Lives of Serum Immunoglobulins in Adult Mice. *Eur. J. Immunol.* **1988**, *18*, 313−316.
(330) Decristoforo, C.; Pickett, R. D.; Verbruggen, A. Feasibility and Availability of 68Ga-Labelled Peptides. *Eur. J. Nucl. Med. Mol. Imaging* **2012**, *39*, 31−40.
(331) Liang, B.; Shao, W.; Zhu, C.; Wen, G.; Yue, X.; Wang, R.; Quan, J.; Du, J.; Bu, X. Mitochondria-Targeted Approach: Remarkably Enhanced Cellular Bioactivities of TPP2a as Selective Inhibitor and Probe toward TrxR. *ACS Chem. Biol.* **2016**, *11*, 425−434.
(332) Isabel, M.; Prata, M. Gallium-68: A New Trend in PET *Radiopharmacy. Curr. Radiopharm.* **2012**, *5*, 142−149.
(333) Roesch, F. Maturation of a Key Resource − The Germanium-68/Gallium-68 Generator: Development and New Insights. *Curr. Radiopharm.* **2012**, *5*, 202−211.
(334) Gaedicke, S.; Braun, F.; Prasad, S.; Machein, M.; Firat, E.; Hettich, M.; Gudihal, R.; Zhu, X.; Klingner, K.; Schüler, J.; Herold-Mende, C. C.; Grosu, A. L.; Behe, M.; Weber, W.; Mäcke, H.;

https://dx.doi.org/10.1021/acs.jmedchem.0c00047
J. Med. Chem. 2020, 63, 14119−14150

Niedermann, G. Noninvasive Positron Emission Tomography and Fluorescence Imaging of CD133+ Tumor Stem Cells. *Proc. Natl. Acad. Sci. U. S. A.* **2014**, *111*, E692−E701.
(335) Cho, Y. W.; Park, S. A.; Han, T. H.; Son, D. H.; Park, J. S.; Oh, S. J.; Moon, D. H.; Cho, K. J.; Ahn, C. H.; Byun, Y.; Kim, I. S.; Kwon, I. C.; Kim, S. Y. Vivo Tumor Targeting and Radionuclide Imaging with Self-Assembled Nanoparticles: Mechanisms, Key Factors, and Their Implications. *Biomaterials* **2007**, *28*, 1236−1247.
(336) Mitra, A.; Nan, A.; Line, B.; Ghandehari, H. Nanocarriers for Nuclear Imaging and Radiotherapy of Cancer. *Curr. Pharm. Des.* **2006**, *12*, 4729−4749.
(337) Yamamoto, F.; Yamahara, R.; Makino, A.; Kurihara, K.; Tsukada, H.; Hara, E.; Hara, I.; Kizaka-Kondoh, S.; Ohkubo, Y.; Ozeki, E.; Kimura, S. Radiosynthesis and Initial Evaluation of ^{18}F Labeled Nanocarrier Composed of Poly(L-Lactic Acid)-Block-Poly-(Sarcosine) Amphiphilic Polydepsipeptide. *Nucl. Med. Biol.* **2013**, *40*, 387−394.
(338) Jerabek, P. A.; Patrick, T. B.; Kilbourn, M. R.; Dischino, D. D.; Welch, M. J. Synthesis and Biodistribution of 18F-Labeled Fluoronitroimidazoles: Potential in Vivo Markers of Hypoxic Tissue. *Int. J. Radiat. Appl. Instrumentation.* **1986**, *37*, 599−605.
(339) Grierson, J. R.; Link, J. M.; Mathis, C. A.; Rasey, J. S.; Krohn, K. A. A Radiosynthesis of Fluorine-18 Fluoromisonidazole. *J. Labelled Compd. Radiopharm.* **1989**, *30*, 343−350.
(340) Lopci, E.; Grassi, I.; Chiti, A.; Nanni, C.; Cicoria, G.; Toschi, L.; Fonti, C.; Lodi, F.; Mattioli, S.; Fanti, S. Pet Radiopharmaceuticals for Imaging of Tumor Hypoxia: A Review of the Evidence. *Am. J. Nucl. Med. Mol. Imaging* **2014**, *4*, 365−384.
(341) Bourgeois, M.; Rajerison, H.; Guerard, F.; Mougin-Degraef, M.; Barbet, J.; Michel, N.; Cherel, M.; Faivre-Chauvet, A. Contribution of [64Cu]-ATSM PET in Molecular Imaging of Tumour Hypoxia Compared to Classical [18F] - MISO - A Selected Review. *Nucl. Med. Rev.* **2011**, *14*, 90−95.
(342) Hoigebazar, L.; Jeong, J. M. Hypoxia Imaging Agents Labeled with Positron Emitters. *Recent Results Cancer Res.* **2013**, *194*, 285−299.
(343) Takasawa, M.; Moustafa, R. R.; Baron, J. C. Applications of Nitroimidazole in Vivo Hypoxia Imaging in Ischemic Stroke. *Stroke* **2008**, *39*, 1629−1637.
(344) Lee, N. Y.; Mechalakos, J. G.; Nehmeh, S.; Lin, Z.; Squire, O. D.; Cai, S.; Chan, K.; Zanzonico, P. B.; Greco, C.; Ling, C. C.; Humm, J. L.; Schöder, H. Fluorine-18-Labeled Fluoromisonidazole Positron Emission and Computed Tomography-Guided Intensity-Modulated Radiotherapy for Head and Neck Cancer: A Feasibility Study. Int. *Int. J. Radiat. Oncol., Biol., Phys.* **2008**, *70*, 2−13.
(345) Padhani, A. R. Where Are We With Imaging Oxygenation in Human Tumours? *Cancer Imaging* **2005**, *5*, 128−130.
(346) Lapi, S. E.; Voller, T. F.; Welch, M. J. PET Imaging of Hypoxia. *PET Clin* **2009**, *4*, 39−47.
(347) Hustinx, R.; Eck, S. L.; Alavi, A. Potential Applications of PET Imaging in Developing Novel Cancer Therapies. *J. Nucl. Med.* **2000**, *11*, 433−441.
(348) Chen, K.; Chen, X. Positron Emission Tomography Imaging of Cancer Biology: Current Status and Future Prospects. *Semin. Oncol.* **2011**, *38*, 70−86.
(349) Zhang, P.; Sadler, P. J. Redox-Active Metal Complexes for Anticancer Therapy. *Eur. J. Inorg. Chem.* **2017**, *2017*, 1541−1548.
(350) Agdeppa, E. D.; Spilker, M. E. A Review of Imaging Agent Development. *AAPS J.* **2009**, *11*, 286−299.
(351) Miller, A.; Hoogstraten, B.; Staquet, M.; Winkler, A. Reporting Results of Cancer Treatment. *Cancer* **1981**, *47*, 207.
(352) O'Connell, M. PET−CT Modification of RECIST Guidelines. *J. Natl. Cancer Inst.* **2004**, *96*, 801.
(353) Frank, R. A.; Långström, B.; Antoni, G.; Montalto, M. C.; Agdeppa, E. D.; Mendizabal, M.; Wilson, I. A.; Vanderheyden, J. L. The Imaging Continuum: Bench to Biomarkers to Diagnostics. *J. Labelled Compd. Radiopharm.* **2007**, *50*, 746−769.
(354) Robertson, C. A.; Evans, D. H.; Abrahamse, H. Photodynamic Therapy (PDT): A Short Review on Cellular Mechanisms and Cancer Research Applications for PDT. *J. Photochem. Photobiol., B* **2009**, *96*, 1−8.
(355) Chauhan, P.; Hadad, C.; Sartorelli, A.; Zarattini, M.; Herreros-Lopez, A.; Mba, M.; Maggini, M.; Prato, M.; Carofiglio, T. Nanocrystalline Cellulose−Porphyrin Hybrids: Synthesis, Supramolecular Properties, and Singlet-Oxygen Production. *Chem. Commun.* **2013**, *49*, 8525−8527.
(356) Adler, A. D.; Longo, F. R.; Finarelli, J. D.; Goldmacher, J.; Assour, J.; Korsakoff, L. A Simplified Synthesis for Meso-Tetraphenylporphine. *J. Org. Chem.* **1967**, *32*, 476.
(357) Mannancherril, V.; Therrien, B. Strategies Toward the Enhanced Permeability and Retention Effect by Increasing the Molecular Weight of Arene Ruthenium Metallaassemblies. *Inorg. Chem.* **2018**, *57*, 3626−3633.
(358) Yoo, J. O.; Ha, K. S. New Insights into the Mechanisms for Photodynamic Therapy-Induced Cancer Cell Death. *Int. Rev. Cell Mol. Biol.* **2012**, *295*, 139−174.
(359) Li, S. Y.; Xie, B. R.; Cheng, H.; Li, C. X.; Zhang, M. K.; Qiu, W. X.; Liu, W. L.; Wang, X. S.; Zhang, X. Z. A Biomimetic Theranostic O_2-Meter for Cancer Targeted Photodynamic Therapy and Phosphorescence Imaging. *Biomaterials* **2018**, *151*, 1−12.

https://dx.doi.org/10.1021/acs.jmedchem.0c00047
J. Med. Chem. 2020, 63, 14119−14150